CR-178849

(NASA-CR-178849) ANALYSIS OF DOPPLER LIDAR WIND MEASUREMENTS Final Technical Report (Chicago Univ.) 67 p CSCL 04B

N86-29465

Unclas
G3/47 43203

ANALYSIS OF DOPPLER LIDAR WIND MEASUREMENTS

FINAL TECHNICAL REPORT

NAS 8 34770

MAY 1986

C\$455749

LABORATORY FOR ATMOSPHERIC PROBING

DEPARTMENT OF THE GEOPHYSICAL SCIENCES

THE UNIVERSITY OF CHICAGO

CHICAGO, IL

CONTRACTOR: Name and Address

The University of Chicago
Research Administration
5801 S. Ellis Avenue
Chicago, Il 60637

TITLE: Analysis of Doppler Lidar Wind Measurements

DATE: May 1986

TYPE OF REPORT AND CONTRACT NUMBER

Final Technical Report: NAS 8 34770

AUTHOR: Ramesh C. Srivastava

Prepared for the George C. Marshall Space Flight Center
Marshall Space Flight Center
Alabama 35812

TABLE OF CONTENTS

1. INTRODUCTION

The distribution of winds in the convectively mixed planetary boundary layer is of considerable practical and theoretical interest. In the past, measurements of the winds have usually been made from instrumented tower or aircraft. A few measurements have been conducted by means of multiple Doppler radar networks. Since the clear air is ordinarily 'invisible' at microwave frequencies, radar reflecting chaff was used in those experiments to make the air 'visible'. The multiple Doppler radar method of measurement is potentially superior in that it can yield practically instantaneous winds over large volumes, whereas both the tower and aircraft methods are considerably limited in that respect.

The Marshall Space Flight Center of the National Aeronautics and Space Administration has developed a method for measuring winds using a Doppler lidar on board a CV 990 aircraft. In contrast to the microwave radar, the lidar senses air motions by scattering from aerosols which are usually present in adequate concentrations, at least in the lower atmosphere, to return detectable signals. The airborne Doppler lidar method offers the potential for measurements in most situations where the plane can be flown.

On 16th July 1981, during the Coperative Convective Precipitation Experiment (CCOPE), the NASA CV 990 Doppler lidar was used to measure the winds in a convectively mixed boundary layer. At the same time, a multiple-Doppler radar network was also used to measure the winds. This report is concerned with an analysis of those measurements. This work was initially undertaken with two objectives in mind: (1) a study of the kinematic structure of the convectively mixed planetary boundary layer, and (2) a comparison between the winds measured by the Doppler lidar and the multiple Doppler radar network.

Analysis of the Doppler lidar measurements for this day was performed by Dr. Robert Lee of Lassen Research. Early in the course of the work, it became clear that the winds deduced by the Doppler lidar and the multiple Doppler network did not compare well. This was not totally surprising. There is a great disparity between the beam widths of the Doppler lidar and the microwave radars used in the experiment, which is compounded by the fact that typically the lidar measurements are made at much closer ranges than the microwave Doppler radar measurements. Thus while the radial velocities measured by the microwave radar were typically averages over a cylinder of radius about 500m (at 30 km range) and length 100m, the radial velocity measured by the Doppler lidar was an average over a cylinder of radius a few meters (at 10 km range) and length 100m. Consequently, the multiple Doppler radar method produced winds averaged

over a volume with typical dimensions of about 500m on each side, while the lidar method produced winds averaged over a much smaller and highly asymmetrical volume. More importantly, the lidar method produced winds with very high resolution in the vertical and this made the comparison even more difficult, especially in the vicinity of the inversion, because the winds often posess a fine-scale structure in that direction. Therefore, this research was mostly devoted to task (1) above, namely, a study of the kinematic structure of the convectively mixed planetary boundary layer.

2. THE EXPERIMENT AND OBSERVATIONS

On the afternoon of 16 July 1981, a boundary layer experiment was carried out in CCOPE. It was a clear day with little cloudiness. Radar reflecting chaff was released from aircraft at a height of approximately 2800m asl, that is, approximately 2100m agl, at about the top of the boundary layer near the inversion. Fig. 1 is a set of contoured reflectivity maps showing the pattern of chaff release from the aircraft. Subsequently, the chaff dispersed rapidly through the depth of the boundary layer, and remained in the area for a considerable period of time. Multiple Doppler radar measurements were taken during this period with the NCAR (National Center for Atmospheric Research) CP2, CP3, and CP4 radars. The CP2 radar is a 10 cm wavelength radar, while the CP3 and CP4 radars transmit at a wavelength of approximately 5.5 cm.

Measurements showed the thermal stratification to be nearly dry-adiabatic below the inversion at a height of approximately 2200m agl. This may be seen from fig. 2 based on aircraft measurements of the vertical profiles of potential temperature and specific humidity. (Subtract 800m from the height scale to get approximate heights above ground level.)

Figure 3 shows the locations of the CCOPE radars used in this study. The data from the CP2, CP3, and CP4 radars for the time period 1443 through 1454 MDT were used to perform the multiple Doppler analyses. Four complete volume scans were performed during that period. The inside rectangle of dimensions 40 km (north-south) by 60 km (east-west) represents the area over which these analyses were performed. Some VAD calculations were also performed using data from the NOAA K band radar but these are not discussed here.

3. METHOD OF MULTIPLE DOPPLER ANALYSIS

A number of steps are involved in calculating wind fields from multiple Doppler radar data. Fig. 4 is an abbreviated flow chart showing the various steps in the processing. A brief description of each of the steps is given below.

The first step, FORMATting, consists of reformatting all the raw radar data tapes to a common format. We have used a fromat different from the so-called 'universal format.' In

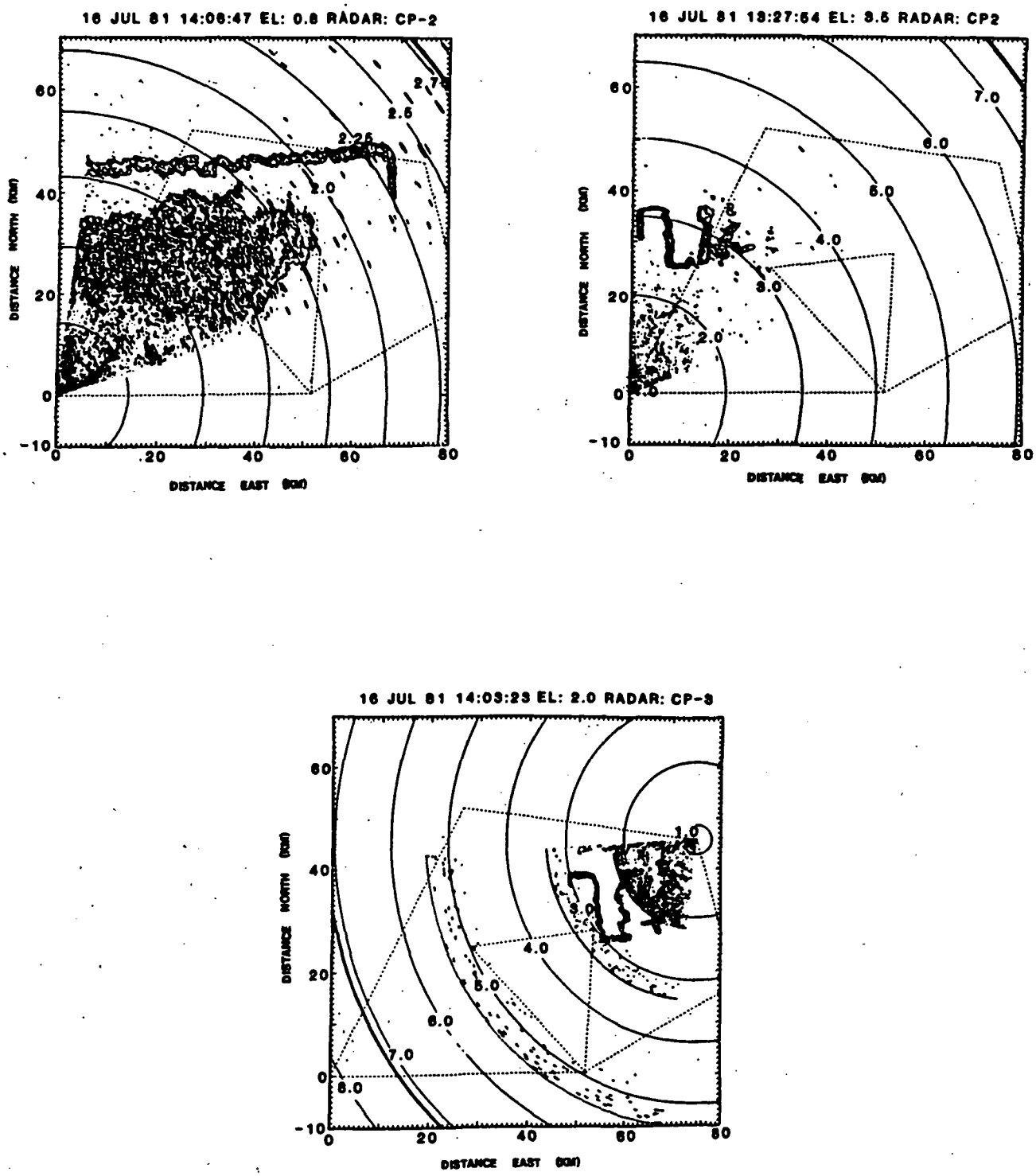

Fig. 1: Shows pattern of chaff dispersal from aircraft. Ground clutter around the radars is evident.

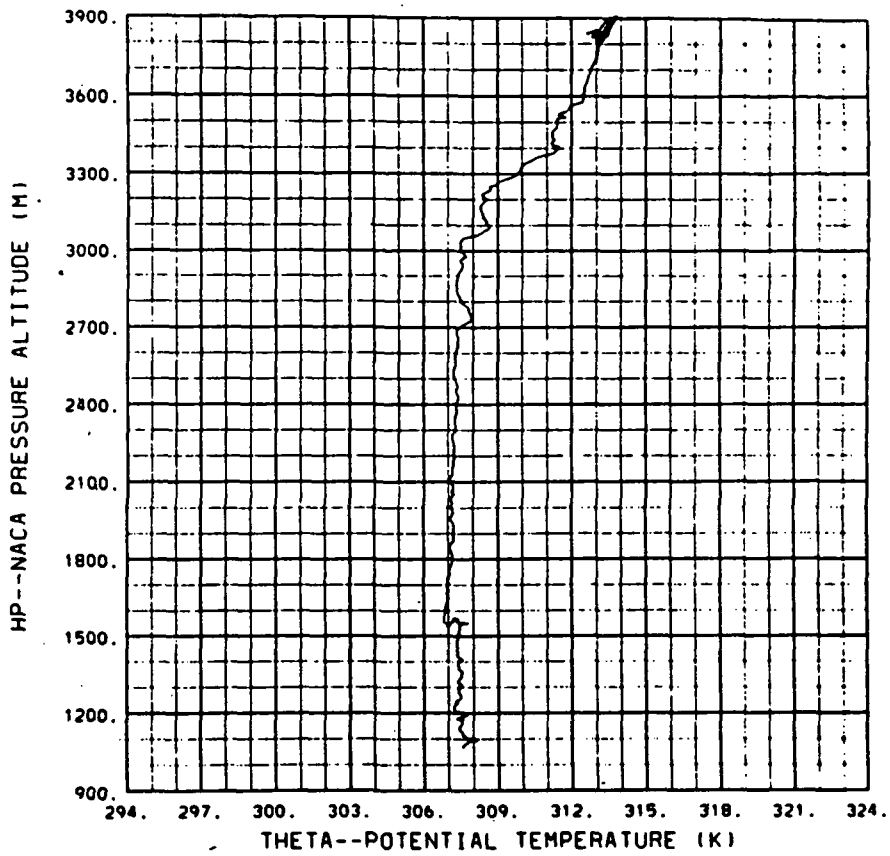

a.

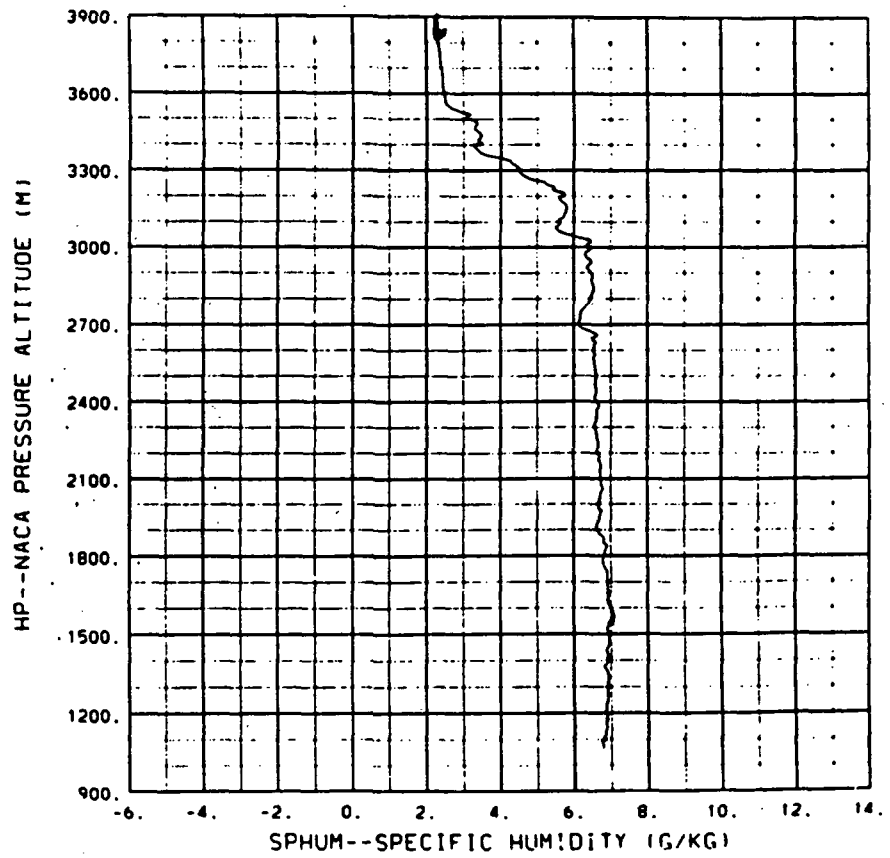

b.

Fig. 2: Profiles of (a) potential temperature, and (b) specific humidity measured by aircraft.

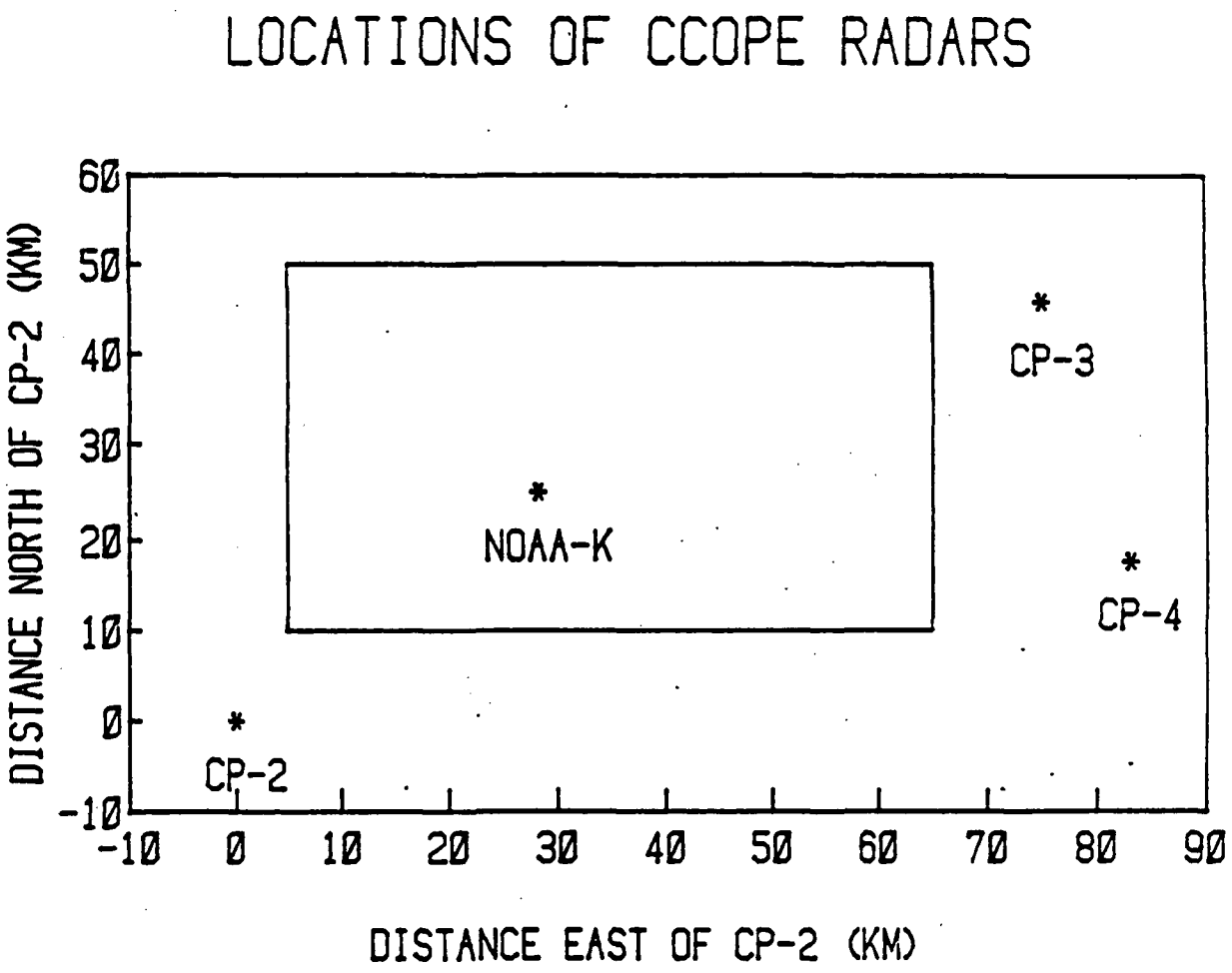

Fig. 3: Locations of some of the CCOPE radars. Data from the CP2, CP3 and CP4 radars were used in the multiple Doppler analysis. The analysis area is represented by the inner rectangle.

the next step, MERGE, data from the various radars (in this case the CP2, CP3, and CP4) are MERGEd. First, a MERGE volume is selected. In this case, it was a volume 40 km by 60 km in the horizontal, shown in fig. 3, by 3.3 km deep. As mentioned before, the inversion was at a height of about 3.0 km above the ground and little chaff was dispersed above it. The data from each of the radars (position, reflectivity, mean Doppler, and time of acquisition) for each range bin within the MERGE volume are written to different 'files' of a random access volume. The different files contain data for pre-selected height intervals. The height intervals are selected depending upon the data density and the meteorological situation. In the present case, 15 layers were used with their centers at heights of 0.2, 0.5, 0.7, 0.9, 1.1, 1.3, 1.5, 1.7, 1.9, 2.1, 2.3, 2.5, 2.7, 2.9, and 3.1 km above ground. This rather fine classification in height was possible because of the high data density-- the data were collected at 'overlapping' elevation angles, that is, the elevation steps in the scans were smaller than the beam widths of the radars; similarly there was 'overlap' in the azimuthal direction as well, that is, the antenna beam rotated by less than a beam width in the time it took to collect returns for a calculation of reflectivity and mean Doppler velocity. Each layer was divided into a 120 by 180 grid, with the smaller number of grids in the north-south direction. Thus the grid resolution was about 333m in both directions. The grid points were numbered 1 through 21,600 (120x180). An ID number was attached to each data point, it being the number of the grid point nearest to it. The EDIT consists in flagging spurious data and unfolding Doppler velocities. In the present case this process was relatively painless because of the high data quality and because the winds were very light and, therefore, no Doppler velocity folding occurred. Most of the editing consisted in flagging ground clutter data recognized by a zero Doppler and substantial reflectivity. Occasional high Doppler velocities were encountered, presumably due to aircraft in the area; these were also flagged. The flagged data are ignored in the subsequent analyses but are nevertheless maintained intact in the MERGE and other data records. The next step of the processing consists in SORTing the data for each layer by ID number and writing it to a random access volume. After the SORT, data from the neighborhood of any point can be readily accessed. In the INTERPOLATION, radial velocities at a set of 'interpolation' grid points are calculated for each of the radars. In the present case, the 'interpolation' grid was taken to be 500m by 500m in the horizontal with vertical extents kept identical to that of the MERGE height classification. That is there were in all 120x80x15 'interpolation' grid points. The interpolation was simply a straight arithmetic average of the radial velocities for each radar lying within each 'interpolation' box of dimensions 500m by 500m in the horizontal by the variable depth determined by the MERGE height classification. A weighted

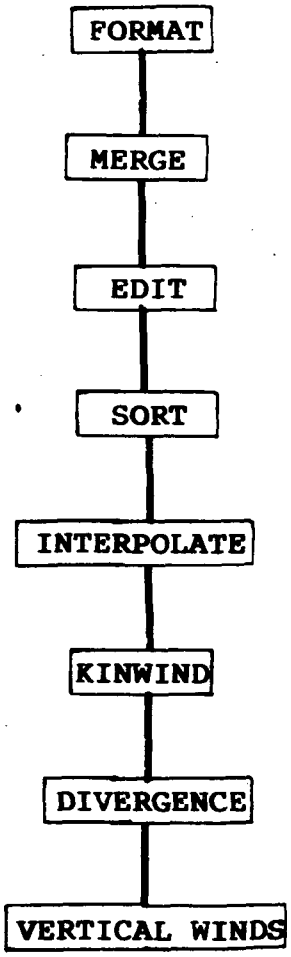

Fig. 4: Abbreviated flow chart for the processing of multiple Doppler radar data

arithmetic average is sometimes performed, with the weights being some function of the distance between the data points and the grid point. This was considered unnecessary in the present case because of the rather high data density which also allowed selection of rather small interpolation boxes. It should be mentioned that the radial velocities contributing to the grid point velocities were all distinct, that is, each radial velocity contributed to only one grid point in the interpolation.

After the interpolation, the horizontal winds were calculated by appropriate matrix inversion neglecting the contribution of vertical velocity of the scaterers to the radial velocities (KINWIND). In the present case, this is certainly justified because of the small vertical velocities and because of the low radar elevation angles. At grid points where only two of the radars had radial velocities, they were sufficient to calculate the two components of the horizontal wind uniquely. At grid points where three radars had radial velocities, we had an overdetermined set of equations and a least-squares method was used to calculate the two components of the horizontal wind vector. From the horizontal winds, their divergence was calculated using straightforward finite difference approximations to the derivatives (DIVERGENCE). The vertical air velocity was then calculated by integrating the anelasic continuity equation, assuming it to be zero at the bottom of the lowest 'merge' (or 'interpolation') layer (VERTCAL WINDS). A simple trapezoidal rule was used for the integration.

4. RESULTS AND DISCUSSION

4.1 Horizontal Winds

A sample plot of the vector horizontal wind is shown in fig. 5 for a height 900m agl at 1445 MDT. (The appendix contains horizontal wind plots for all the 15 heights for the times 1445, 1450 and 1452, that is a total of 45 plots; plots for 1448 MDT are not included) Straight lines connecting the CP2 radar to the CP3 and CP4 radars are shown. A few of the wind vectors are clearly erroneous. These occur near the base lines connecting pairs of radars; examination of the data showed that the erroneous wind vectors are the result of combining radial velocities from two radars only lying along the base line. These vectors were flagged and ignored in the subsequent calculations. The density of the wind vectors generally decreases with height with the concentration of the chaff. If the region had been completely filled with chaff, a wind vector would have been calculated at every grid point, that is, at points separated by 500m in either horizontal direction.

The winds are very light. They are cellular which is characteristic of thermal convection. Especially noteworthy are the sharp shears in the horizontal, and the sharp demarcation between the cells. The typical distance from the

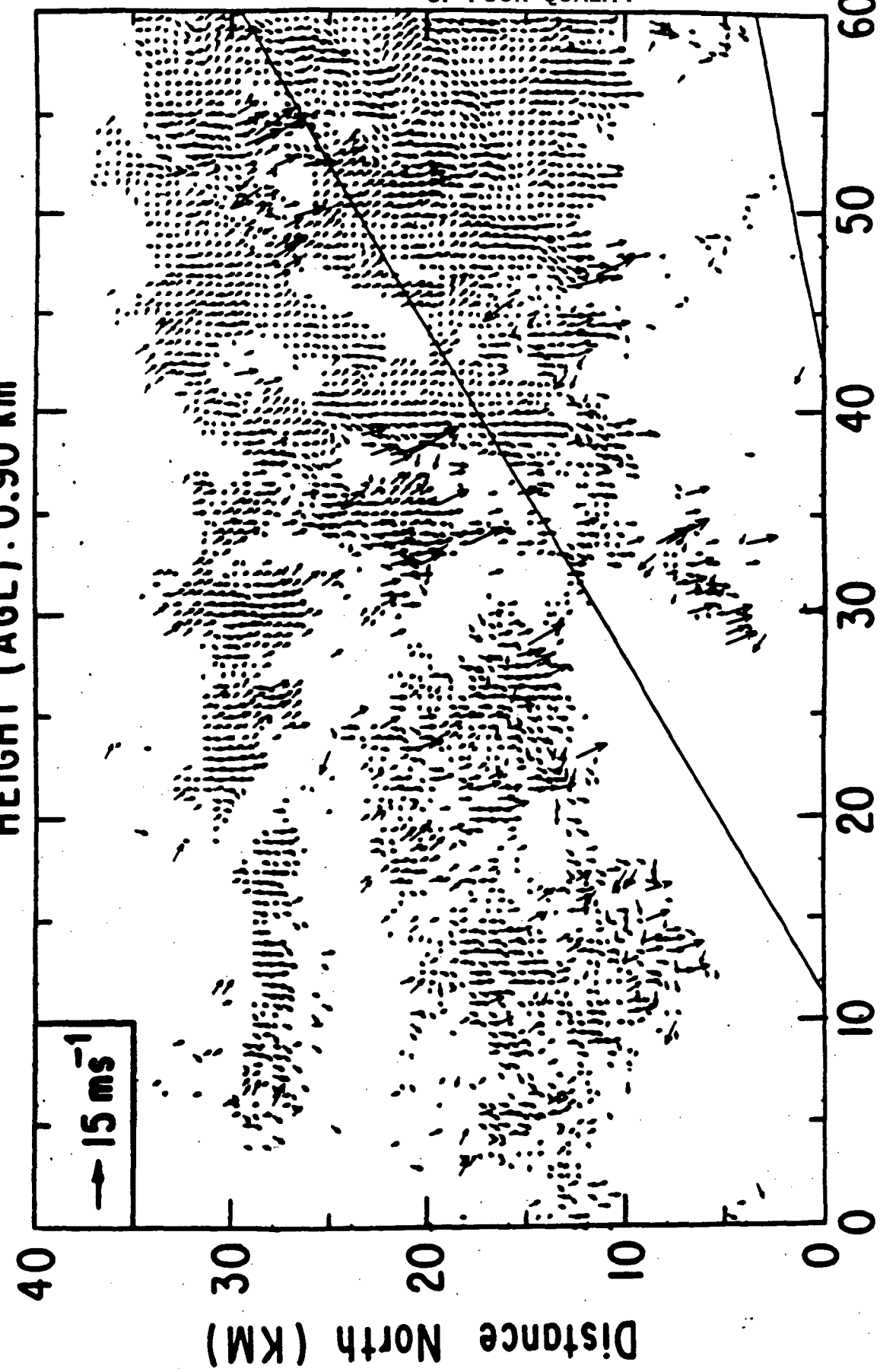

Fig. 5: Sample plot of horizontal winds for 900m agl at 14:45 MDT.

CP2 and CP3 radars to the area of dense wind vectors is about 30 km. At this distance, the half-power full beam width has a linear dimension of approximately 500m. Therefore, it is perhaps not surprising that the winds show substantial changes from grid point to grid point. But it is clear that the finite radar pulse volume must produce some averaging and, therefore, the demarcation from one cell to the next must in reality be sharper than depicted in the figure. In the vertical direction, we have aimed for higher resolution than warranted by the radar beam width because there were 'overlapping' scans and sharp changes in the vertical may be expected to manifest themselves even though degraded by the pulse-volume averaging.

An examination of the winds for successive heights (see figures in the appendix) shows remarkable continuity in the vertical, and in time. Some continuity is to be expected because of the pulse volume averaging, but the continuity is evident even when comparing winds separated by say more than 500m in height. Another point worth noting is that the positions of the prononuced cells (towards the location of the CP3 and CP4 radars) changes little over the 7 minute time period from 1445 to 1452. This may be due to the light winds and/or control of the cell locations by surface features.

A plot of the vertical profiles of the areal averages of u and v (east and north components of the wind vector) is shown in figs. 6a and b. Note again the consistency in time and height.

4.2 Vertical Winds

As mentioned above the vertical air velocity (w) was calculated by first finding the divergence of the horizontal wind and then integrating the anelastic continuity equation with the boundary condition w=0 at the ground. Because of the integration most of the deep vertically continuous records of w occurred in the eastern portion of the analysis region. Values of w that were obviously erroneous (magnitudes exceeding about 10 m/s) occurred near the edges of regions of chaff, that is at the boundaries between data-filled and data-void regions. These were obviously due to errors in the horizontal divergence in those regions. These w values were edited out.

Vertical sections of w through two of the convection 'cells' are shown in fig. 7. The vectors drawn are the magnitude and direction of the winds in the plane of the section. A scale of wind magnitude is shown on the figure. Typical magnitudes of w are 1 m/s with peak magnitudes of about 5 m/s. Note that w tends to approach zero near the inversion in rising air; downward motions also tend to be continuous in the vertical with non-zero w near the inversion. Both the rising and descending columns of air are fairly erect. These features were found in other vertical sections as well. These profiles of vertical air velocity are entirely reasonable.

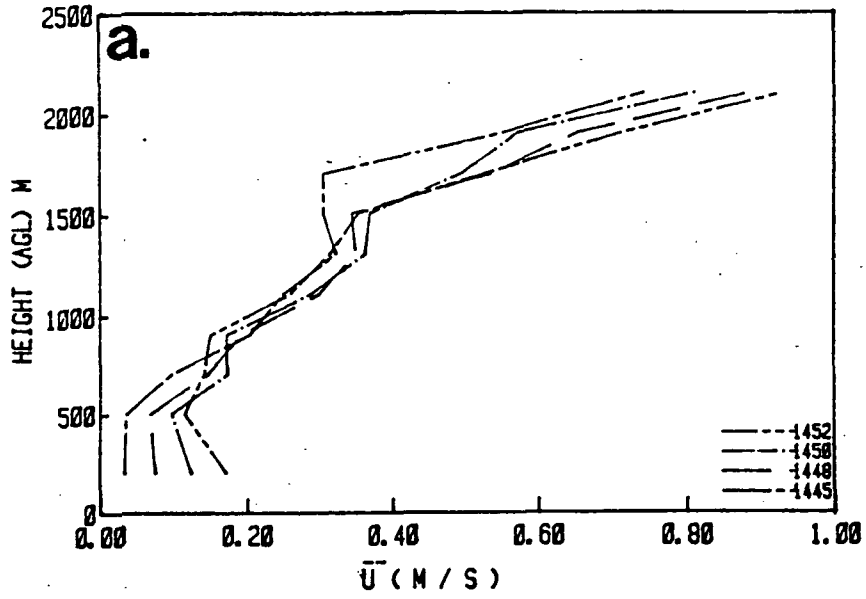

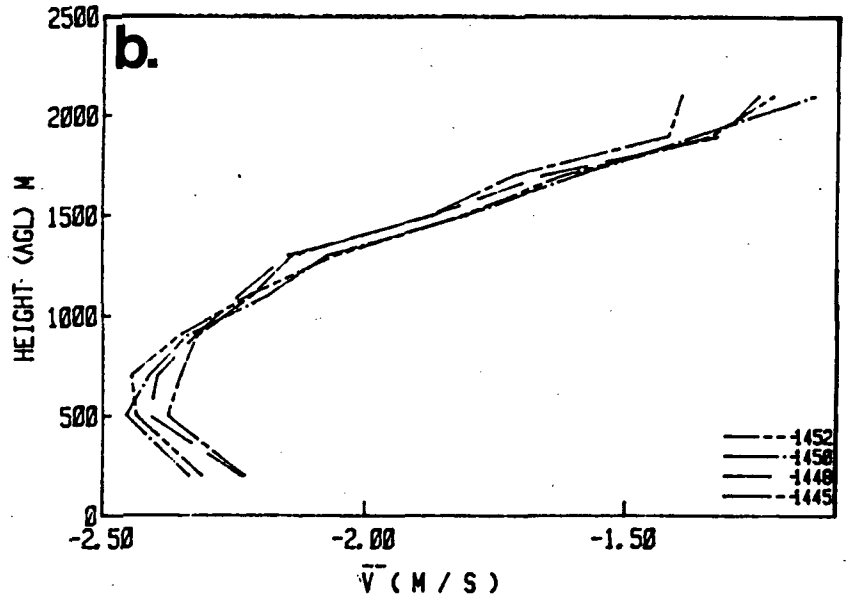

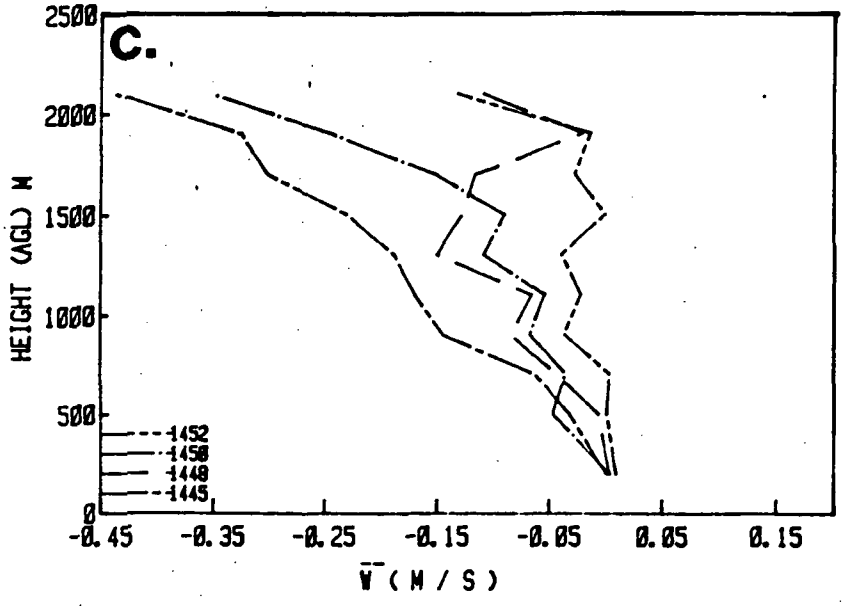

Fig. 6: Vertical profiles of averages of the three components of the wind for the four time periods.

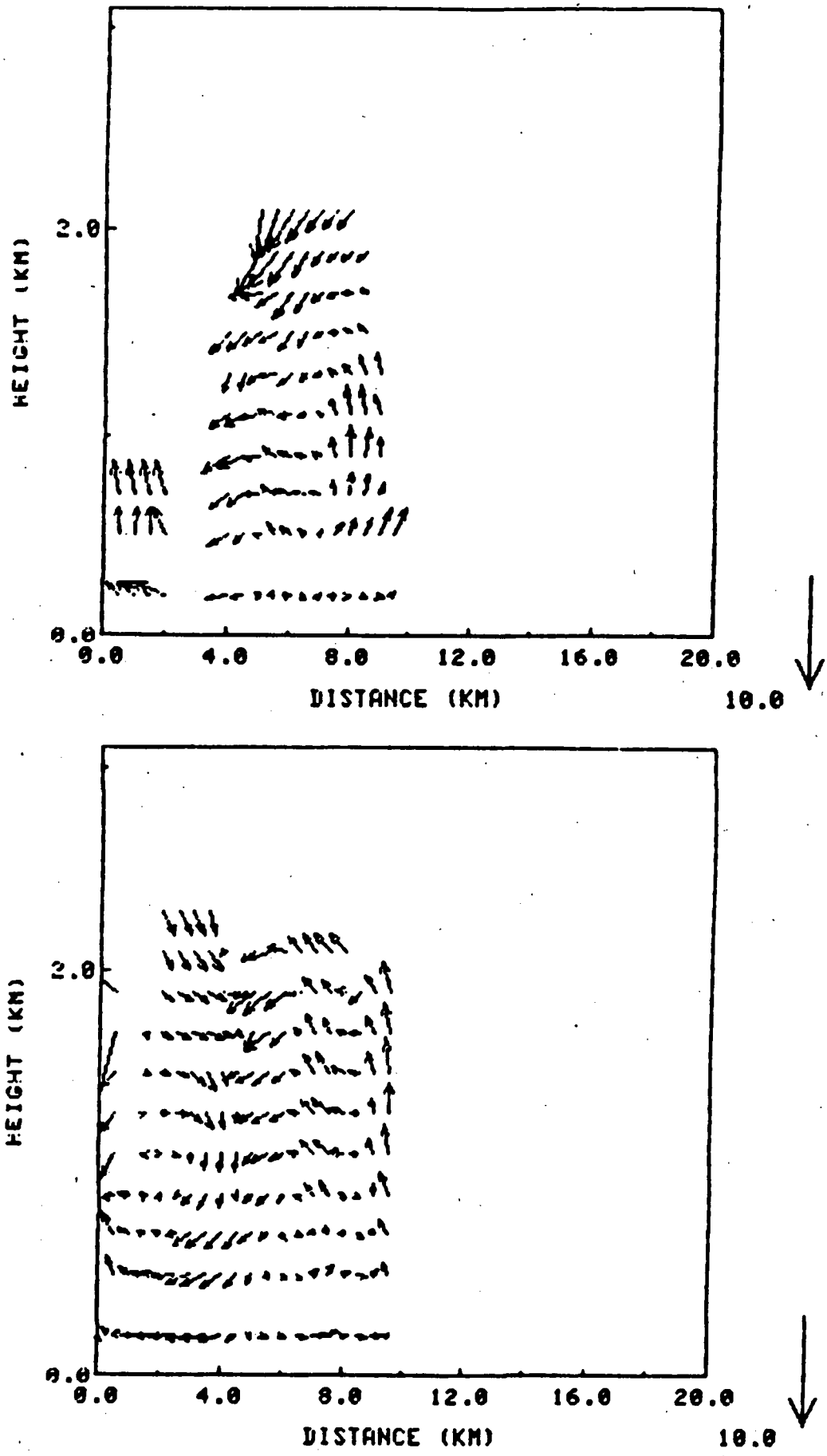

Fig. 7: Vertical cross section of vertical air velocity in the planetary boundary layer.

The quality of the results of the w calculations was somewhat of a surprise to the author given his experience and that of other researchers with the calculation of w in convective storms by multiple Doppler radar methods. In that case random errors of some m/s, and even systematic errors affecting the sign of calculated w do occur at variance with theoretical expectations of the possible magnitudes of the errors (Bohne and Srivastava, 1976; Lhermitte and Gilet, 1976; and Doviak et al, 1976). The author believes that the reason for the discrepancy is that the assumptions of the theoretical error analyses are not satisfied in the case of convective storms. In the present situation, the assumptions are apparently satisfied and, therefore, the errors are also within the theoretical limits. Point values of vertical air velocities are believed to be accurate to better than 1 m/s.

The main reasons for the discrepancy in the case of convective storms are: 1) errors in the boundary condition on w, and 2) high frequency variability of the storm. In convective storms rather large values of the horizontal divergence (or convergence) occur near the ground. (This is especially true of the more interesting regions.) Those divergence values remain unobserved by the radar because of earth curvature effects, or are in error because of ground clutter contamination. Therefore, a systematic offset occurs in the w obtained by integration of the continuity equation assuming w=0 at the ground. This is attributed in the literature, somewhat erroneously, as an error due to an error in the boundary condition on w. The implication is that w is non-zero at the level where the integration of w is started, namely, the lowest level at which horizontal divergence is available from the multiple Doppler analysis. The second source of error is due to the fact that convective storms change much faster than the time it takes to perform a volume scan (typically about 3 minutes). The discrepancy in the time of acquisition of radial velocity data from the different radars for any given 'point' then manifests itself as an error in the horizontal winds, thence in the horizontal divergence, and finally in the vertical air velocity. In the present case these sources of errors are minimal. Extreme values of divergence were probably not present near the ground; the lowest radar scans were at an elevation angle equal to a fraction of the radar beamwidth and, as we saw above, the wind conditions were changing rather slowly with respect to the volume scan time (about 90 seconds).

The random errors in the vertical air velocity were apparently not large. This was evidenced by the fact that regions of positive (or negative) w, and divergence of the horizontal wind as well, formed coherent patterns encompassing many grid points, in the horizontal and the vertical, rather than a checkerboard pattern that would have occurred if the random errors were large. A further test of the accuracy of the w calculation is shown in fig. 6c which is a plot of the mean w as a function of the height. These are mostly less than 1/4 th of a m/s, and are consistent from

level to level rather than changing sign from one level to the next. It is not known if any significane can be attached to the descending motions.

4.3 Turbulence Quantities

With the success of the horizontal velocity and w calculations, we took the next logical step of calculating 'turbulence' quantities, namely, 1) the kinetic energy in the fluctuations of u, v and w, and 2) the vertical momentum transfers by the fluctuations. As usual, we shall denote the fluctuations by primes; further we shall call them turbulent fluctuations. The fluctuations were obtained as the difference between the area averages and the grid point values.

Fig. 8 shows the height profiles of components of twice the turbulent kinetic energy per unit mass in the east, north, and vertical directions, that is, <u'u'>, <v'v'>, and <w'w'>, where <x> signifies the area average of x. First we note that the quantities are remarkably consistent from one time period to the next, and from one height level to the next. This gives us some confidence in the results. Recall that the data contributing to each grid point calculation are totally independent because of the manner in which the analysis was carried out. An implicit dependence does, however, exist in height, and to a lesser extent in the horizontal, due to radar pulse volume averaging effects but no dependence was introduced by the analysis procedures.

It is seen that the fluctuations are not isotropic in the sense that the contributions to the kinetic energy from the three directions are different. The magnitudes are reasonable in the sense that they are comparable to those measuremed by aircraft in similar physical situations.

Fig. 9 is a plot of vertical profiles of the turbulent 'momentum transfers', <u'w'> and <v'w'>. Worthy of note again is the consistency of the quantities in time and height and the fact that their magnitudes are similar to those found in comparable situations by more direct measurements. The sign of the turbulent momentum transfers is consistent with the vertical shears of the mean u and v (see figs. 6a and b) and the idea that horizontal momentum is approximately conserved in vertical displacements.

4.4 General Remarks

This is believed to be a first calculation of turbulence quantities in the boundary layer by multiple Doppler radar methods. The results are internally consistent and reasonable but unfortunately no independent confirmation has been obtained so far. As part of an ongoing study, a comparison is planned to be made with available aircraft measurements. If the comparison turns out to be good then this may be a proven technique for turbulence studies in the planetary boundary layer superior to methods utilizing

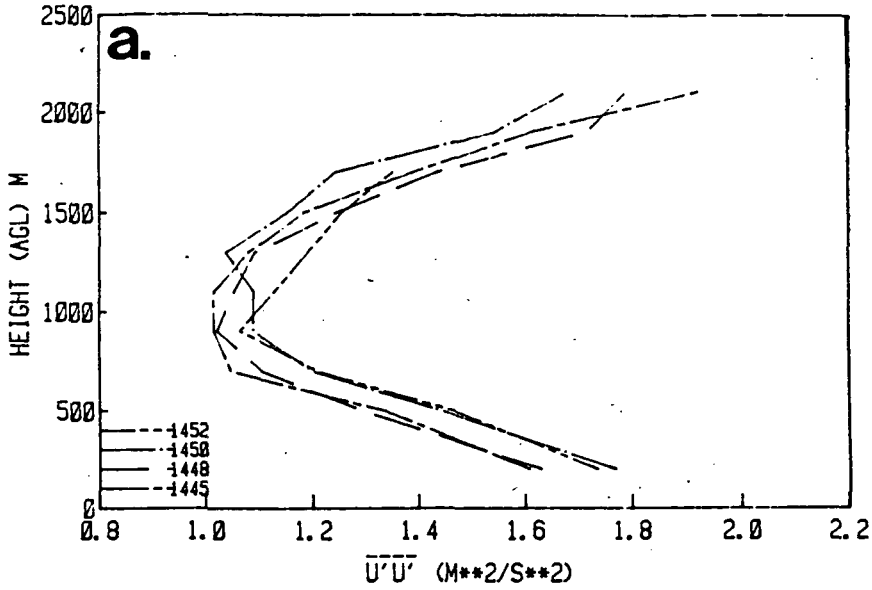

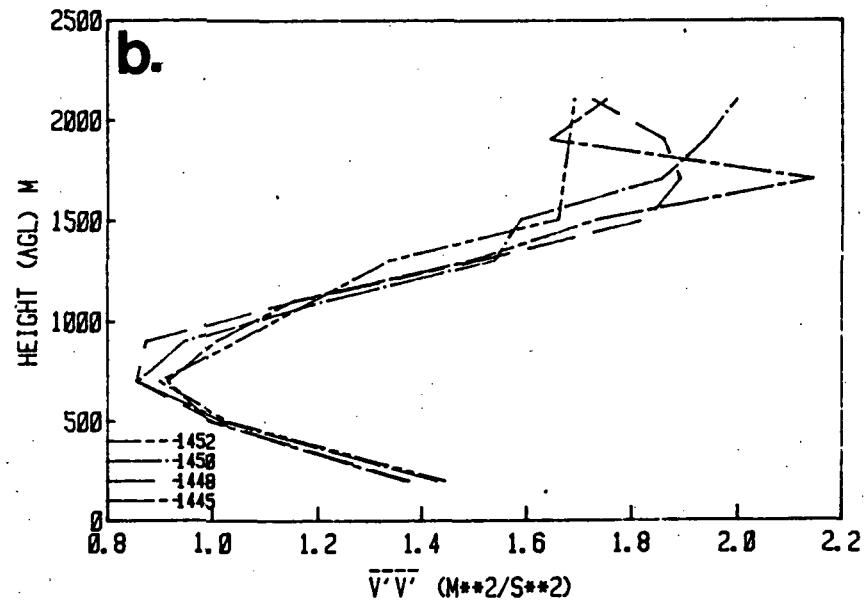

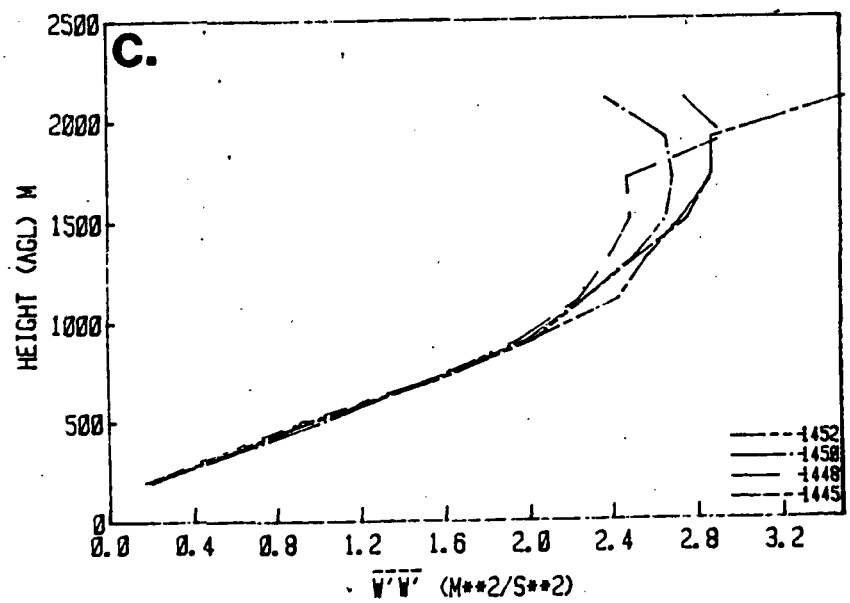

Fig. 8: Vertical profiles of the average squares of the fluctuations in the three components of the wind vector for the four time periods.

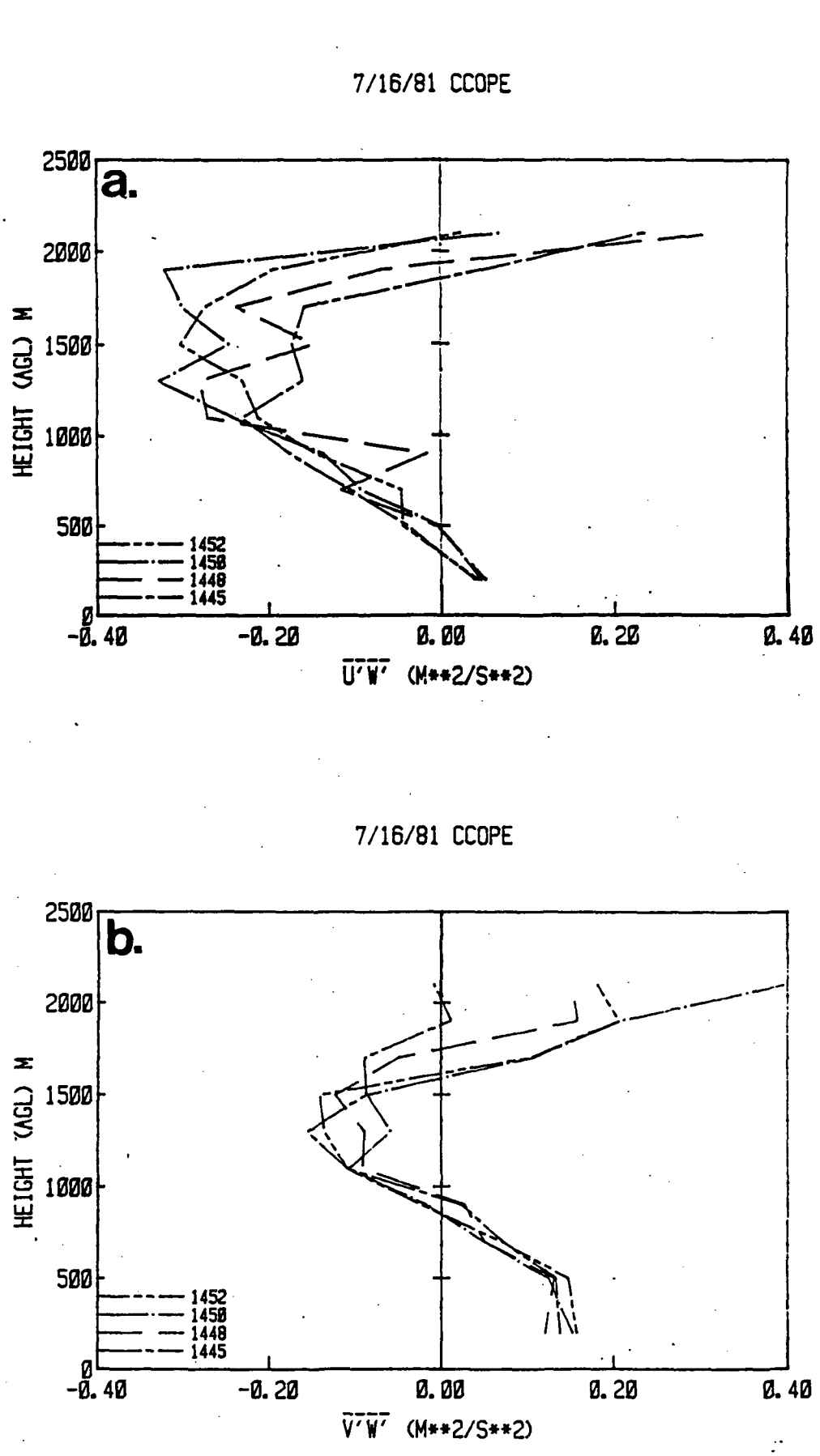

Fig. 9: Vertical profiles of the correlations between the fluctuations of the vertical component and the (a) east and (b) north components of the wind vector.

instrumented aircraft. This data may then also perhaps be a unique data set for turbulence studies. One additional study that could be done with this data set includes the inversion of the time sequence of wind fields to obtain fields of pressure perturbation and thermal buoyancy. If the comparison is not good, a resolution of the discrepancies will be called for. That should shed important light on multiple Doppler radar methods of wind measurement. Some differences are anticipated because of the effects of pulse-volume averaging. Differences can also arise as a result of incorrect spatial positioning of radial velocities with respect to each other. As was seen above, the winds sometimes changed significantly over one grid point, that is, over a distance of 500m. Therefore, one would want all the positioning information to be accurate to better than a small fraction of 500m. Technically this is possible, of course, but not always guaranteed because of numerous operations intervening between the radar echo return and the final product.

5. SUMMARY AND CONCLUDING REMARKS

On 16th July 1981, Doppler lidar and multiple Doppler radar data were obtained in a convectively mixed planetary boundary layer. The lidar measurements were possible due to scattering from existing aerosols; radar reflecting chaff was released in the atmosphere to make it visible to the multiple Doppler radar network. The data were analyzed to obtain detailed horizontal wind structures. The divergence of the horizontal wind was calculated and the anelastic continuity equation integrated to obtain vertical air motions. Differences between the areally averaged quantities and the grid point values provided a measure of the fluctuations in the wind components or the turbulent wind fluctuations. Vertical profiles of the mean winds and quantities related to the turbulent kinetic energy components, namely, $\langle u'u' \rangle$, $\langle v'v' \rangle$, and $\langle w'w' \rangle$, and the turbulent momentum transfers, namely, $\langle u'w' \rangle$ and $\langle v'w' \rangle$, were also calculated. All the results are internally consistent and this data set is potentially perhaps a unique source for the study of winds and turbulence in the convectively mixed boundary layer.

6. REFERENCES

Bohne, A. R., and R. C. Srivastava, 1976: Random errors in wind and precipitation fall speed measurement by a triple Doppler radar sysytem. **Preprints, 17th Conference on Radar Meteorology,** October 26-29, 1976, Seattle, Washington. Published by the American Meteorological Society. pp. 7-14.

Doviak, R. J., P. S. Ray, R. G. Strauch and L. J. Miller, 1976: Error estimation in wind fields derived from dual-Dopler radar measurement. J. App. Meteor., 15, 868-878.

Lhermitte, R. M., and M. Gilet, 1976: Acquisition and processing of tri-Doppler radar data. **Preprints, 17th Conference on Radar Meteorology**, October 26-29, 1976, Seattle, Washington. Published by the American Meterological Society. pp. 1-6.

APPENDIX

HORIZONTAL WIND VECTORS ON 15 CONSTANT HEIGHT SURFACES FOR 1445, 1450 AND 1452 MDT.

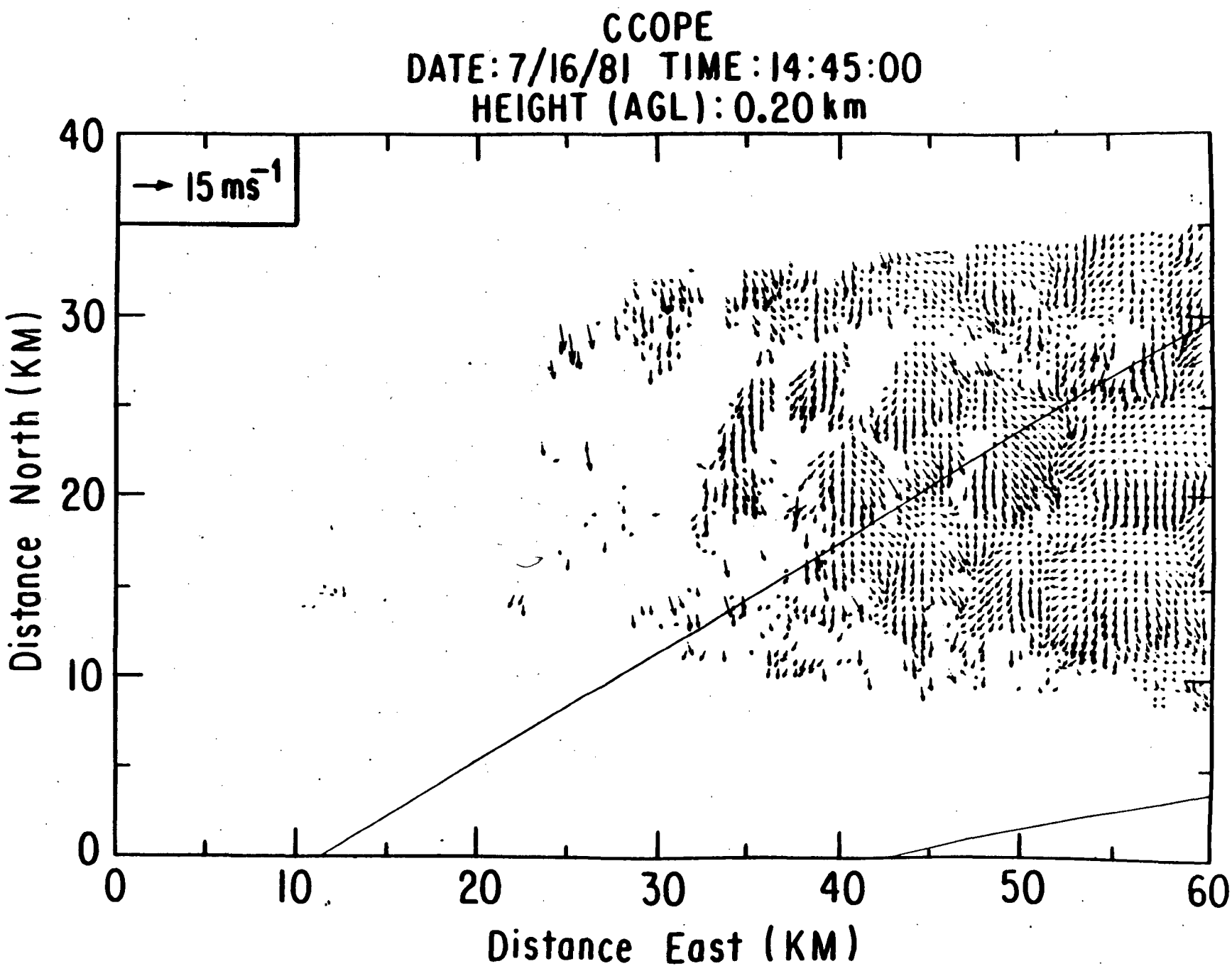
CCOPE
DATE: 7/16/81 TIME: 14:45:00
HEIGHT (AGL): 0.20 km
→ 15 ms⁻¹
Distance North (KM)
Distance East (KM)
0
10
20
30
40
50
60

A2

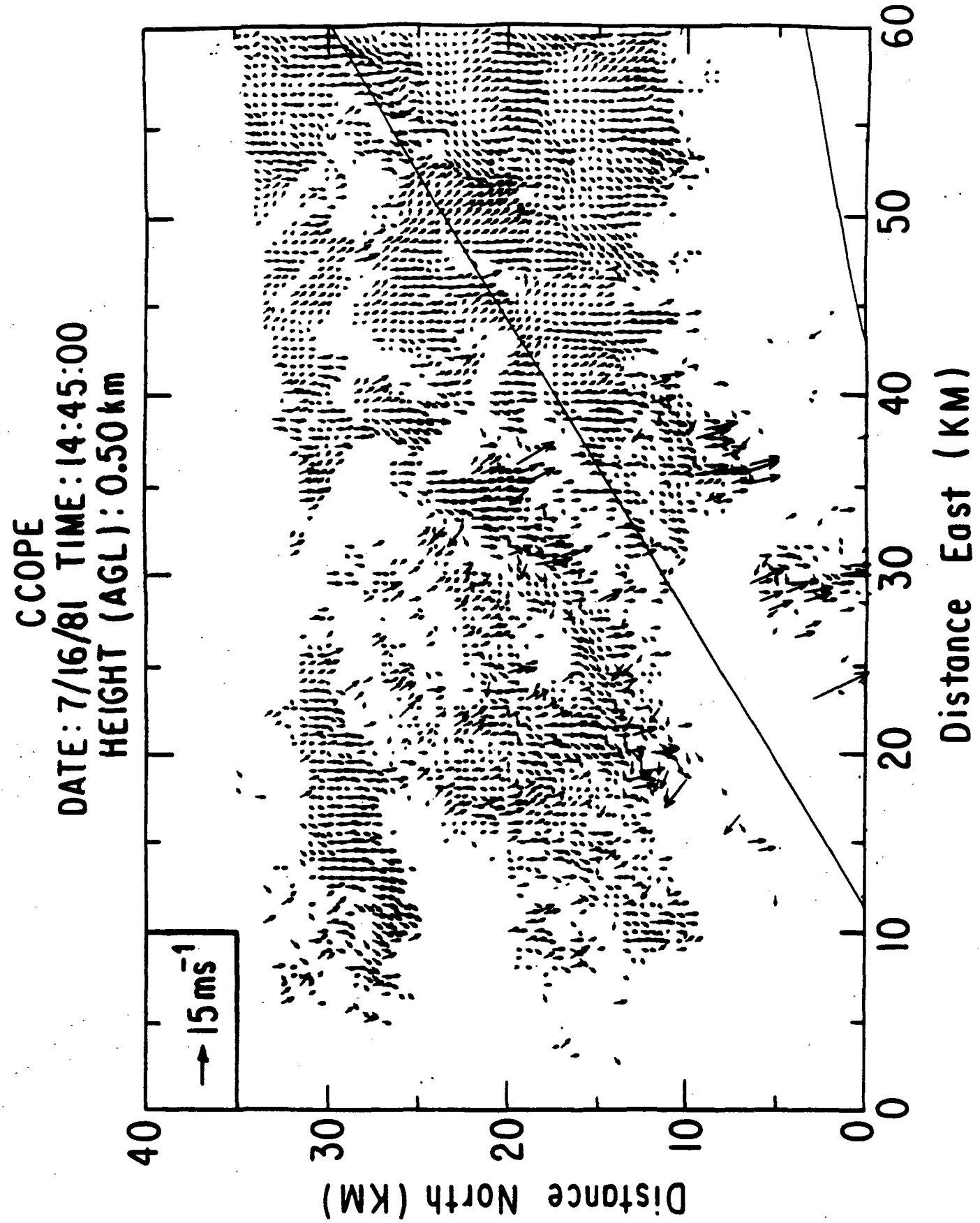
CCOPE
DATE: 7/16/81 TIME: 14:45:00
HEIGHT (AGL): 0.50 km
15 ms⁻¹
Distance East (KM)
Distance North (KM)
0
10
20
30
40
50
60

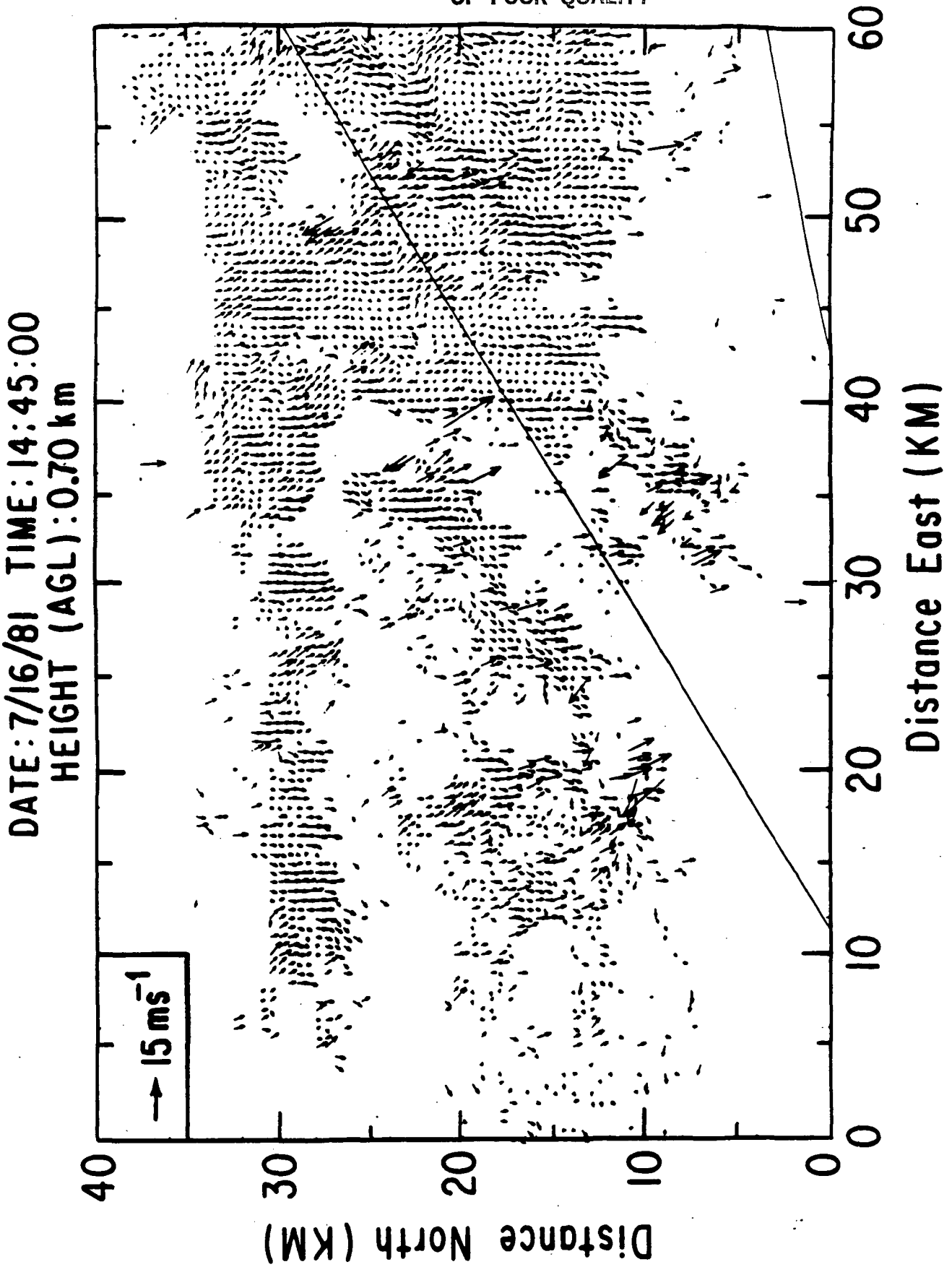

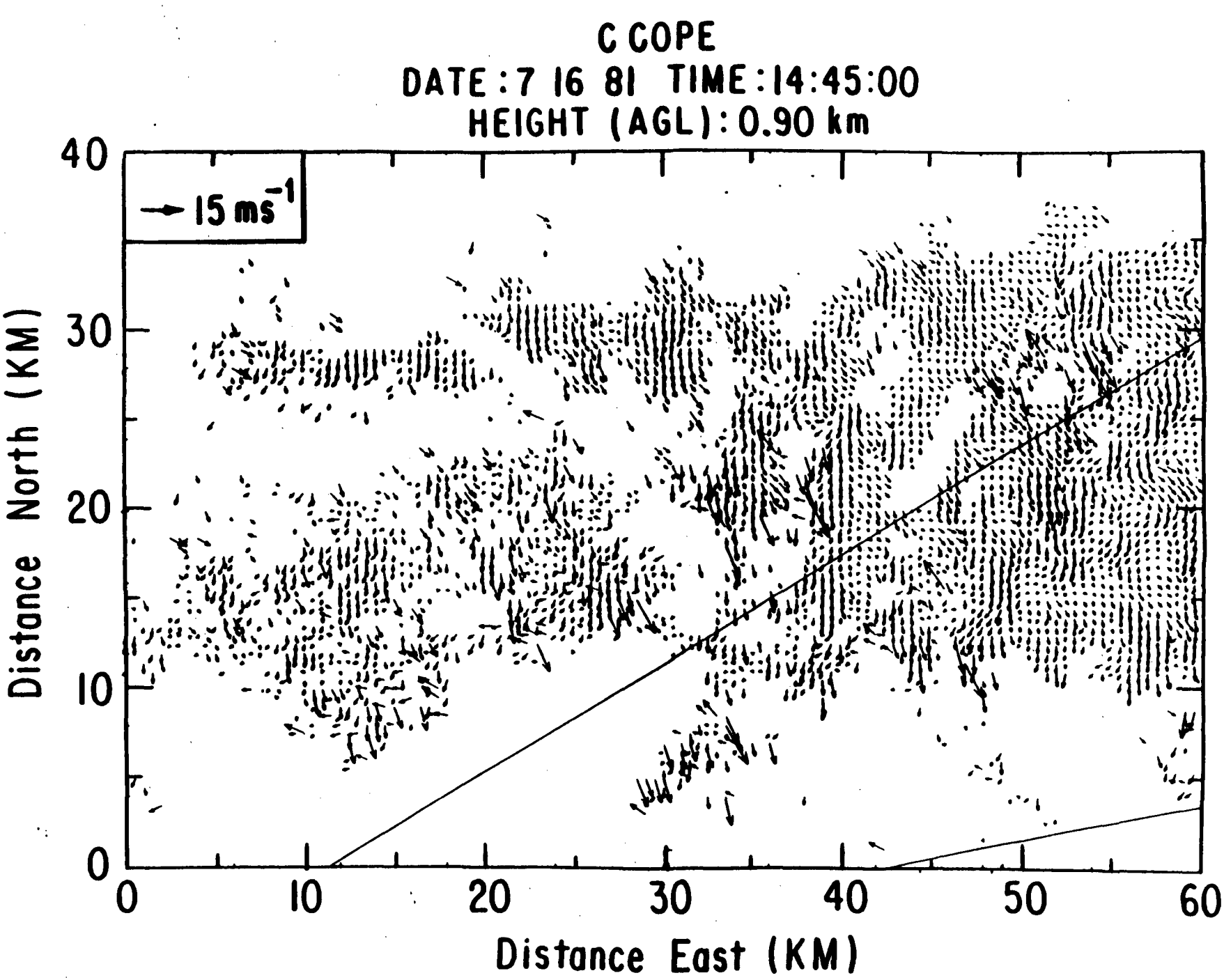
C COPE
DATE : 7 16 81 TIME : 14:45:00
HEIGHT (AGL) : 0.90 km
15 ms⁻¹
Distance North (KM)
Distance East (KM)
0
10
20
30
40
50
60

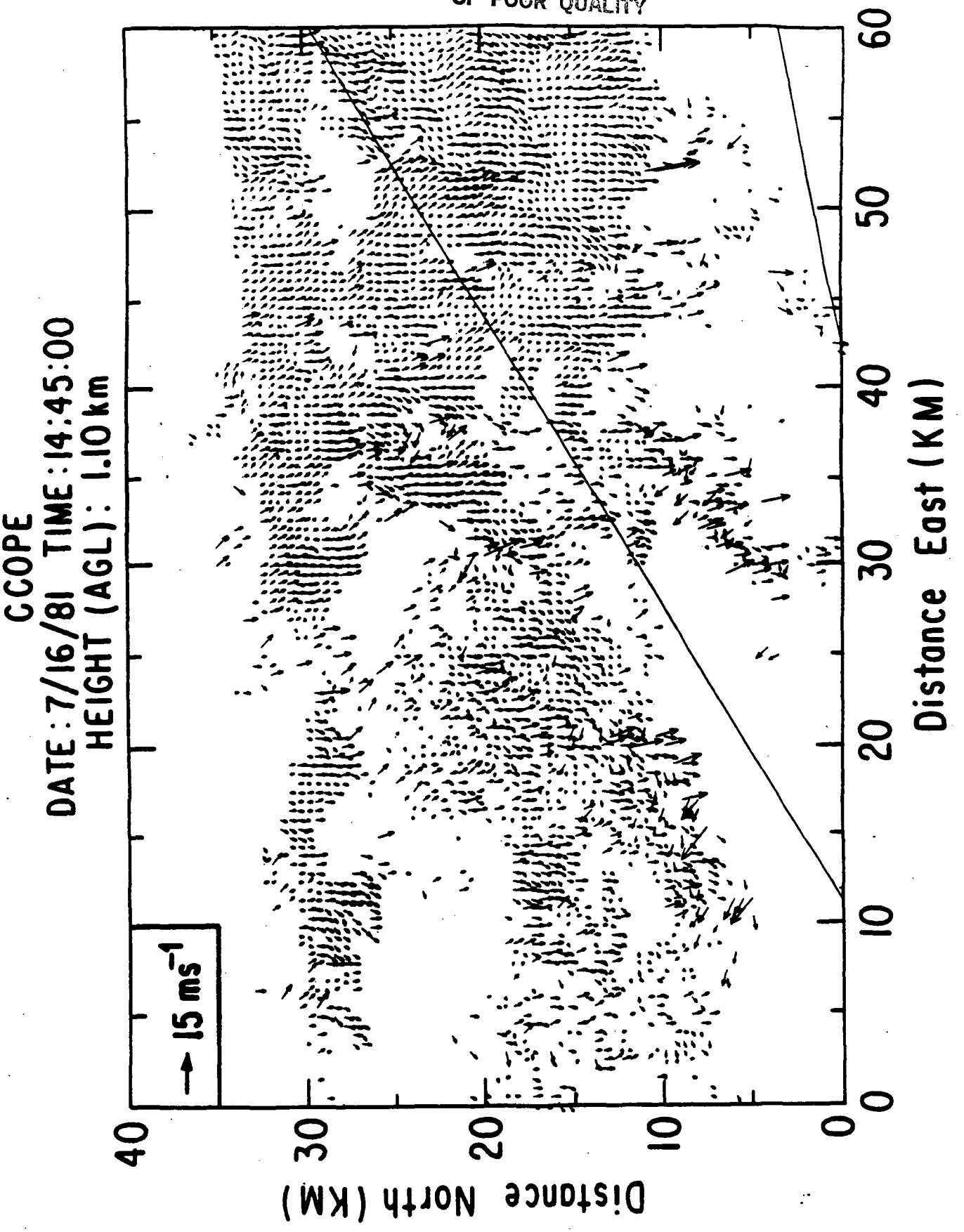

A6

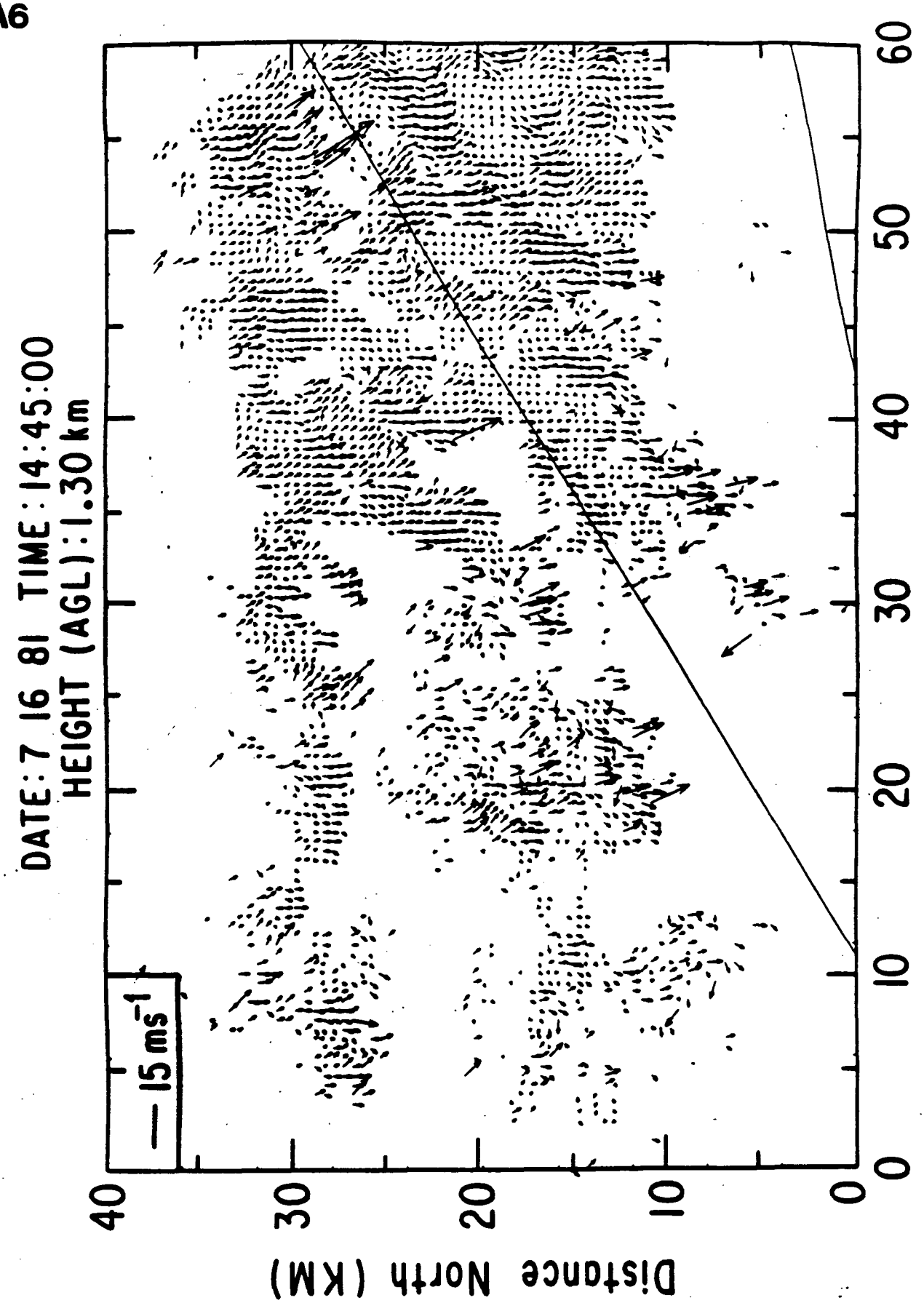
DATE: 7 16 81 TIME: 14:45:00
HEIGHT (AGL): 1.30 km
— 15 ms⁻¹
Distance East (KM)
Distance North (KM)
0
10
20
30
40
50
60

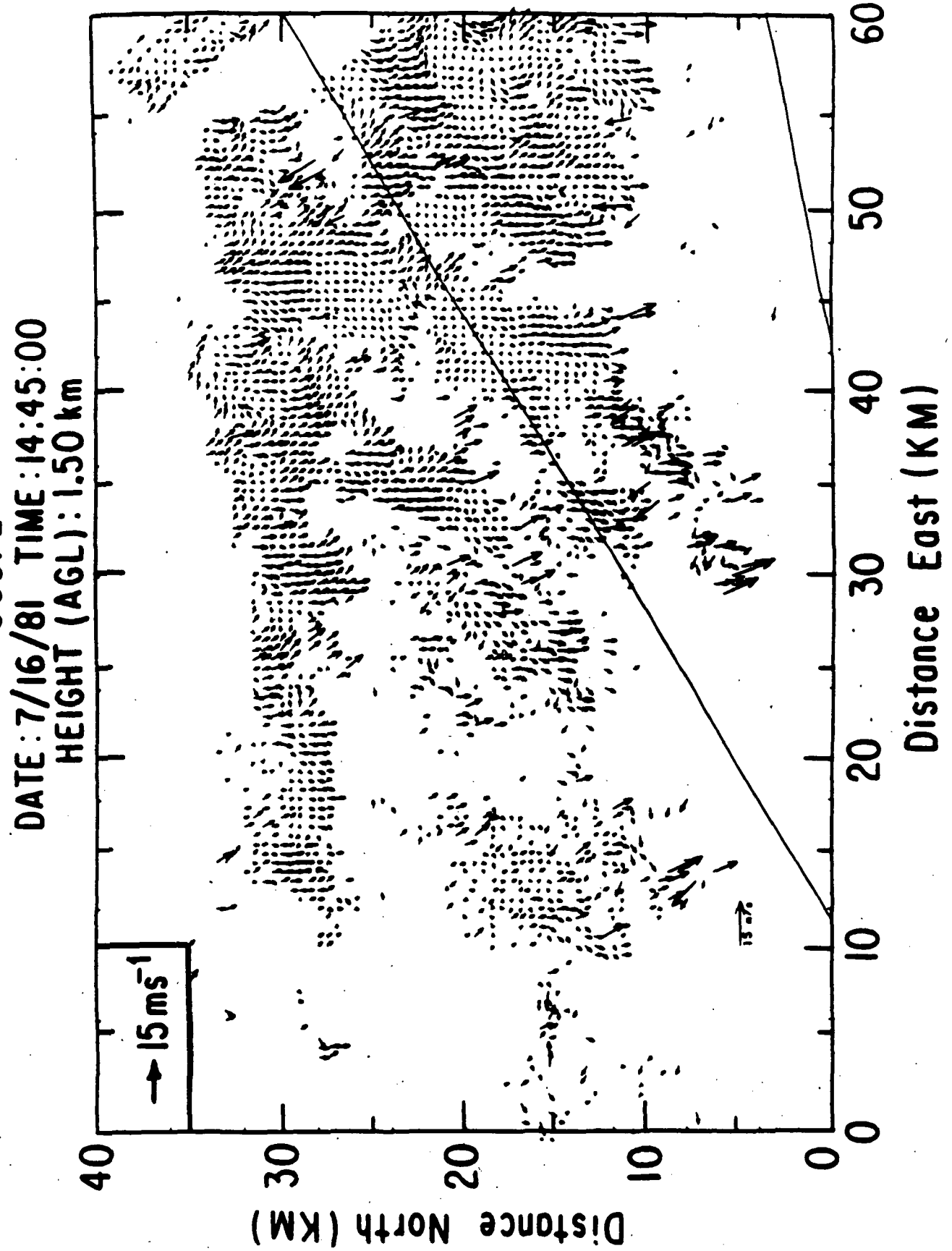

A8

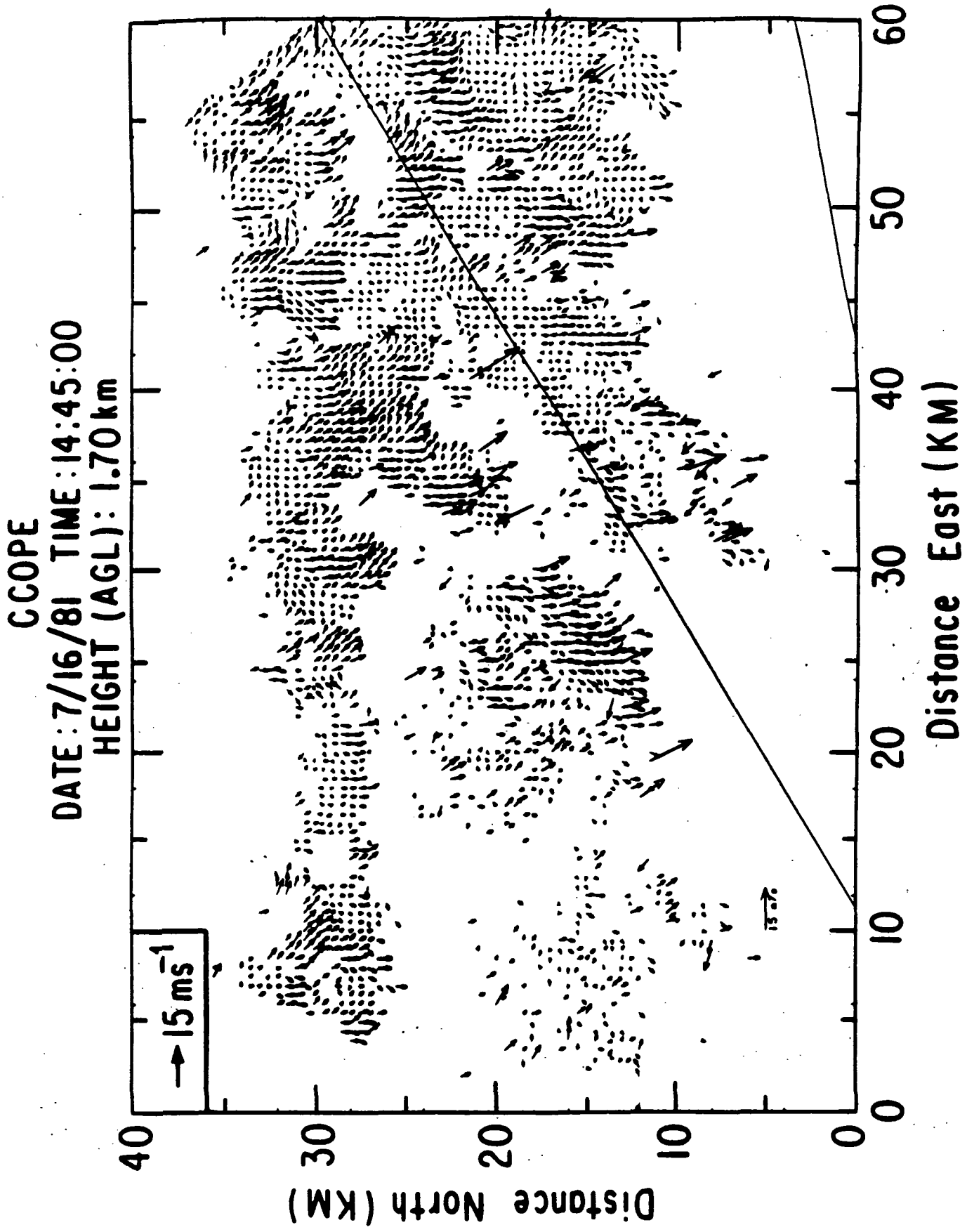
CCOPE
DATE: 7/16/81 TIME: 14:45:00
HEIGHT (AGL): 1.70 km
15 ms⁻¹
Distance East (KM)
Distance North (KM)
0
10
20
30
40
50
60

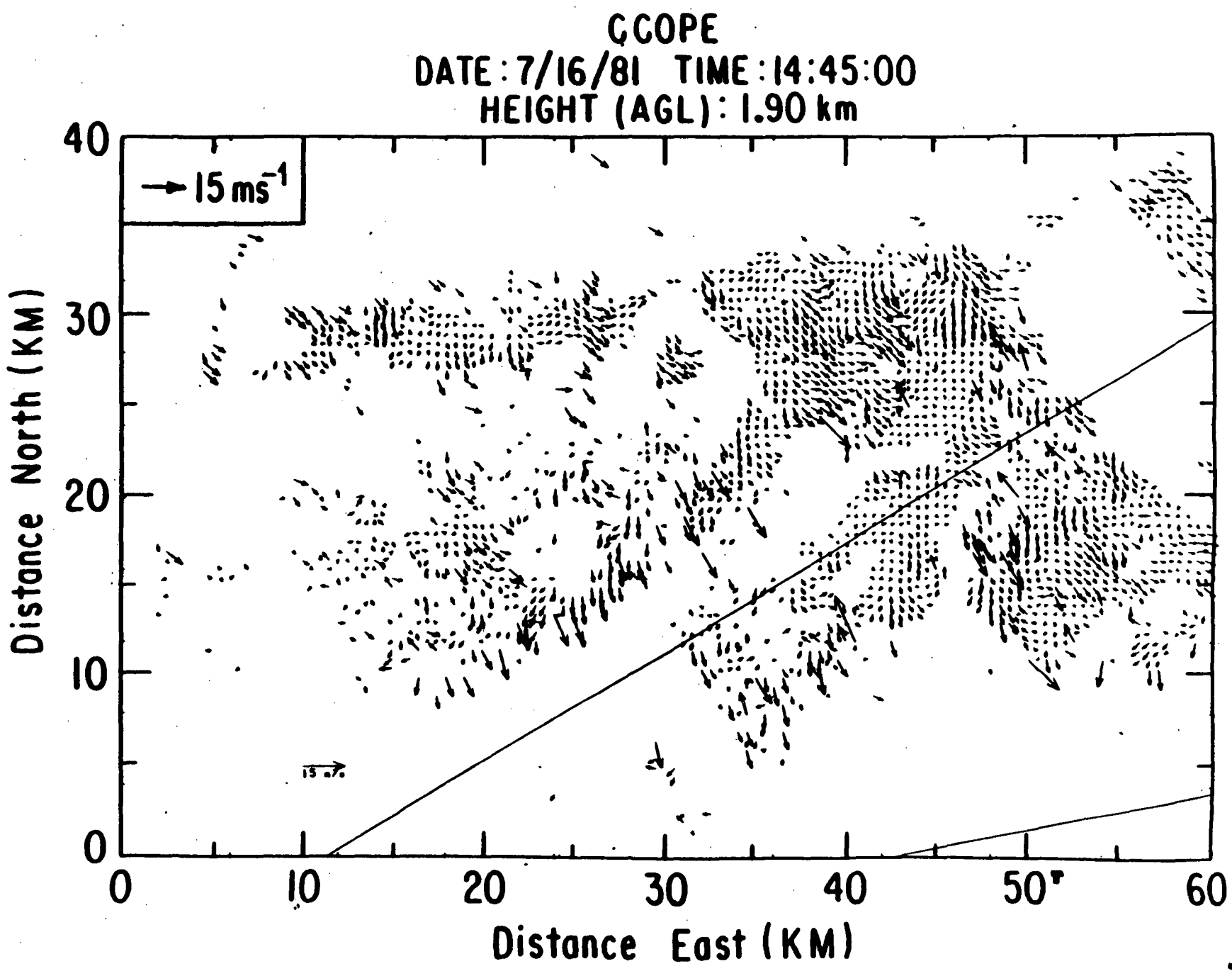
CCOPE
DATE: 7/16/81 TIME: 14:45:00
HEIGHT (AGL): 1.90 km
15 ms⁻¹
Distance North (KM)
Distance East (KM)
0
10
20
30
40
50
60

A10

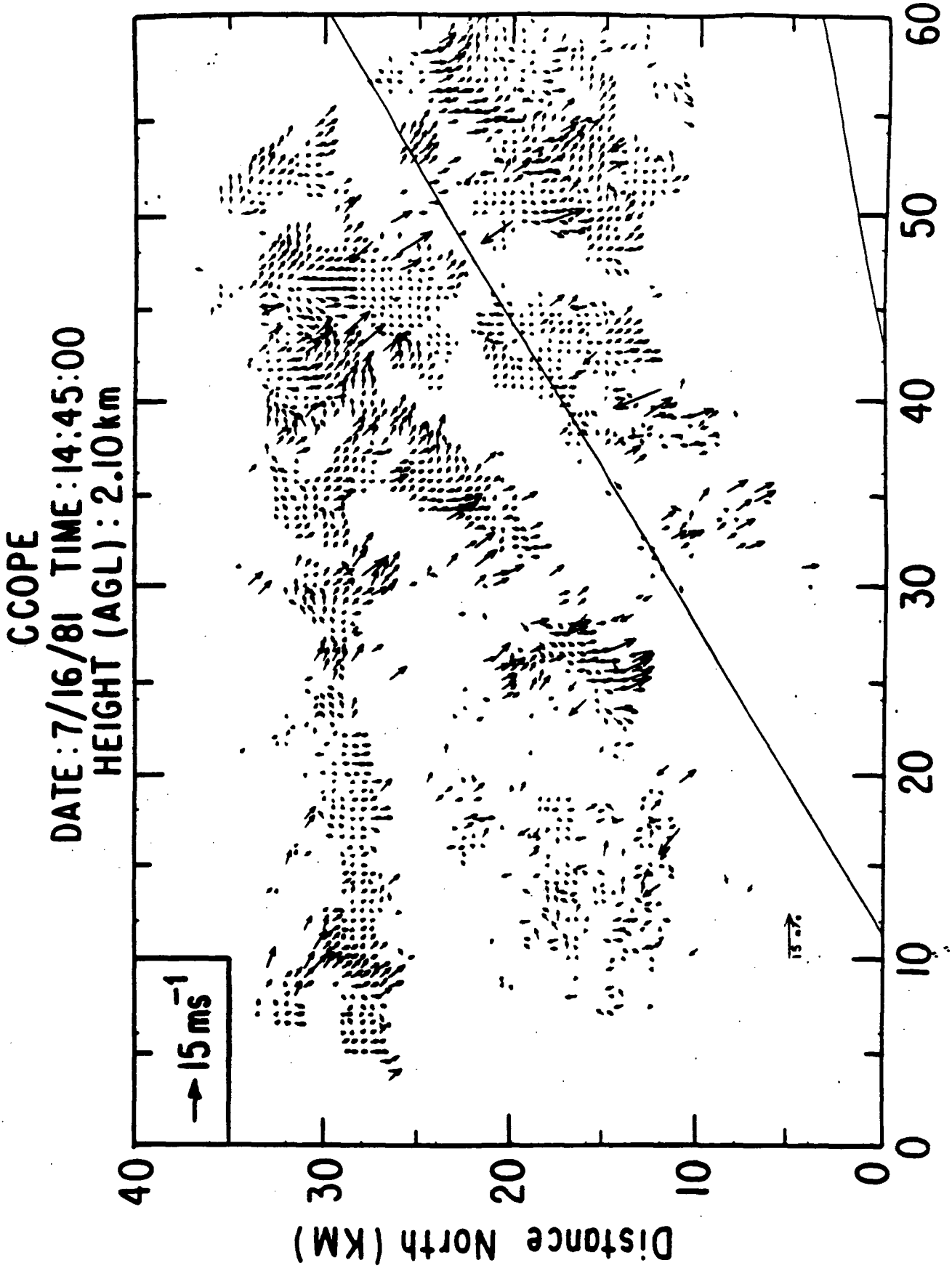
CCOPE
DATE: 7/16/81 TIME: 14:45:00
HEIGHT (AGL): 2.10km
15 ms⁻¹
Distance East (KM)
Distance North (KM)
0
10
20
30
40
50
60

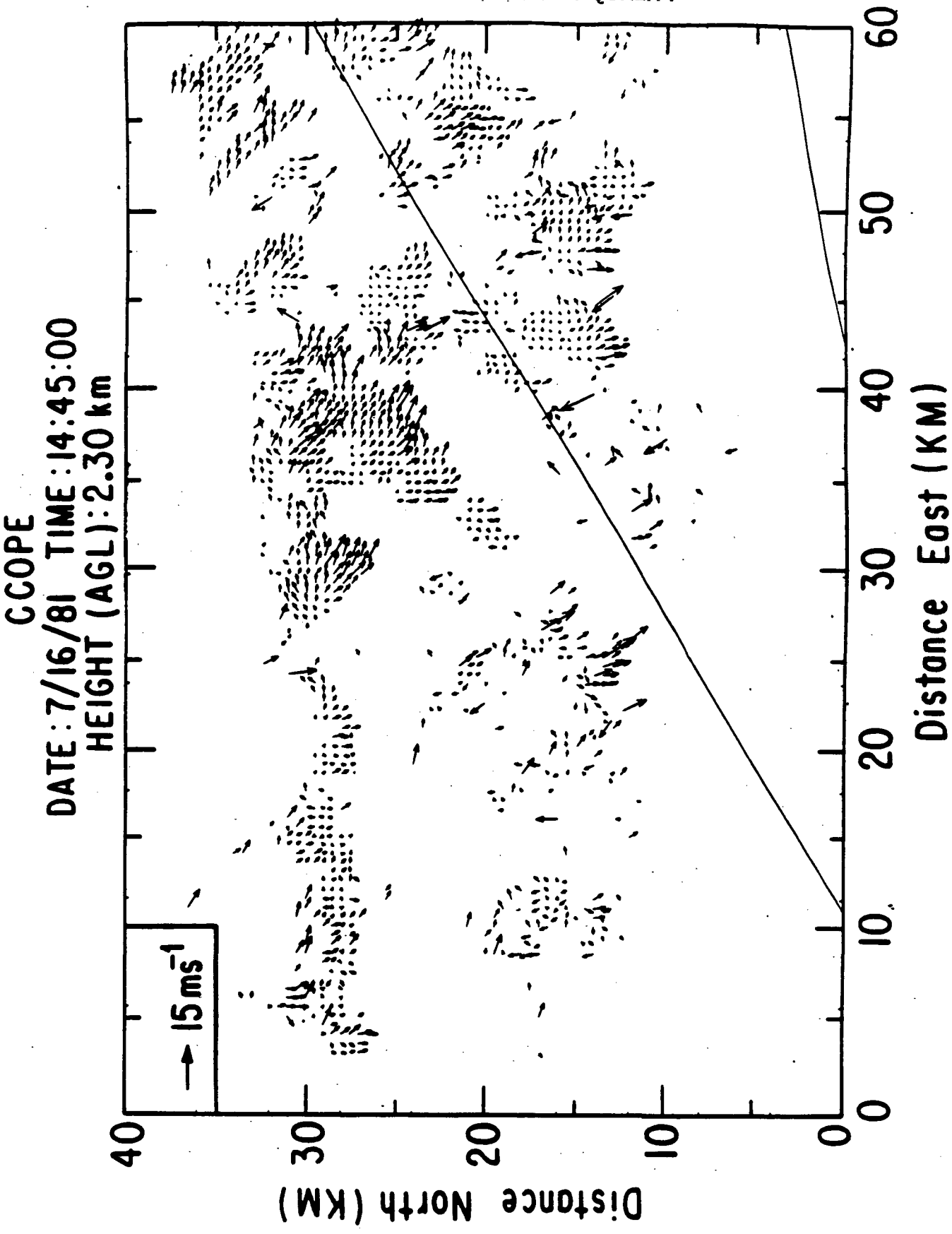

A12

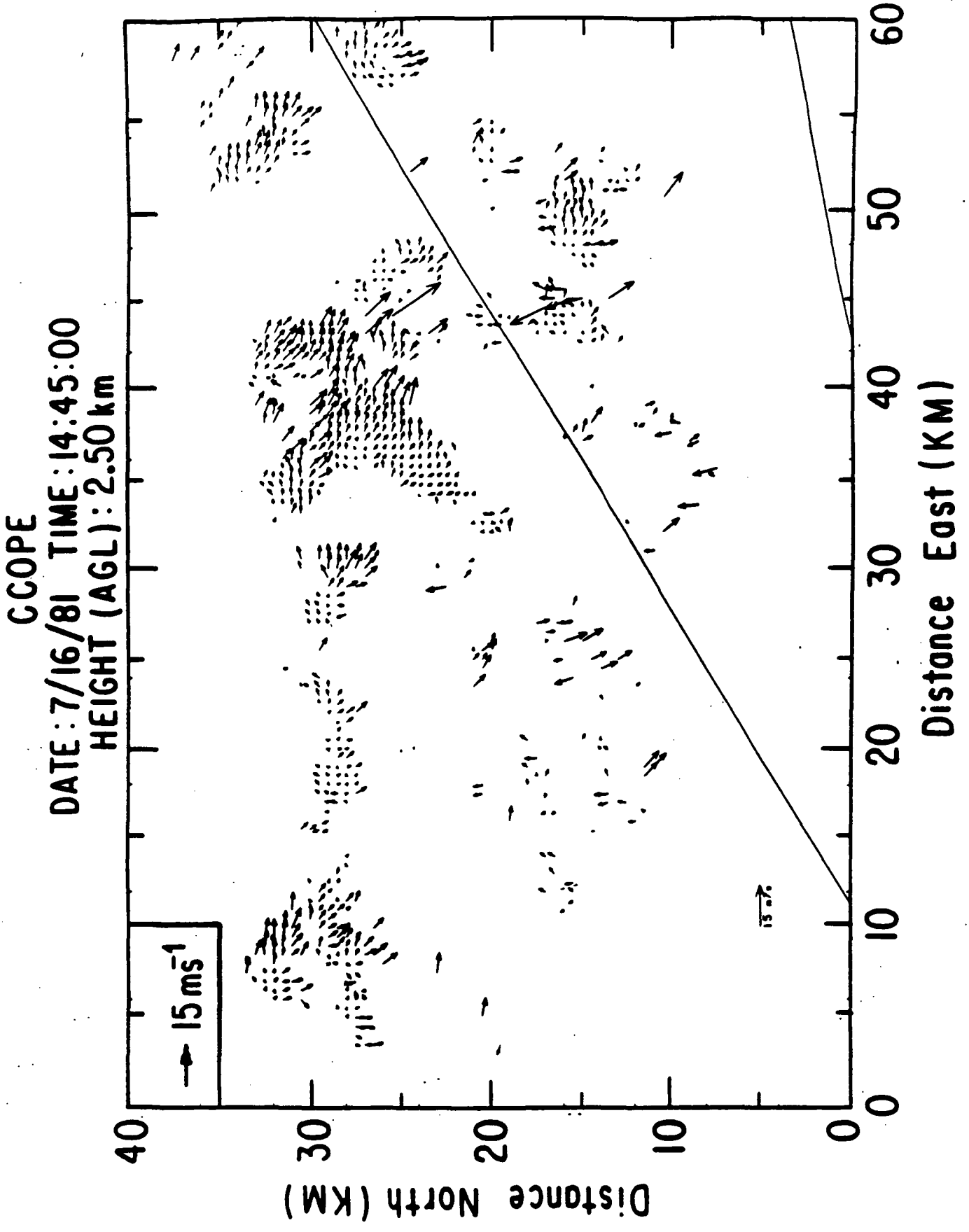
CCOPE
DATE: 7/16/81 TIME: 14:45:00
HEIGHT (AGL): 2.50 km
15 ms⁻¹
Distance East (KM)
Distance North (KM)
0
10
20
30
40
50
60

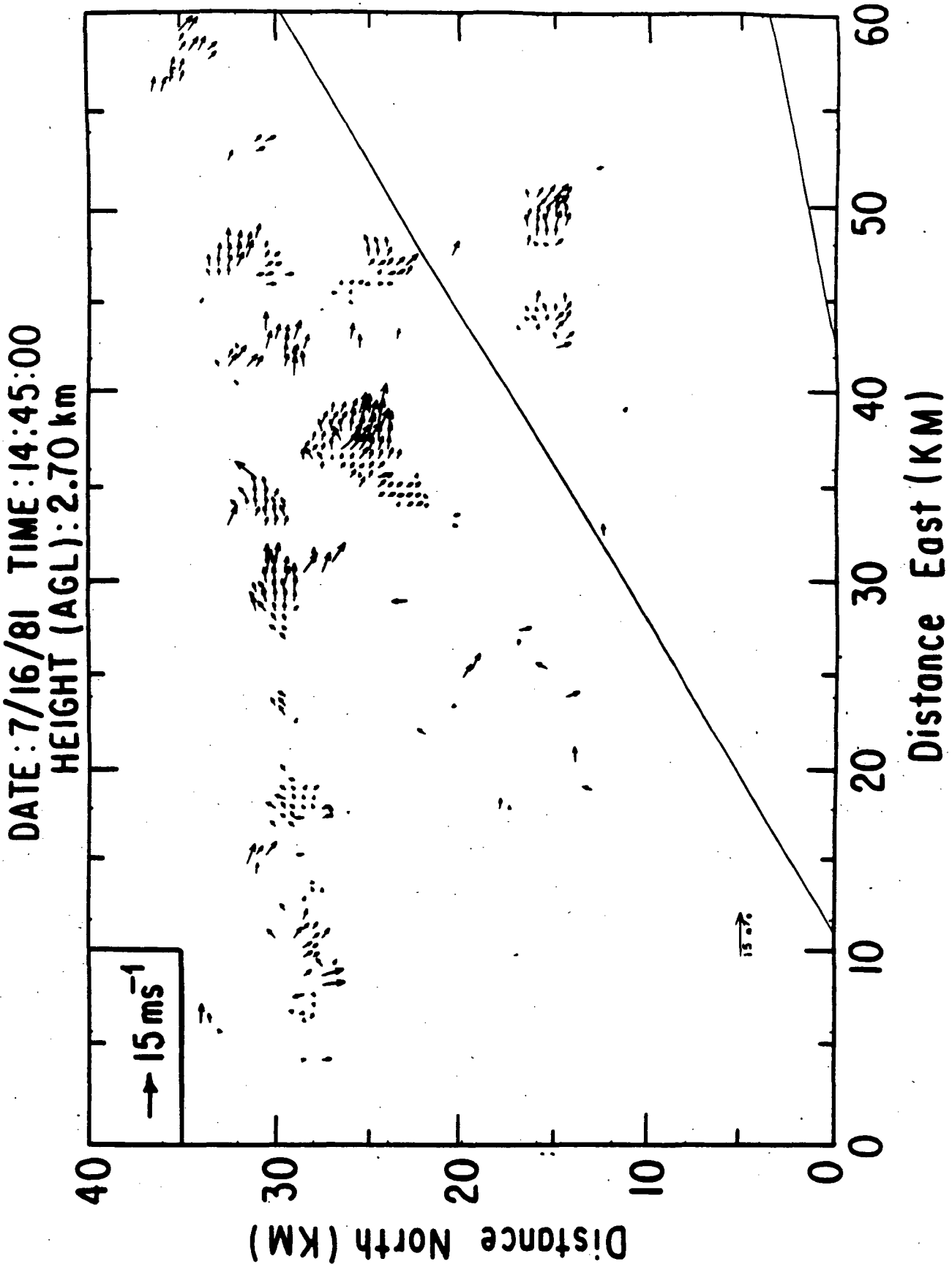

A14

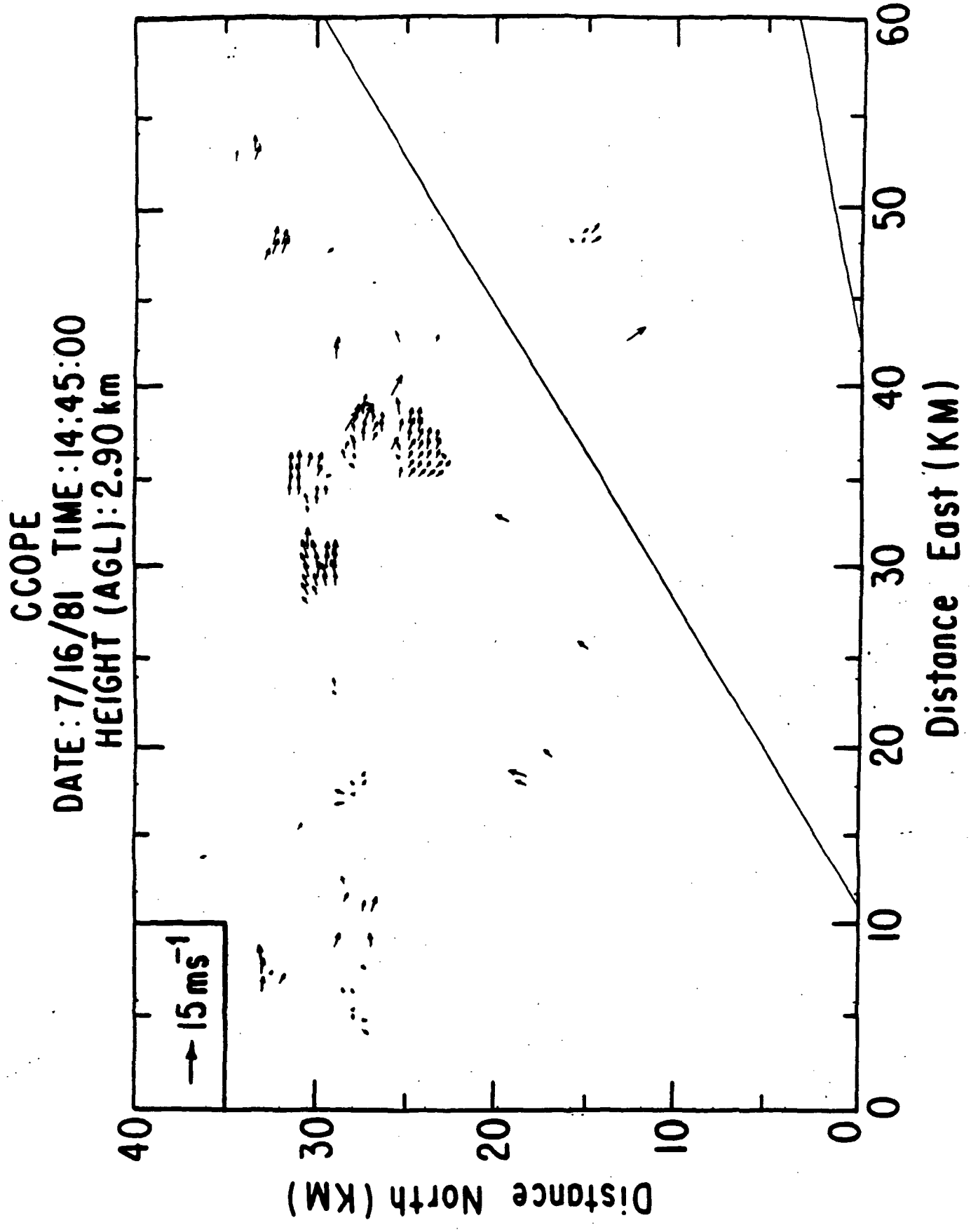
CCOPE
DATE: 7/16/81 TIME: 14:45:00
HEIGHT (AGL): 2.90 km
15 ms⁻¹
Distance East (KM)
Distance North (KM)
0
10
20
30
40
50
60

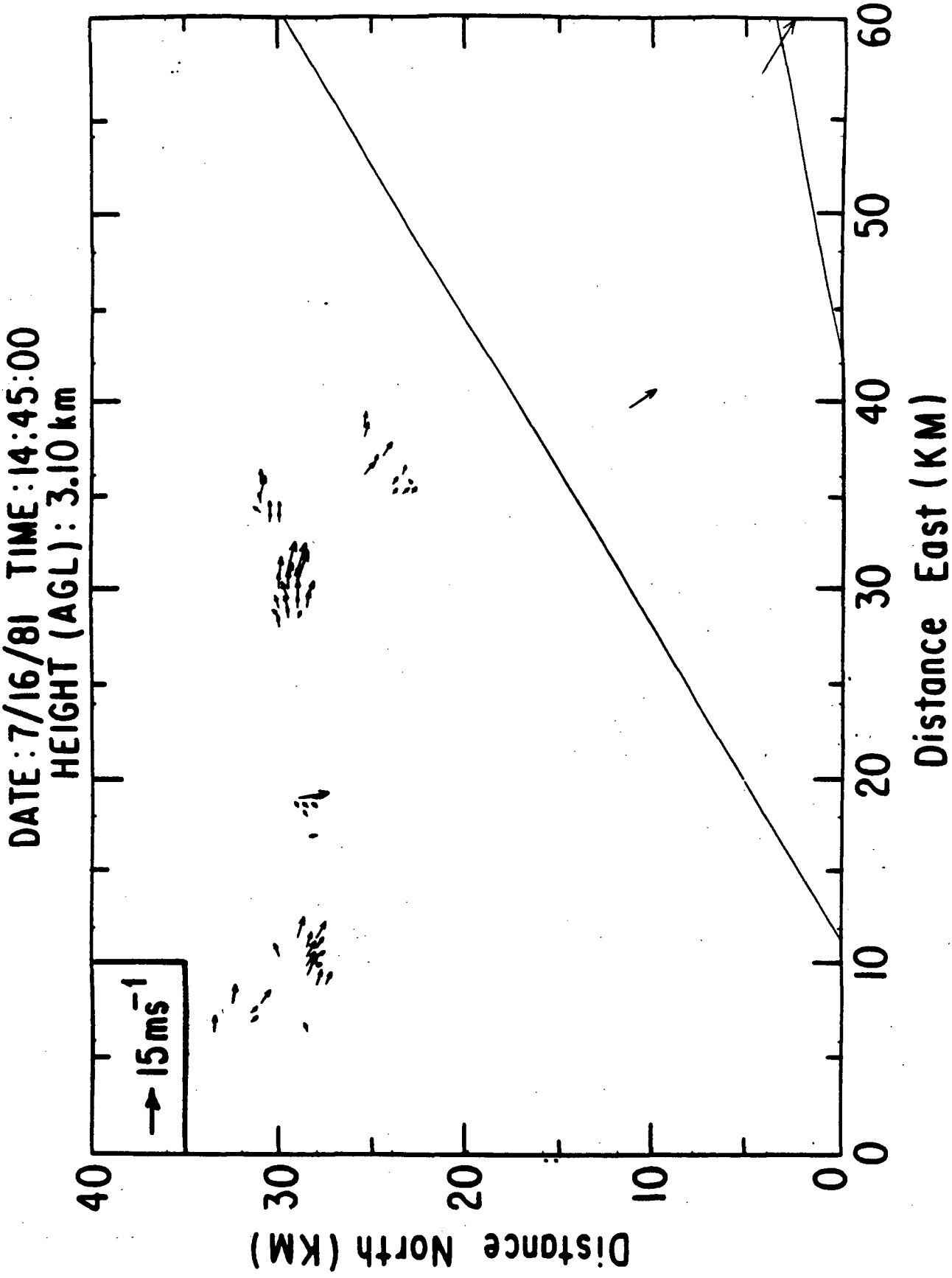
CCOPE
DATE: 7/16/81 TIME: 14:45:00
HEIGHT (AGL): 3.10 km
15 ms⁻¹
Distance North (KM)
Distance East (KM)
0
10
20
30
40
50
60

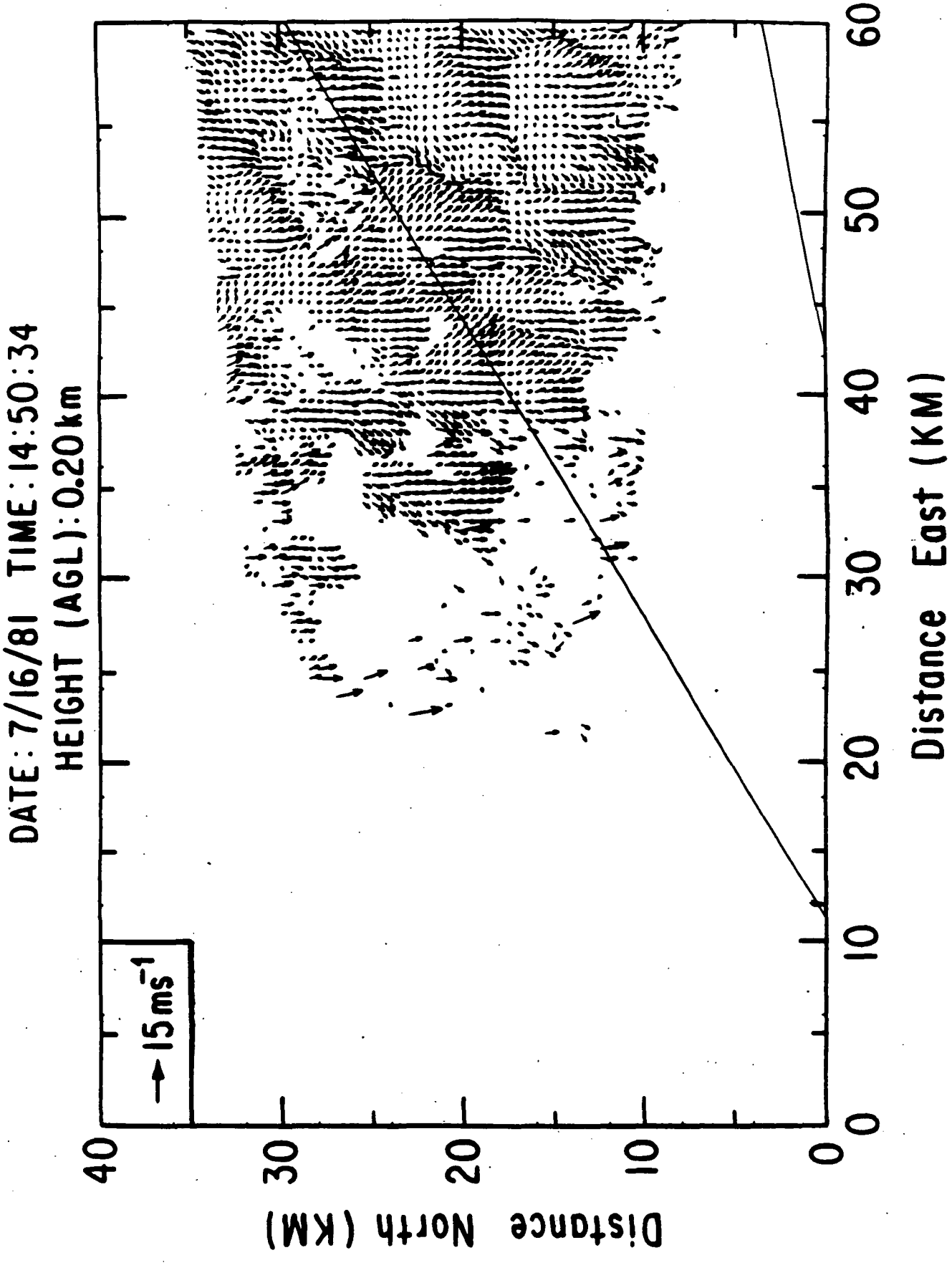

A17

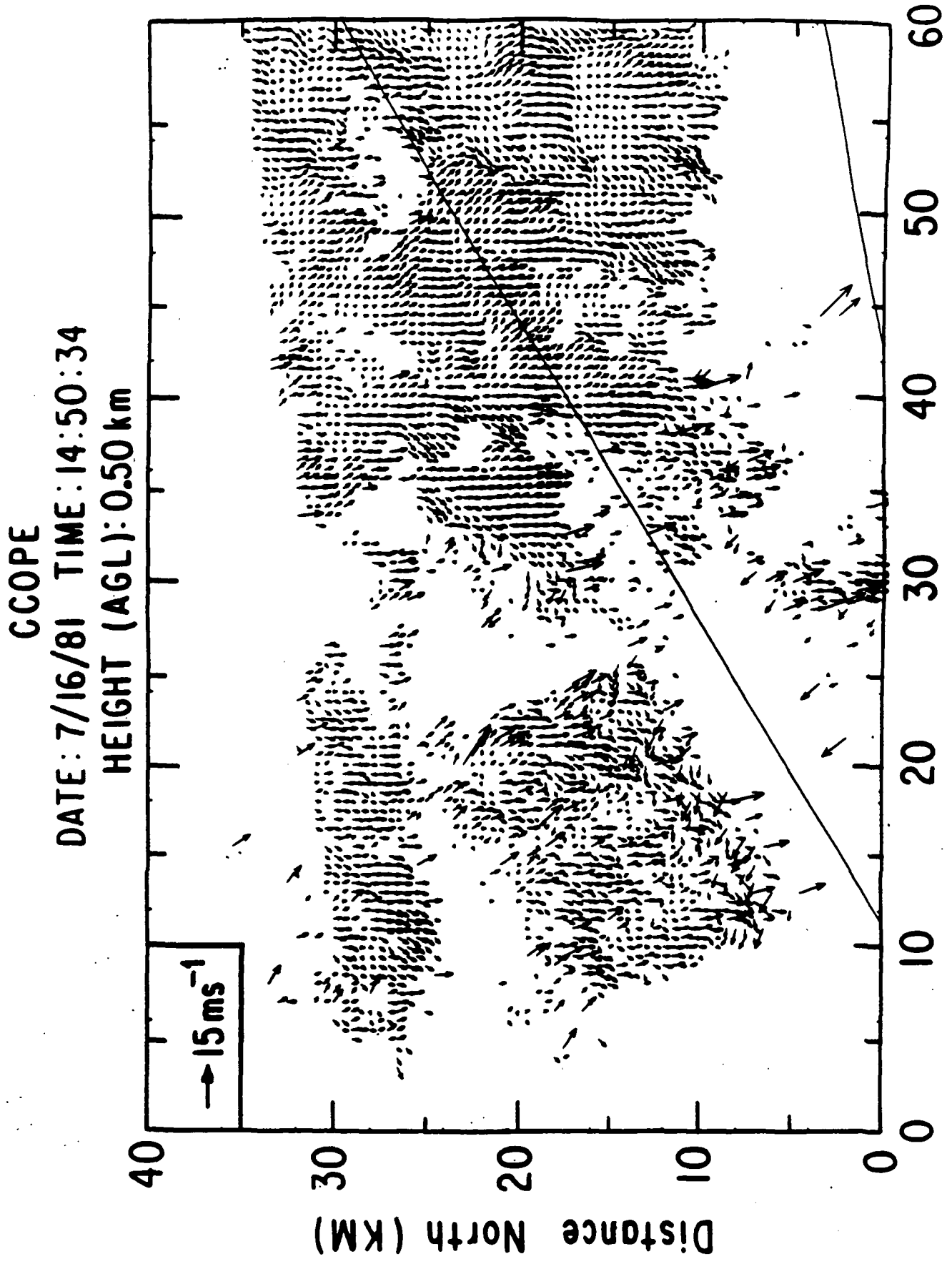
CCOPE
DATE: 7/16/81 TIME: 14:50:34
HEIGHT (AGL): 0.50 km
15 ms⁻¹
Distance East (KM)
Distance North (KM)
0
10
20
30
40
50
60

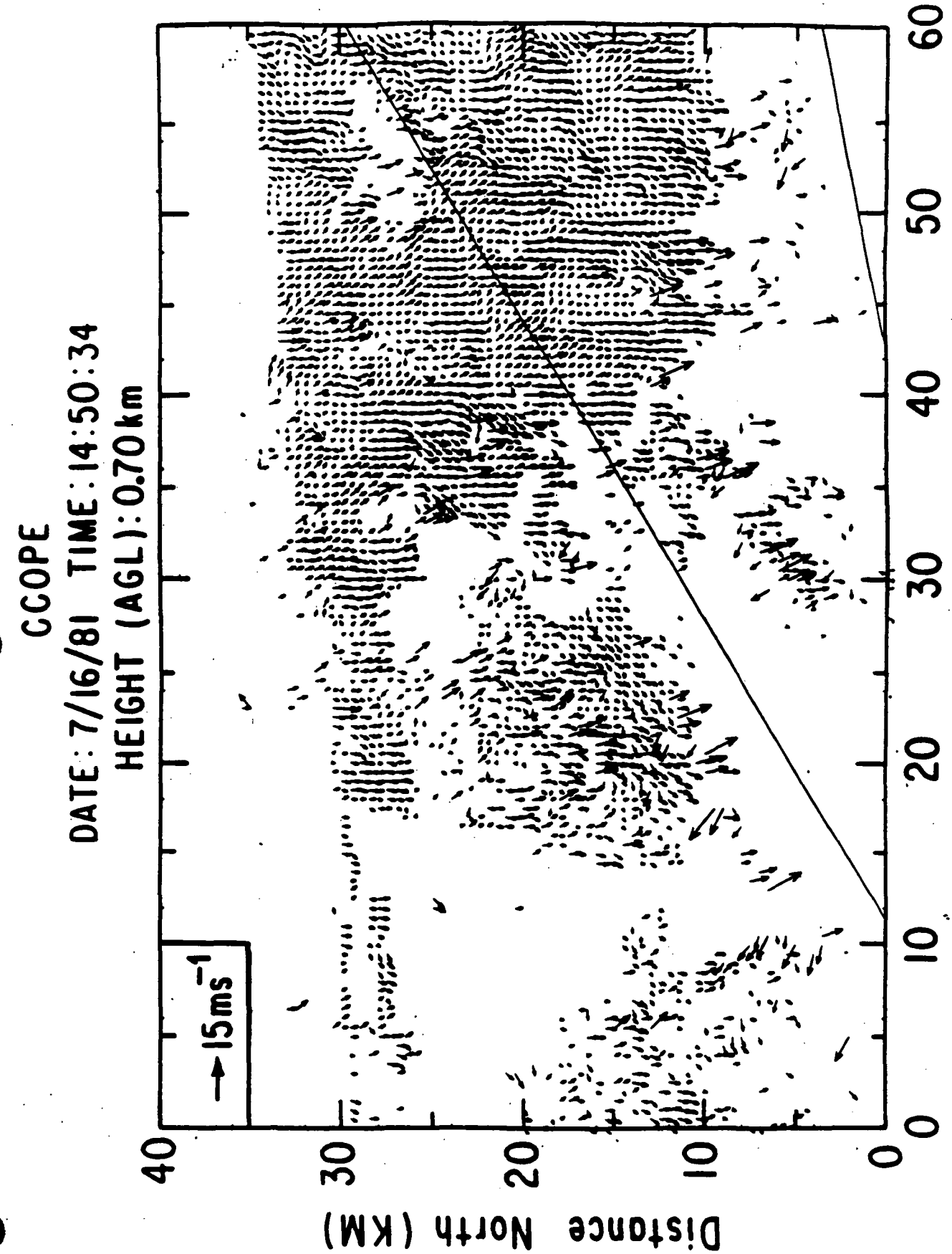
CCOPE
DATE: 7/16/81 TIME: 14:50:34
HEIGHT (AGL): 0.70 km
15ms⁻¹
Distance East (KM)
Distance North (KM)
0
10
20
30
40
50
60

A19

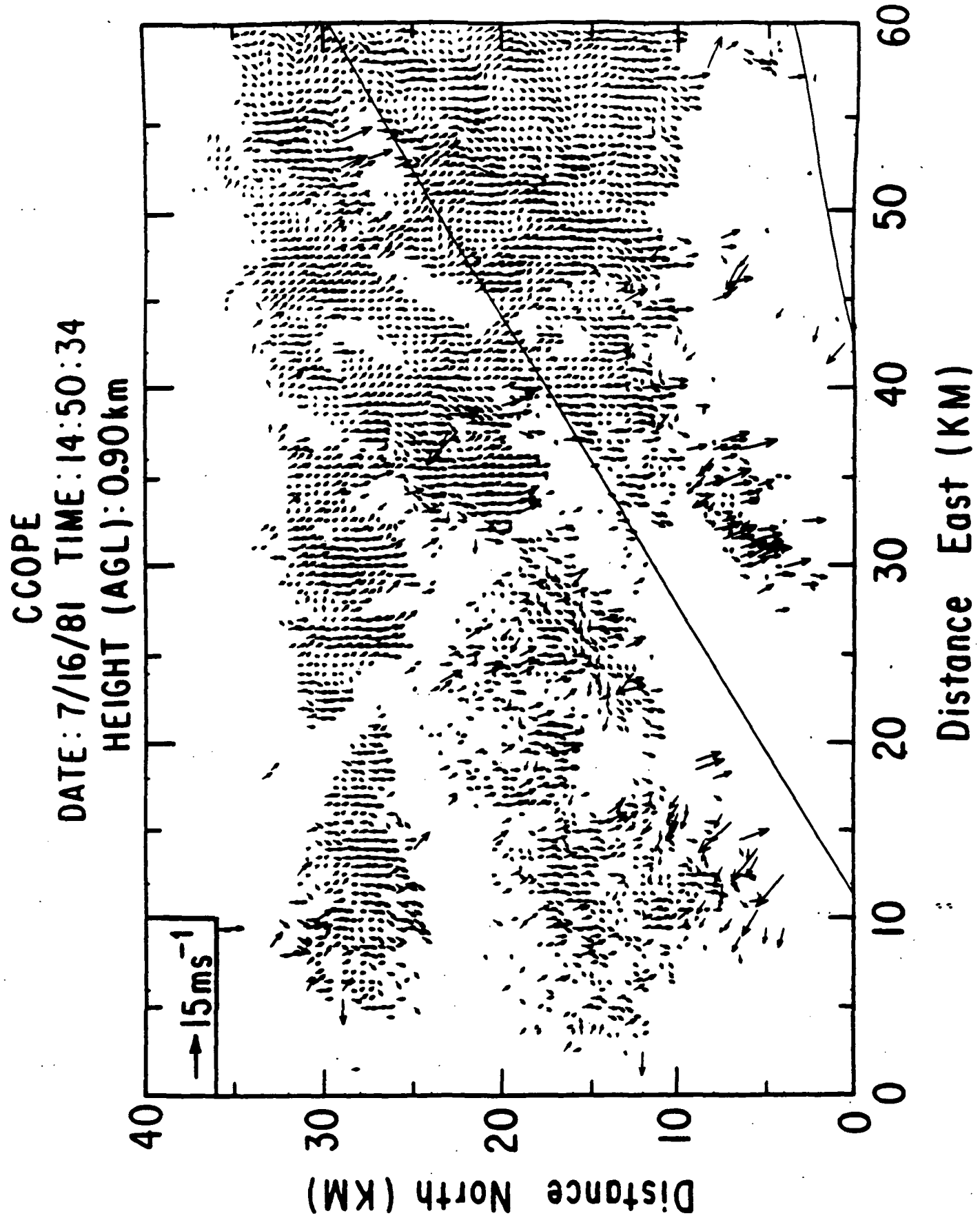
CCOPE
DATE: 7/16/81 TIME: 14:50:34
HEIGHT (AGL): 0.90km
15ms⁻¹
Distance East (KM)
Distance North (KM)
0
10
20
30
40
50
60

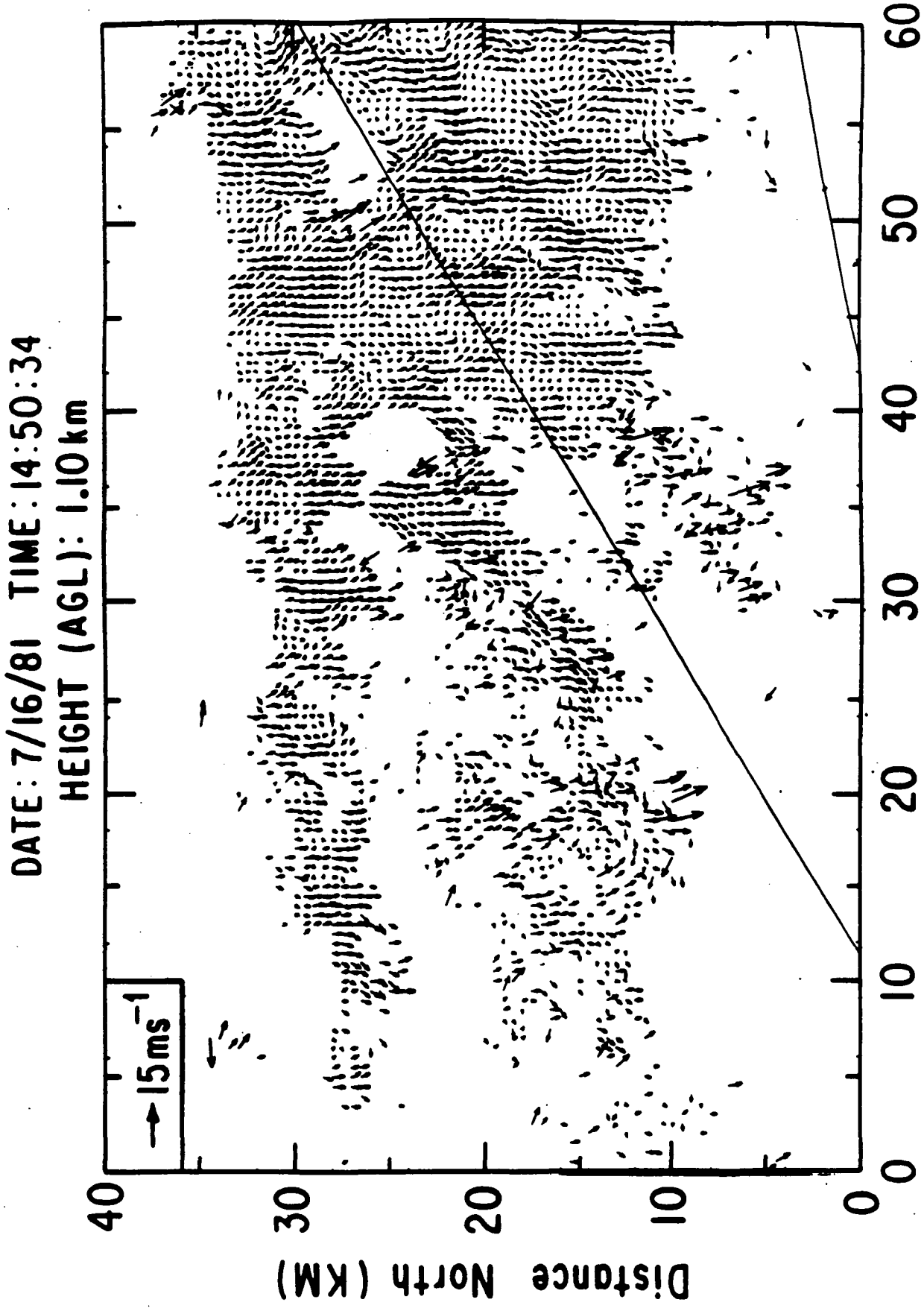

A21

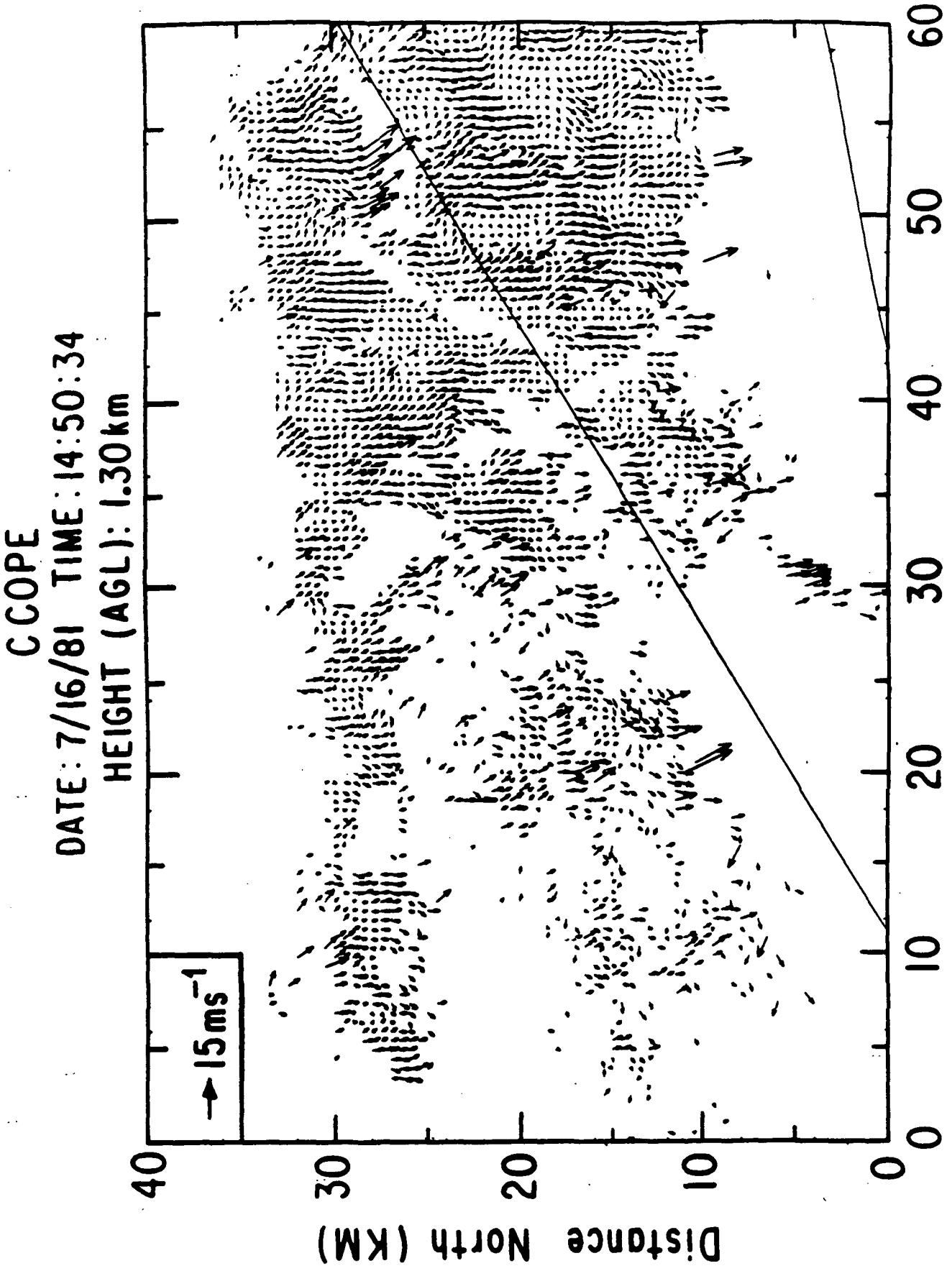
CCOPE
DATE: 7/16/81 TIME: 14:50:34
HEIGHT (AGL): 1.30km
15ms⁻¹
Distance East (KM)
Distance North (KM)
0
10
20
30
40
50
60

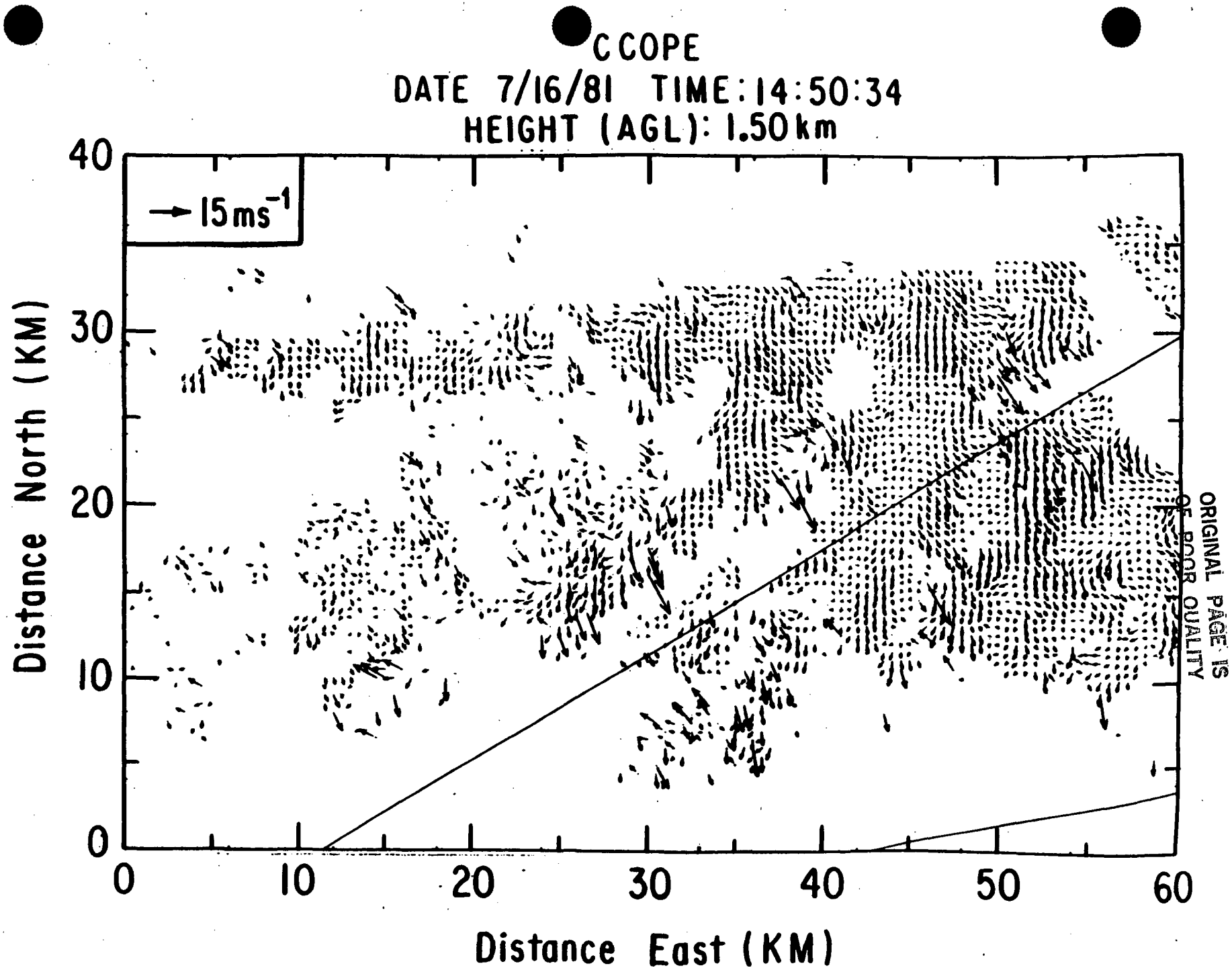

A23

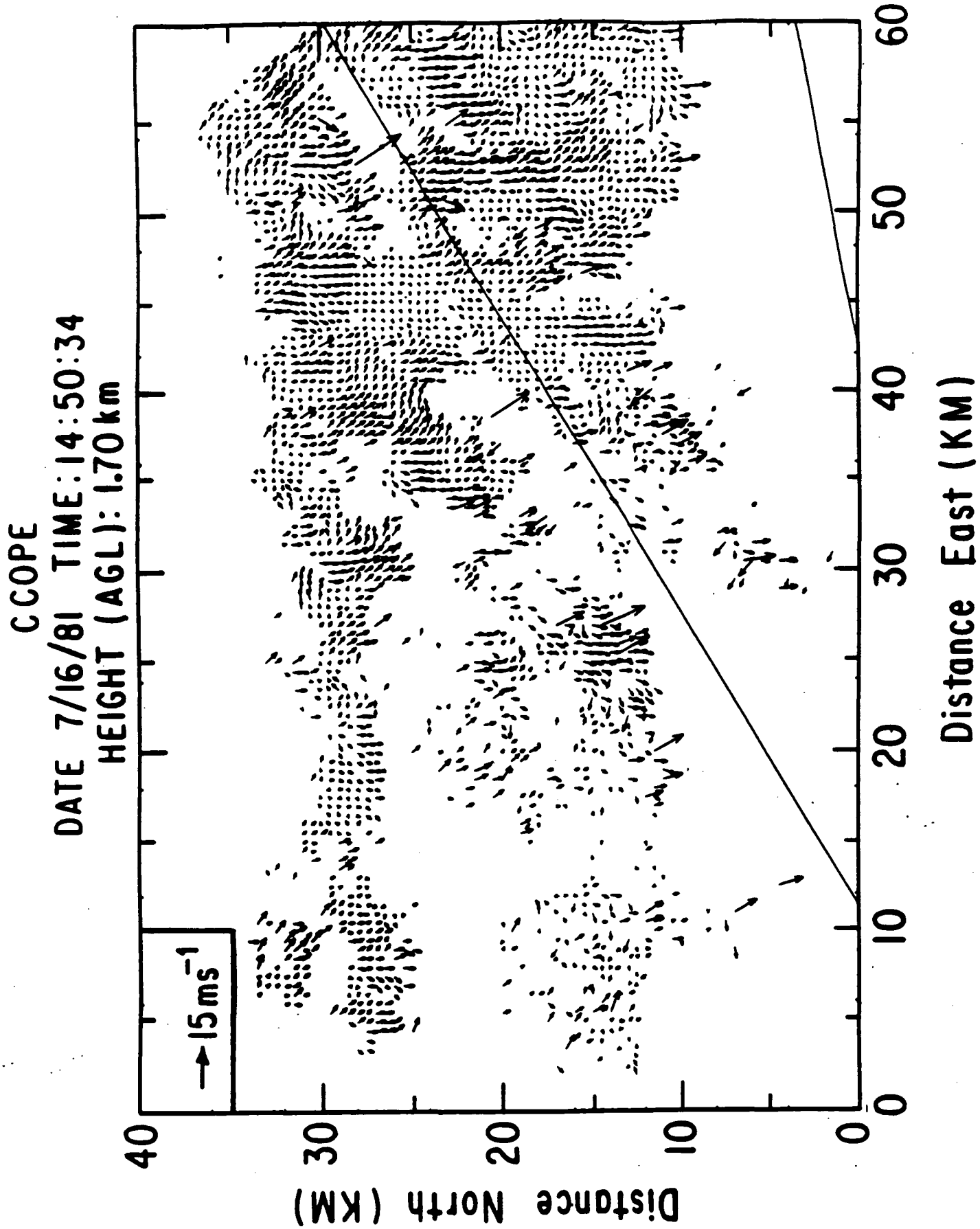
CCOPE
DATE 7/16/81 TIME: 14:50:34
HEIGHT (AGL): 1.70 km
15 ms⁻¹
Distance East (KM)
Distance North (KM)
0
10
20
30
40
50
60

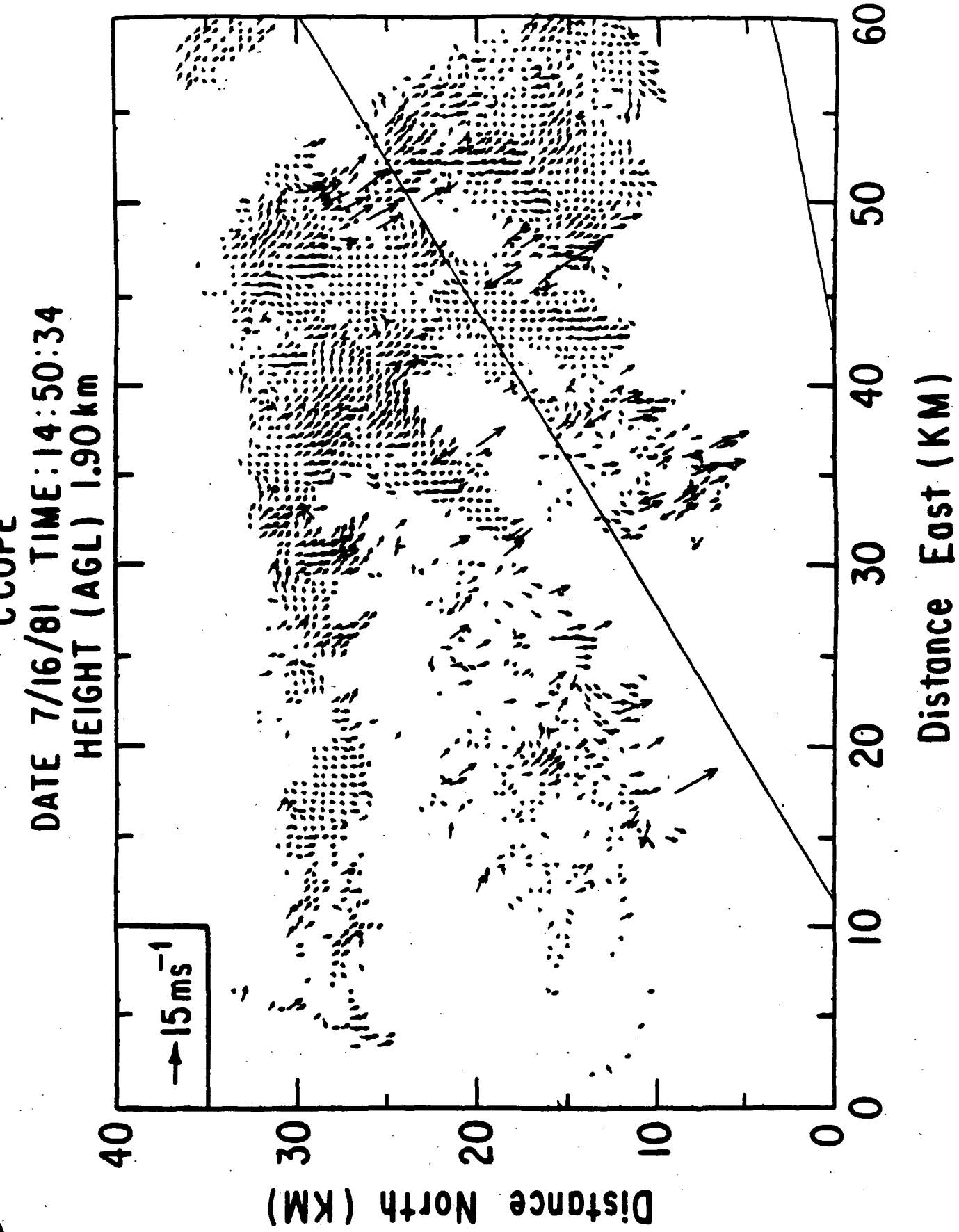

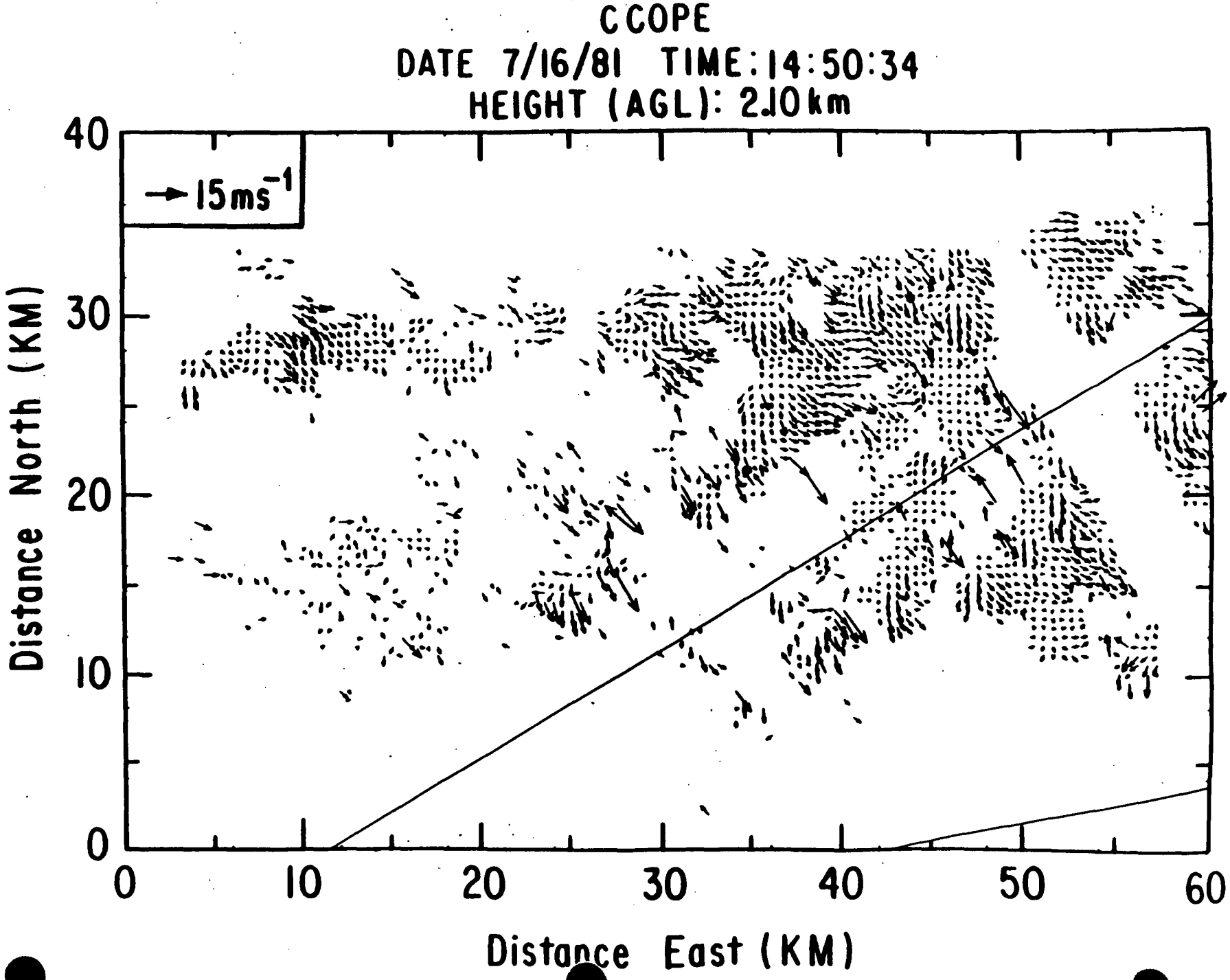
CCOPE
DATE 7/16/81 TIME:14:50:34
HEIGHT (AGL): 2.10 km
→ 15 ms⁻¹
Distance North (KM)
Distance East (KM)
0
10
20
30
40
50
60

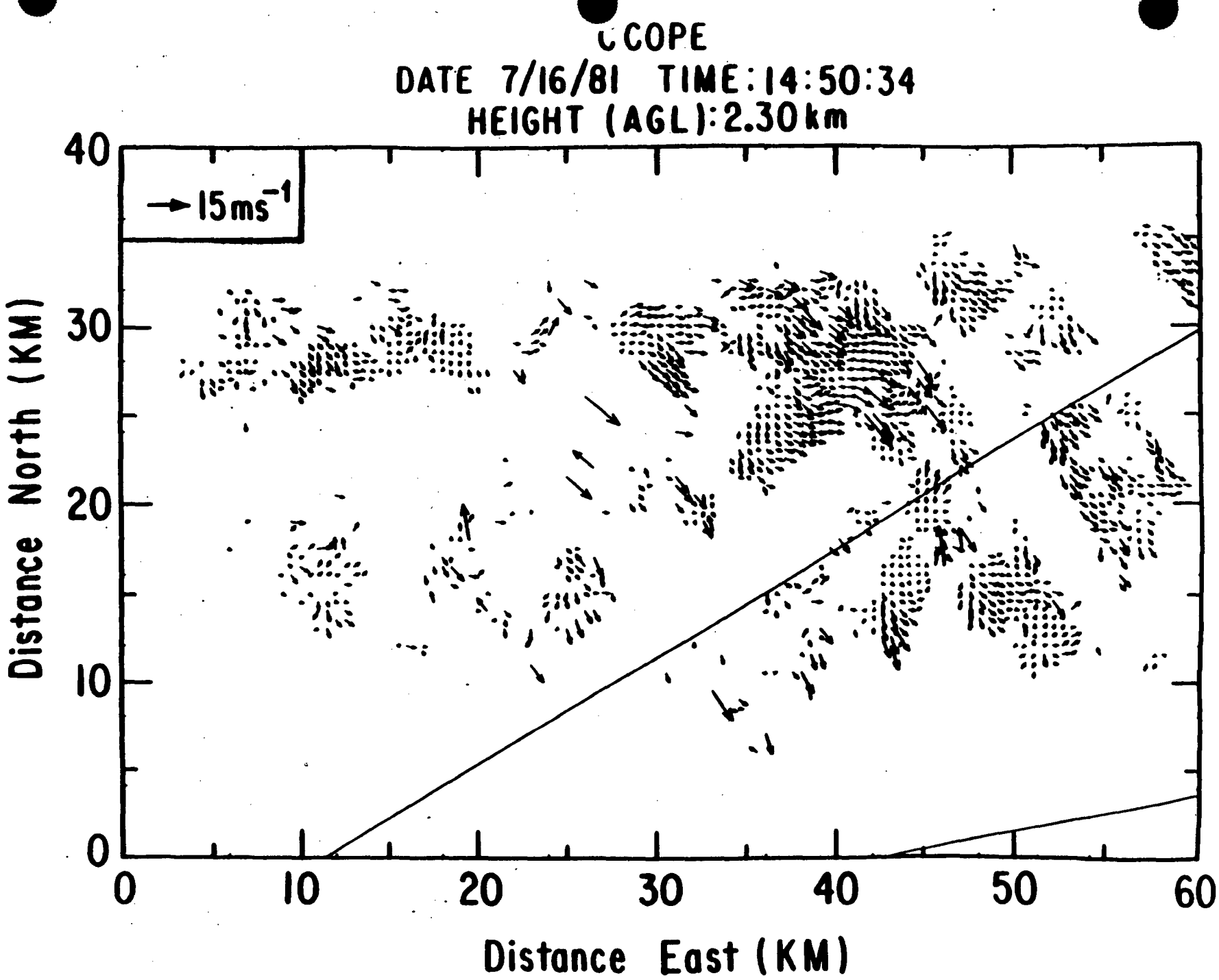
CCOPE
DATE 7/16/81 TIME: 14:50:34
HEIGHT (AGL): 2.30 km
15 ms⁻¹
Distance North (KM)
Distance East (KM)
0
10
20
30
40
50
60

A27

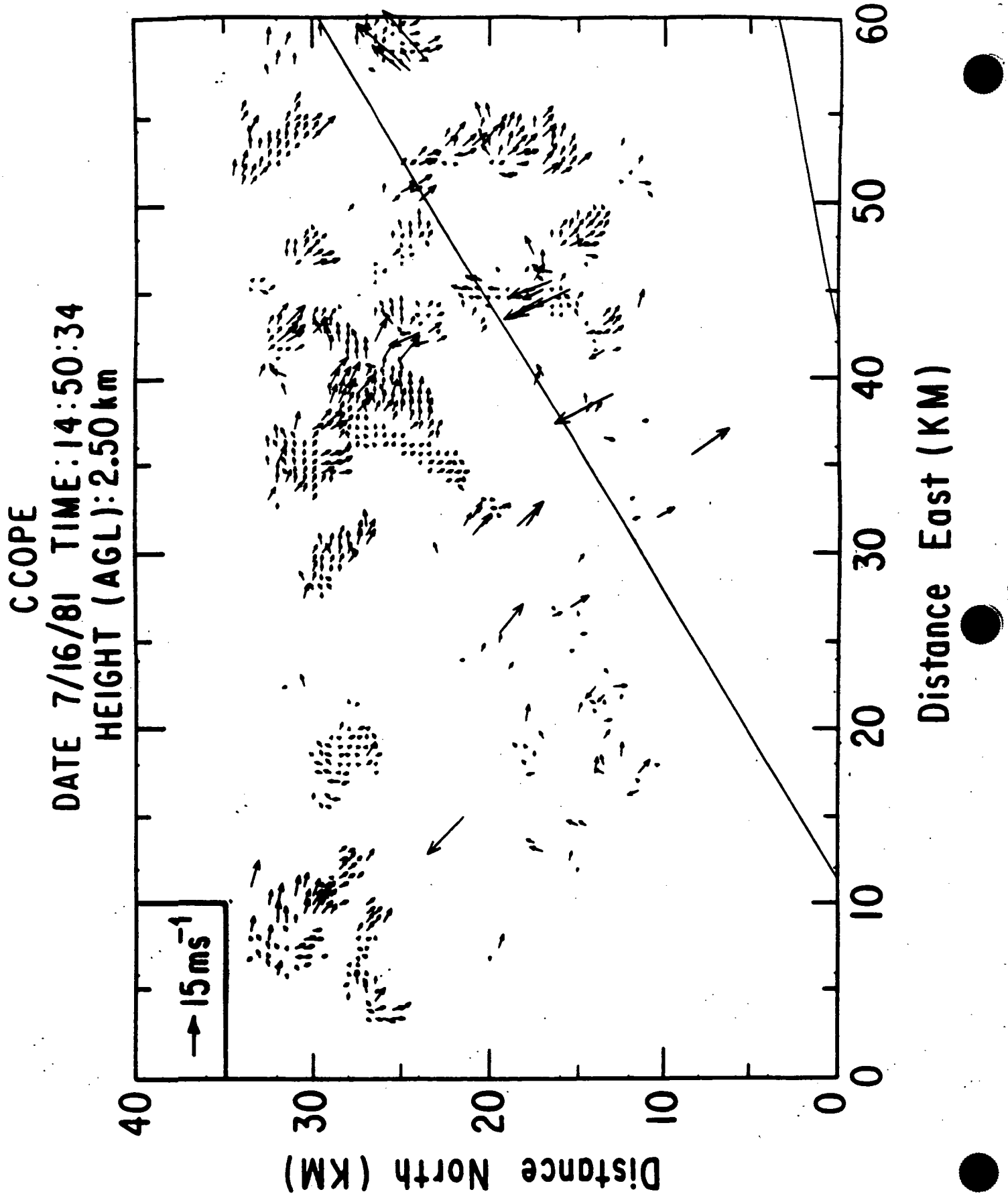
CCOPE
DATE 7/16/81 TIME: 14:50:34
HEIGHT (AGL): 2.50 km
15 ms⁻¹
Distance North (KM)
Distance East (KM)
0
10
20
30
40
50
60

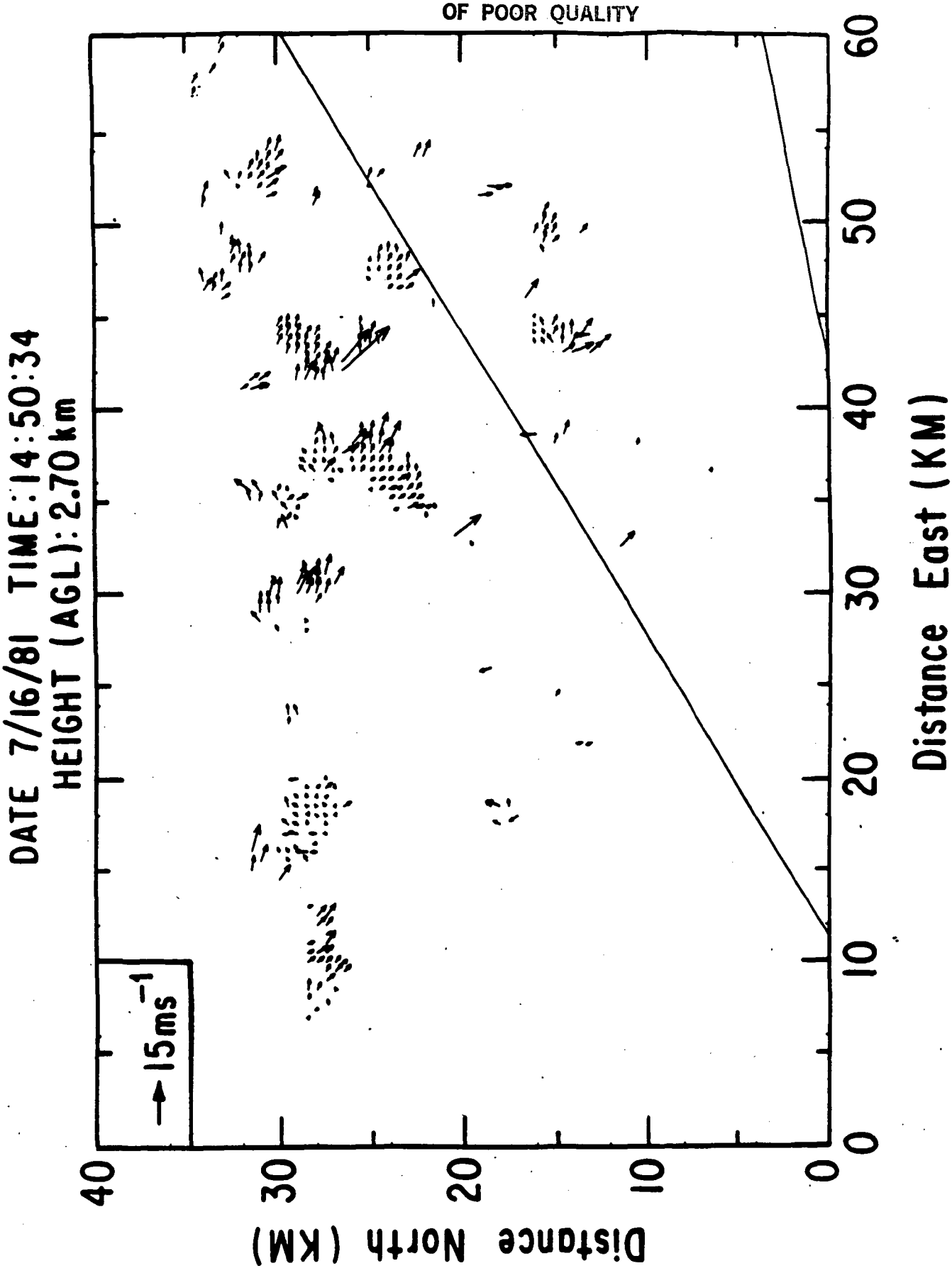

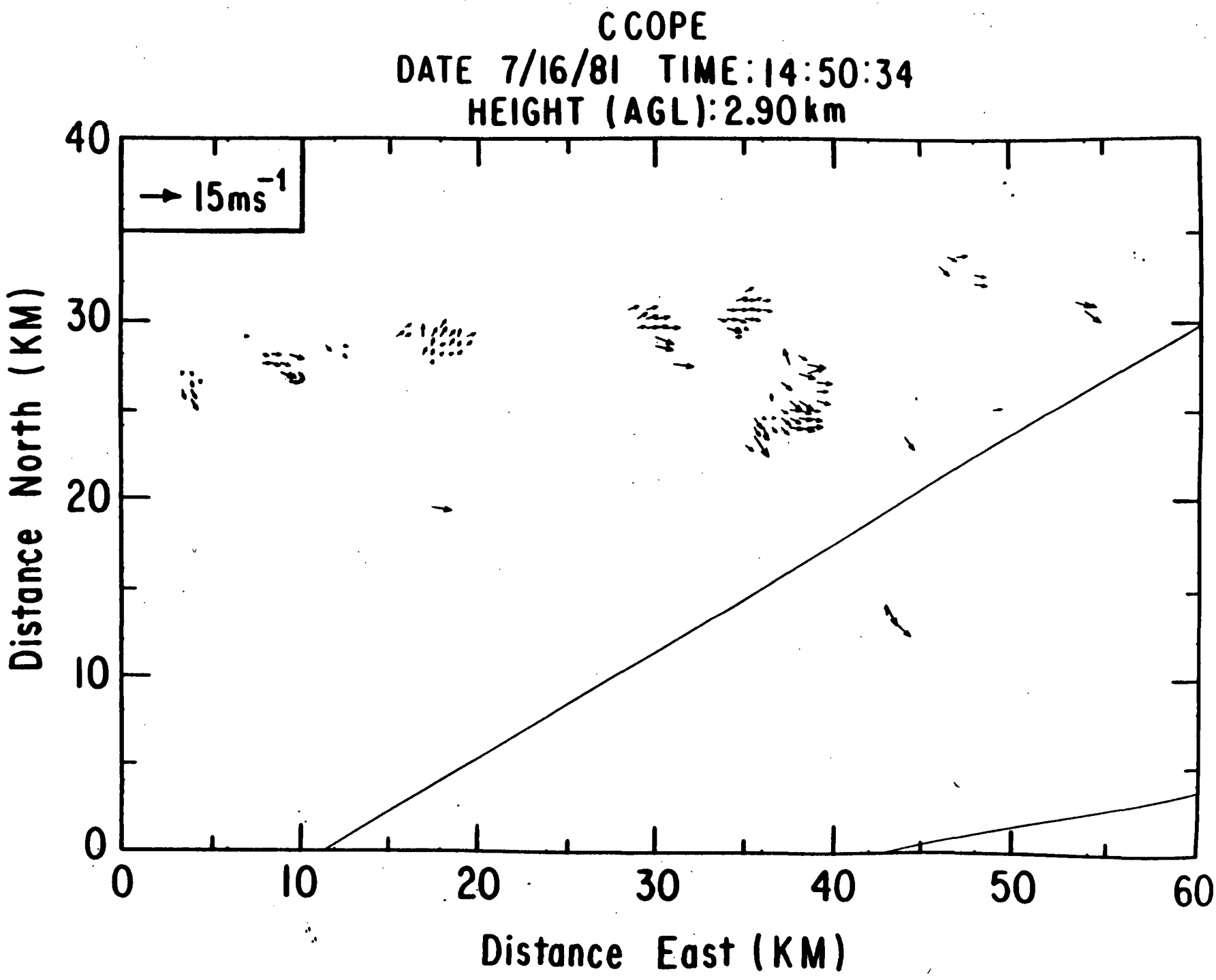
CCOPE
DATE 7/16/81 TIME:14:50:34
HEIGHT (AGL):2.90km
→ 15ms⁻¹
Distance North (KM)
Distance East (KM)
0
10
20
30
40
50
60

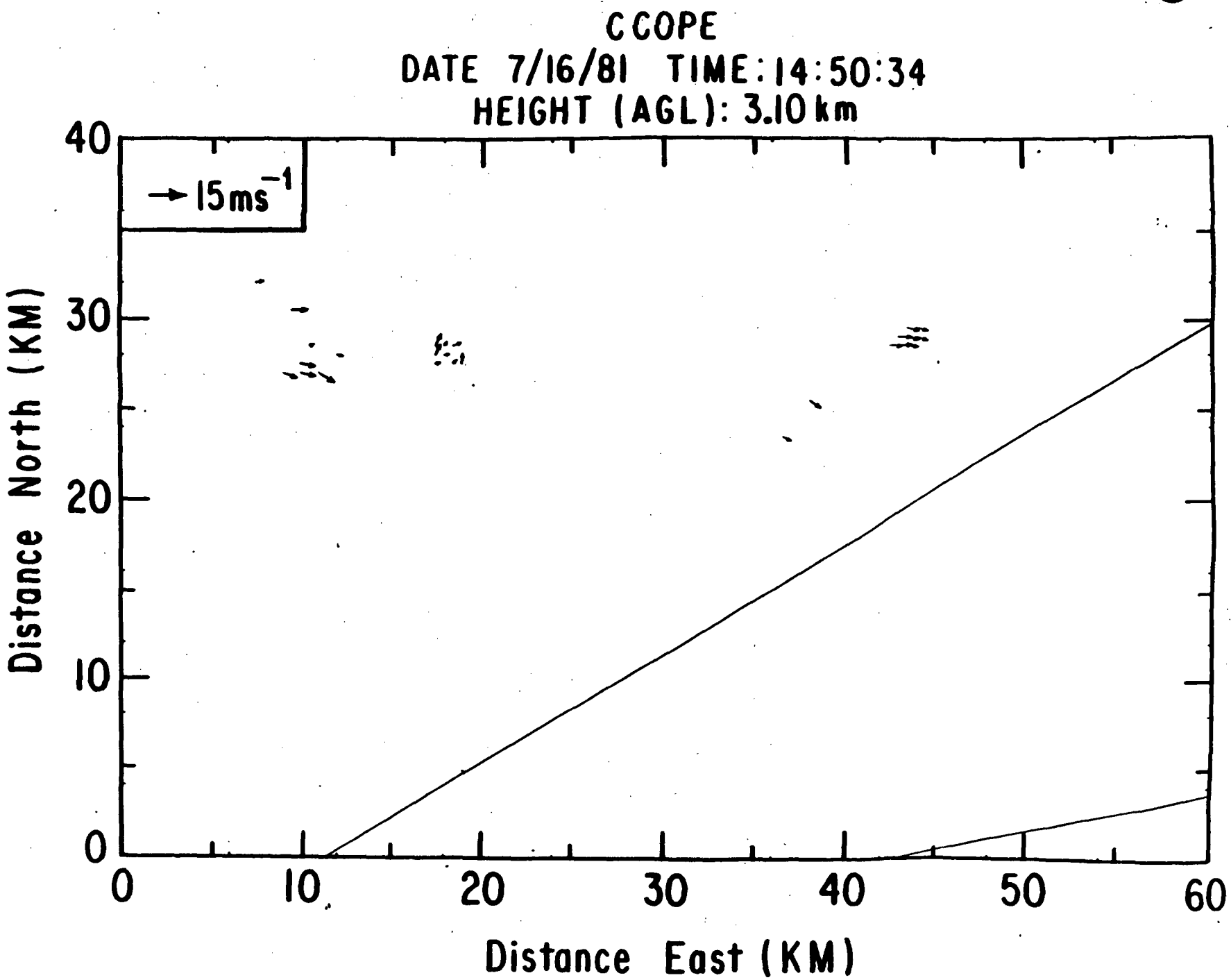
CCOPE
DATE 7/16/81 TIME: 14:50:34
HEIGHT (AGL): 3.10 km
→ 15 ms⁻¹
Distance North (KM)
Distance East (KM)
0
10
20
30
40
50
60

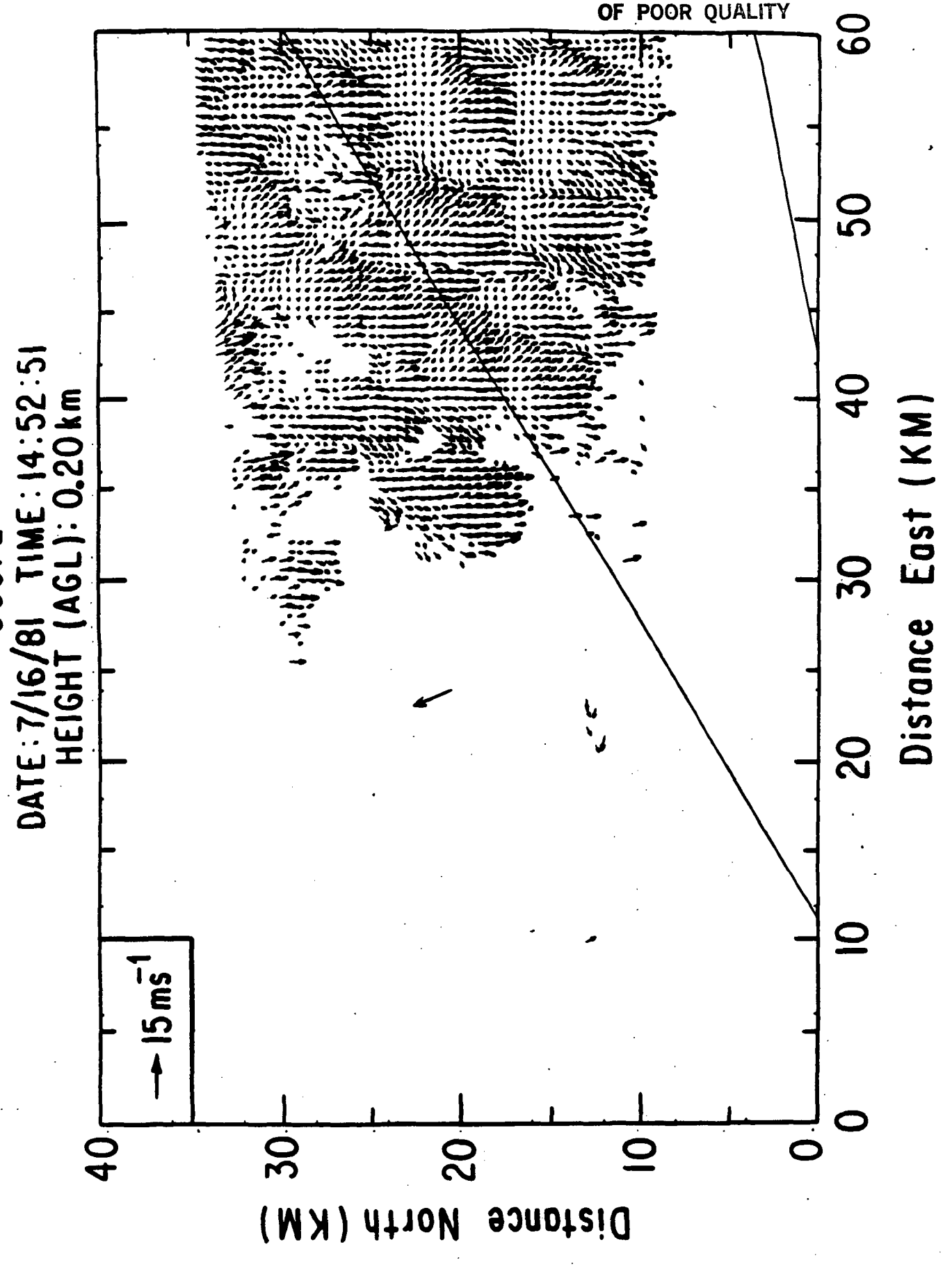

A32

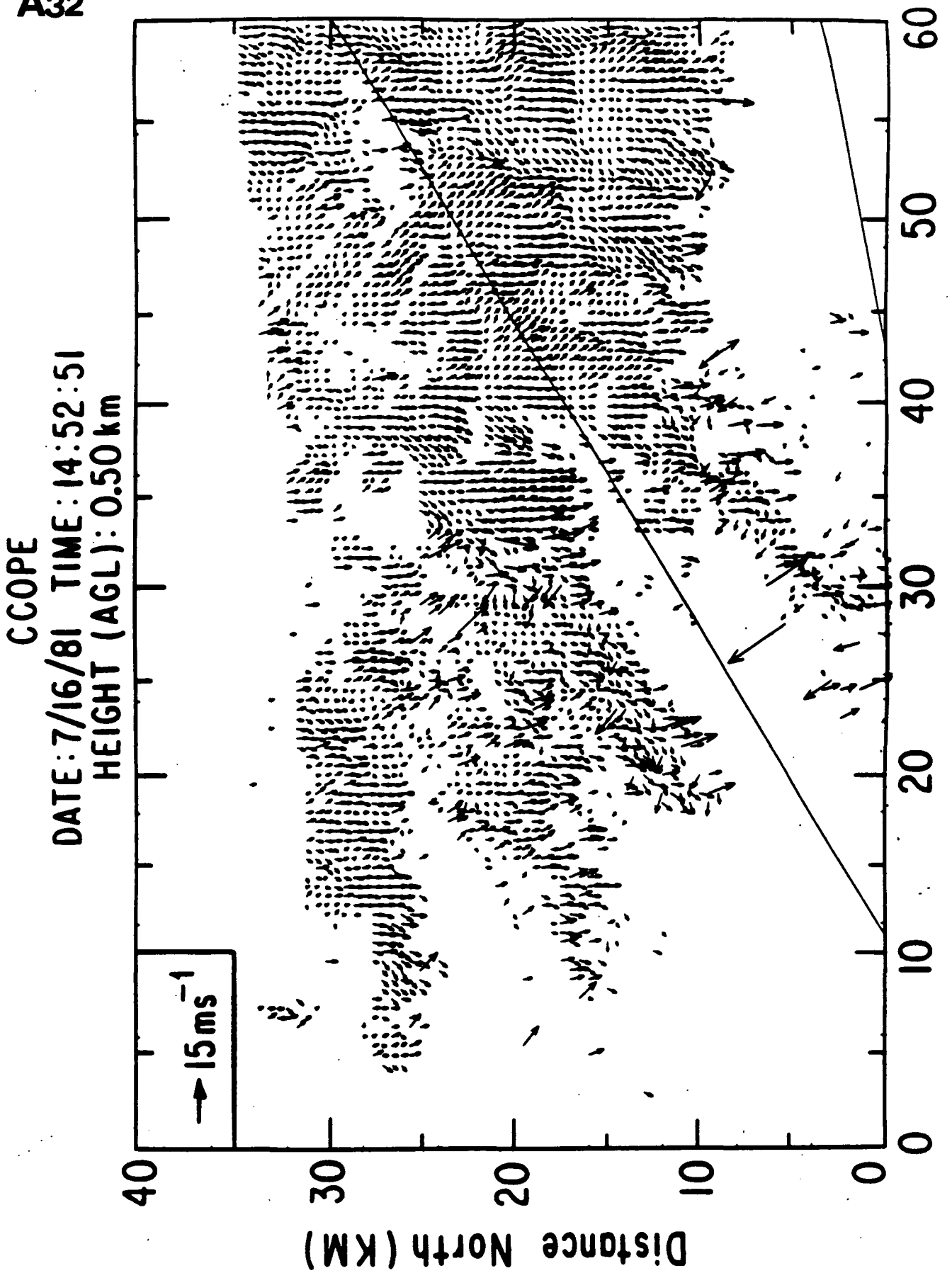
CCOPE
DATE: 7/16/81 TIME: 14:52:51
HEIGHT (AGL): 0.50 km
15 ms⁻¹
Distance East (KM)
Distance North (KM)
0
10
20
30
40
50
60

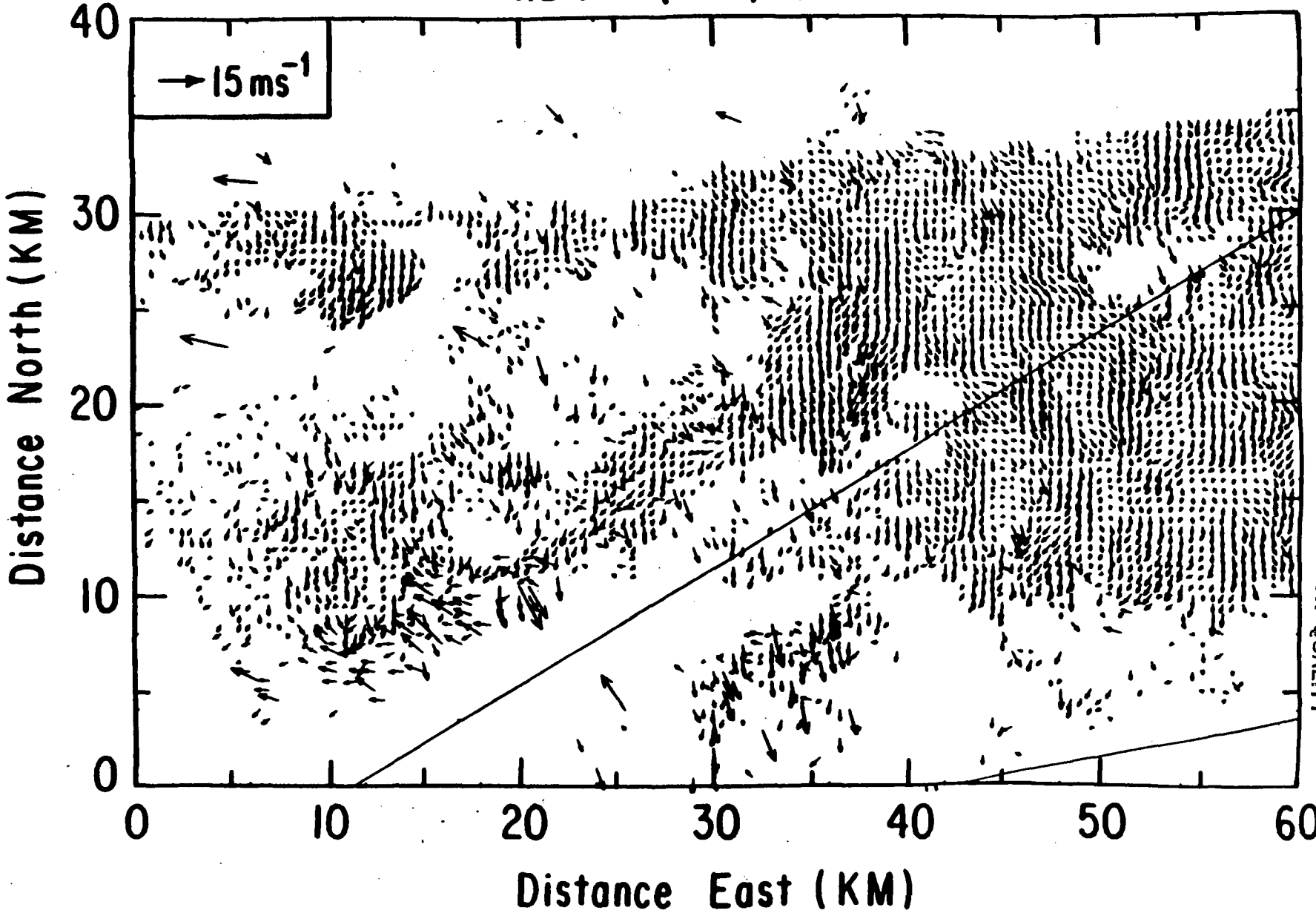

A34

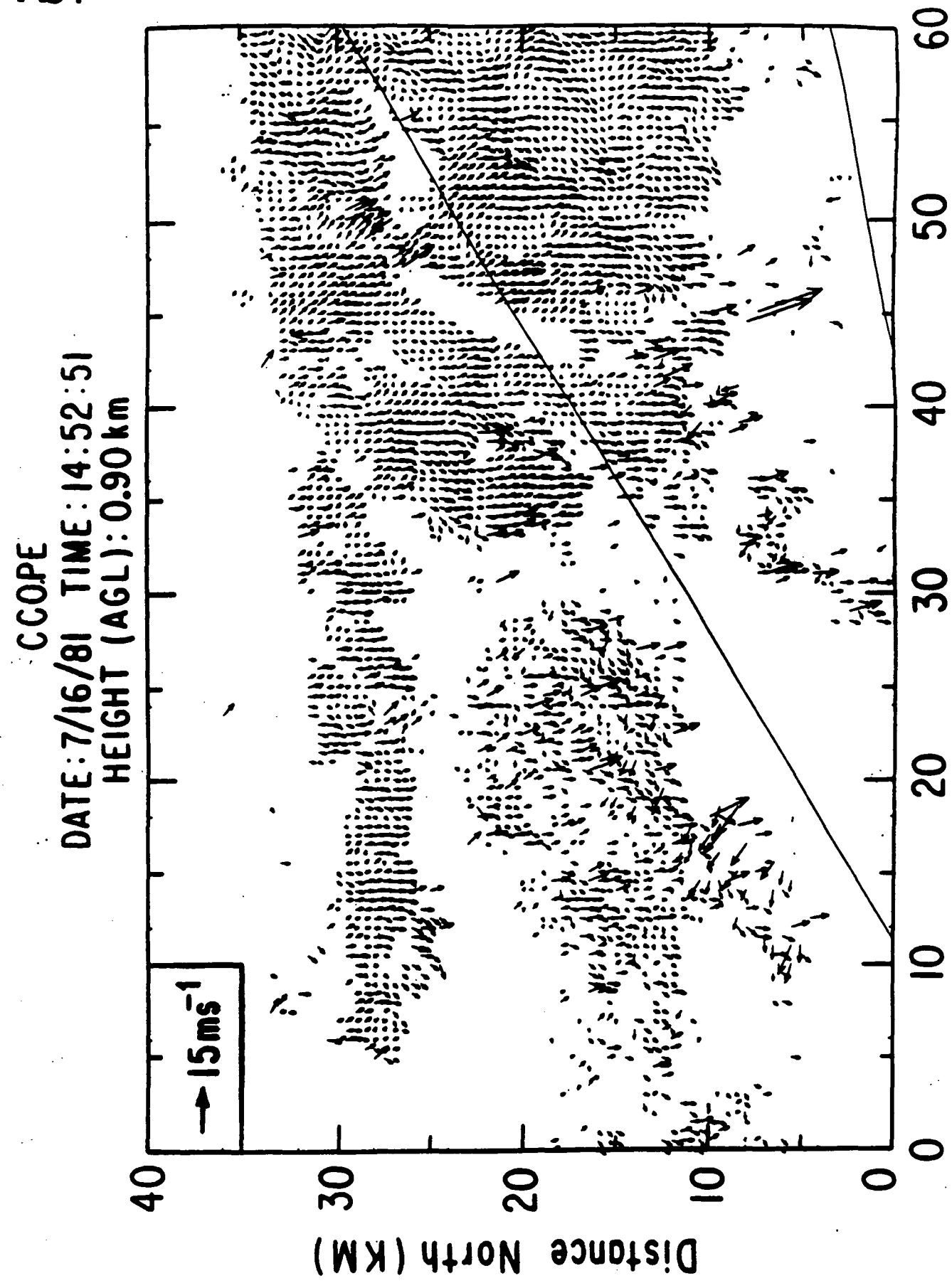
CCOPE
DATE: 7/16/81 TIME: 14:52:51
HEIGHT (AGL): 0.90 km
15ms⁻¹
Distance North (KM)
Distance East (KM)
0
10
20
30
40
50
60

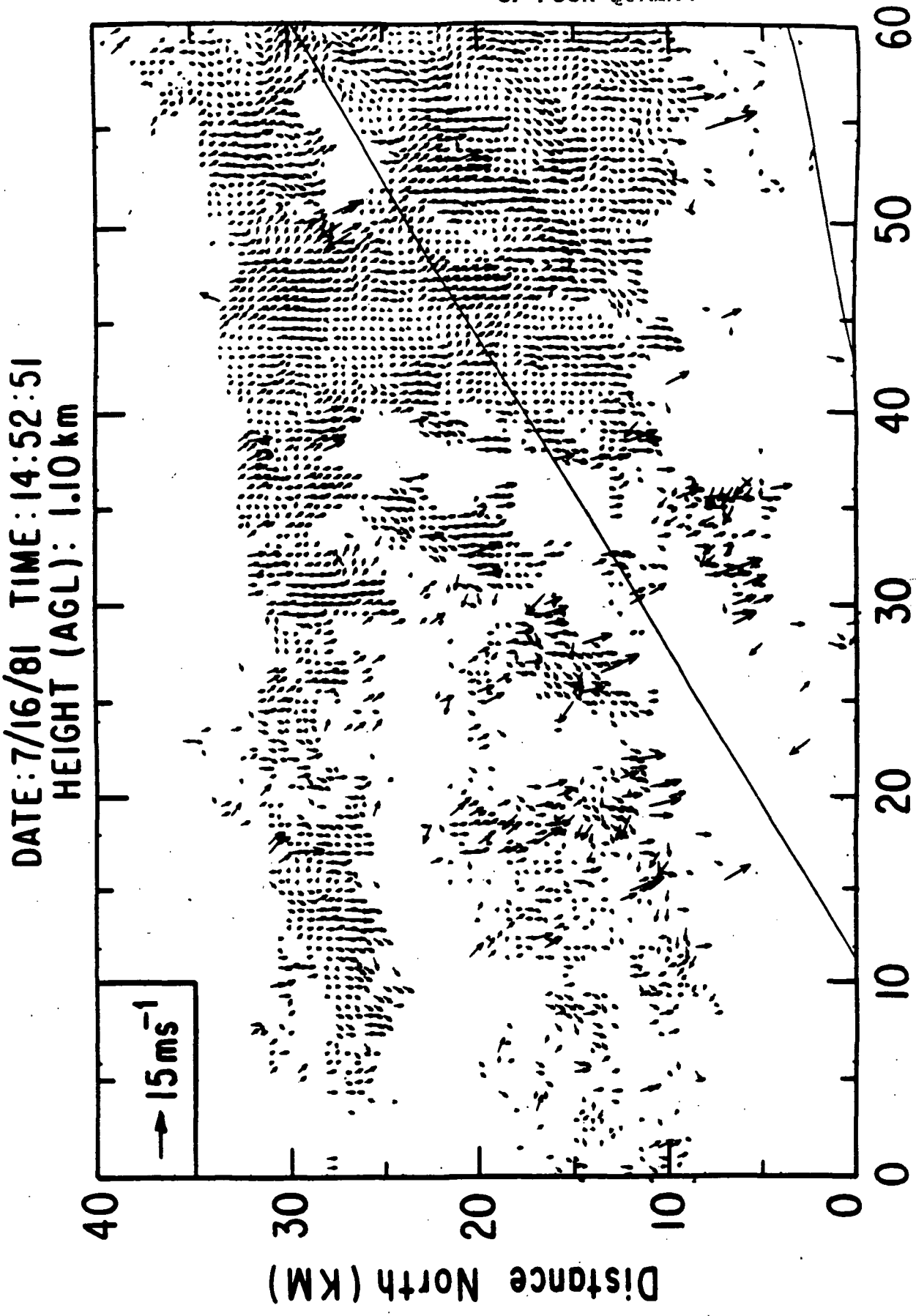

A36

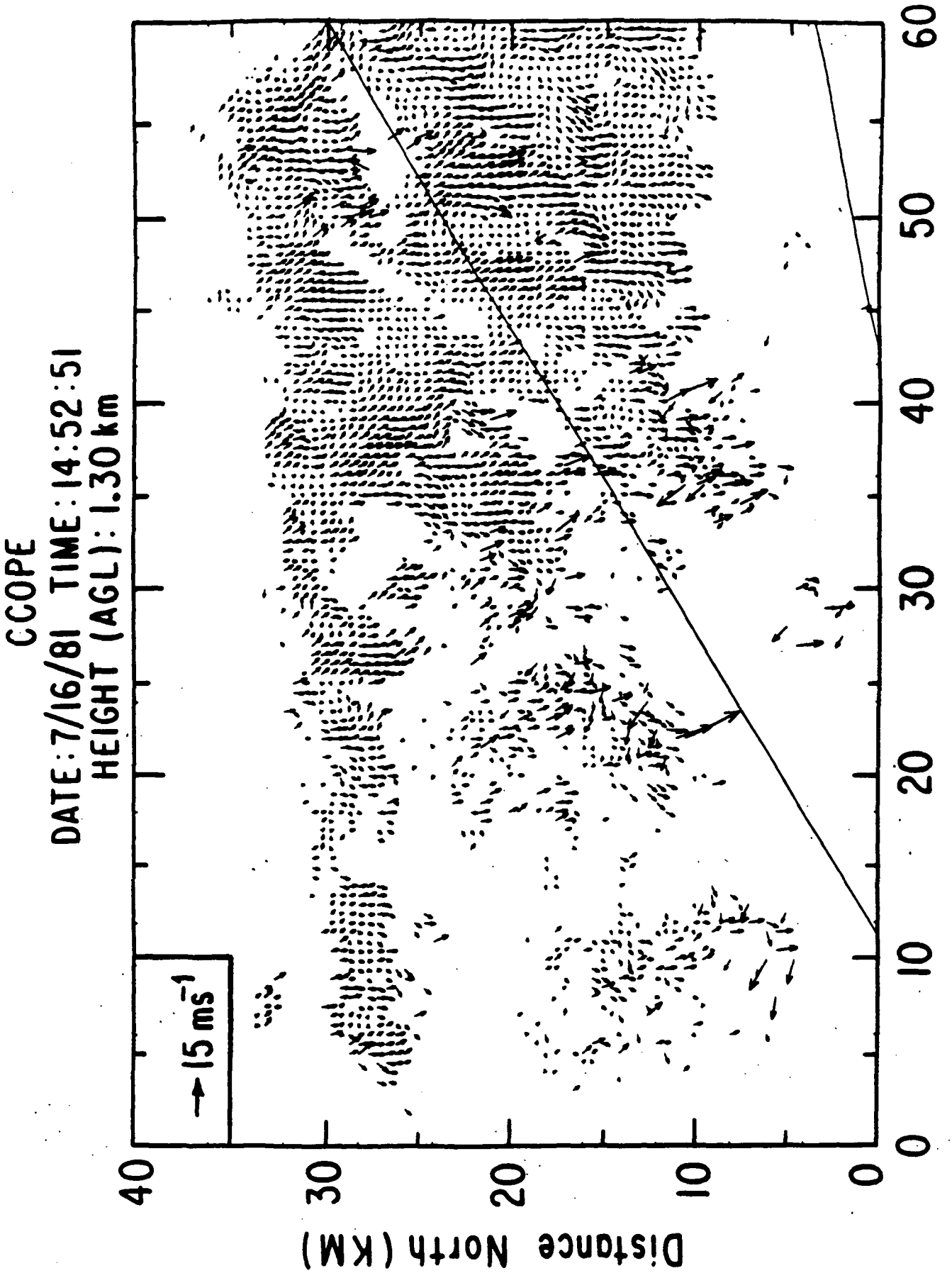
CCOPE
DATE: 7/16/81 TIME: 14:52:51
HEIGHT (AGL): 1.30 km
15 ms⁻¹
Distance East (KM)
Distance North (KM)
0
10
20
30
40
50
60

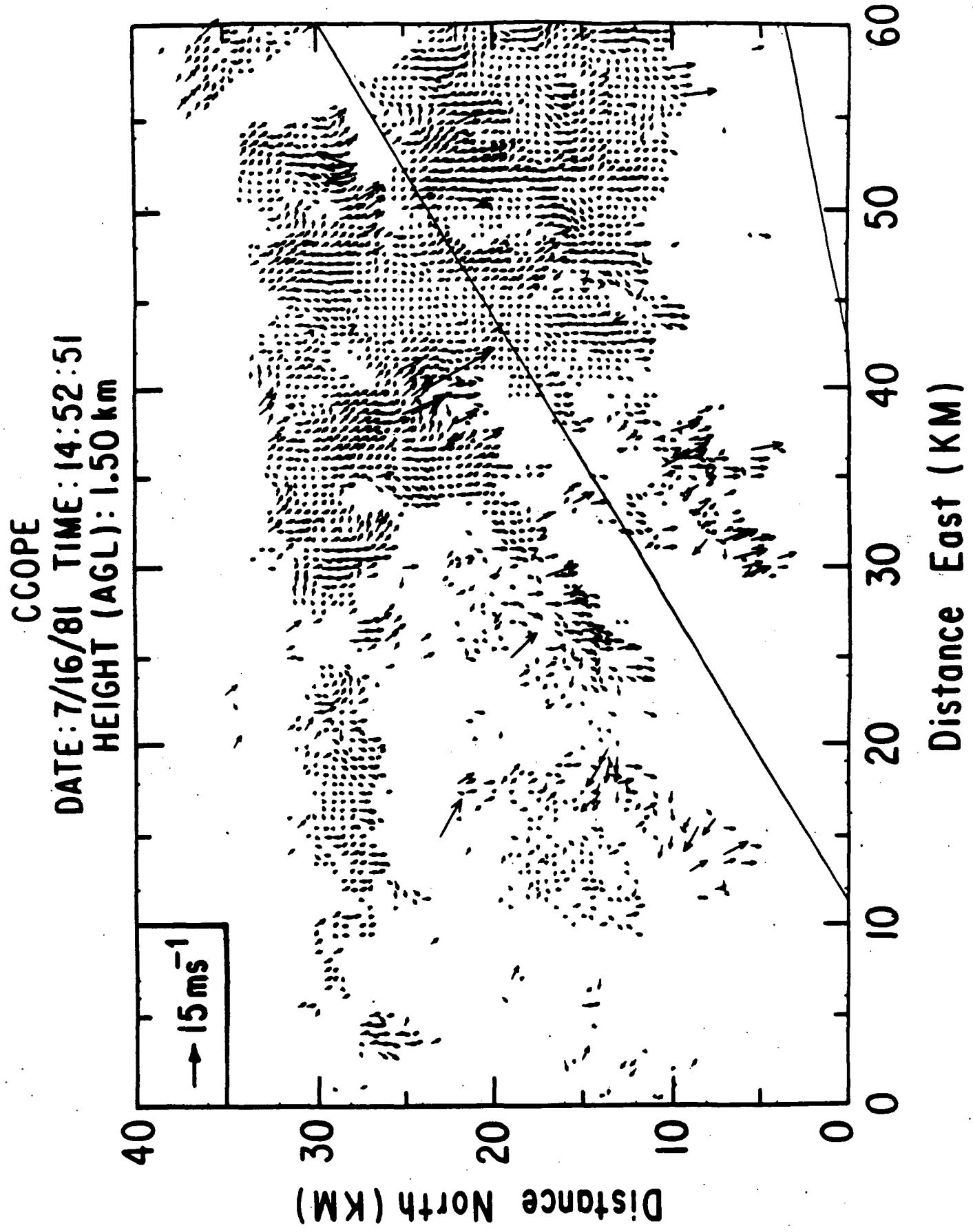

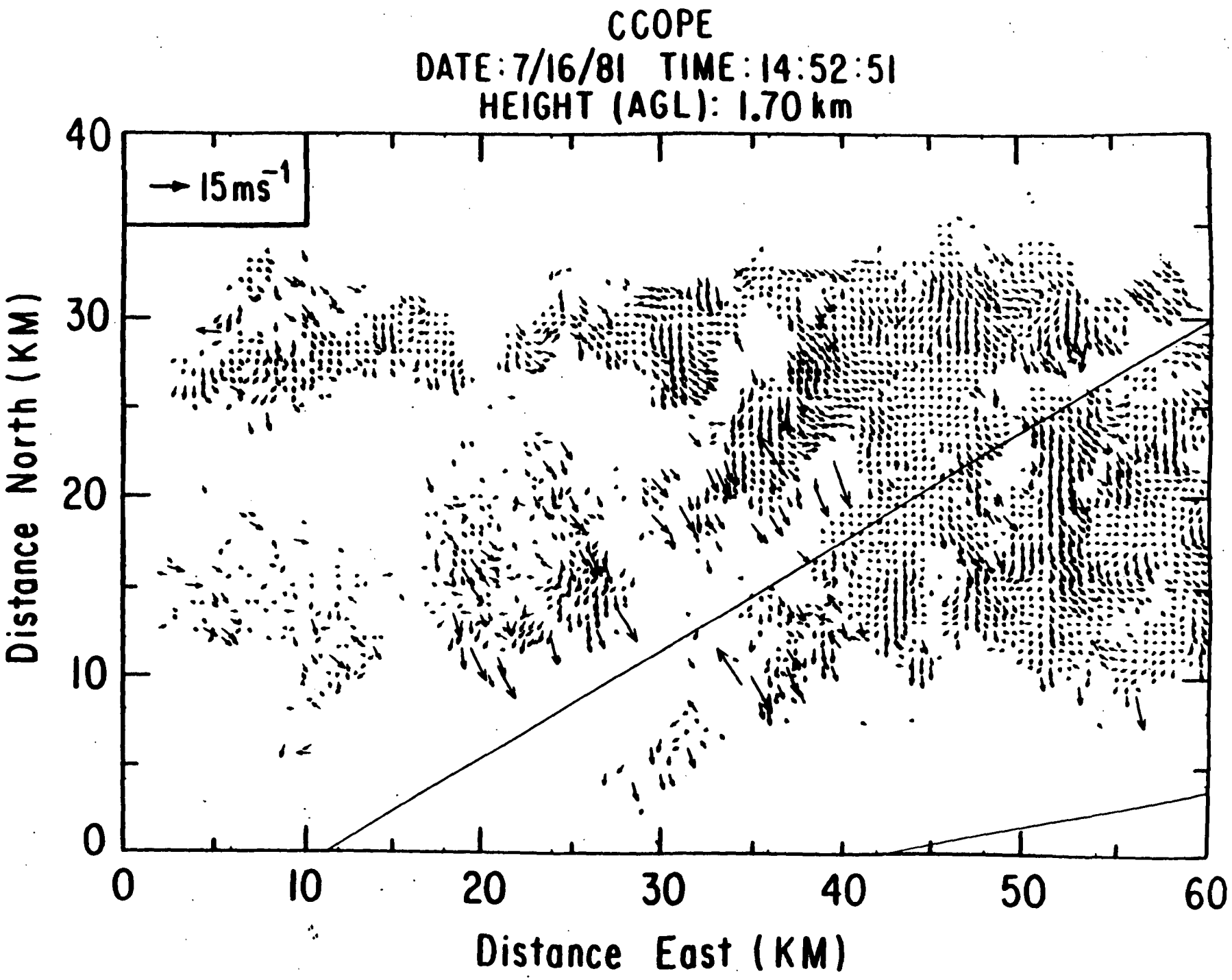
CCOPE
DATE: 7/16/81 TIME: 14:52:51
HEIGHT (AGL): 1.70 km
→ 15 ms⁻¹
Distance North (KM)
Distance East (KM)
0
10
20
30
40
50
60

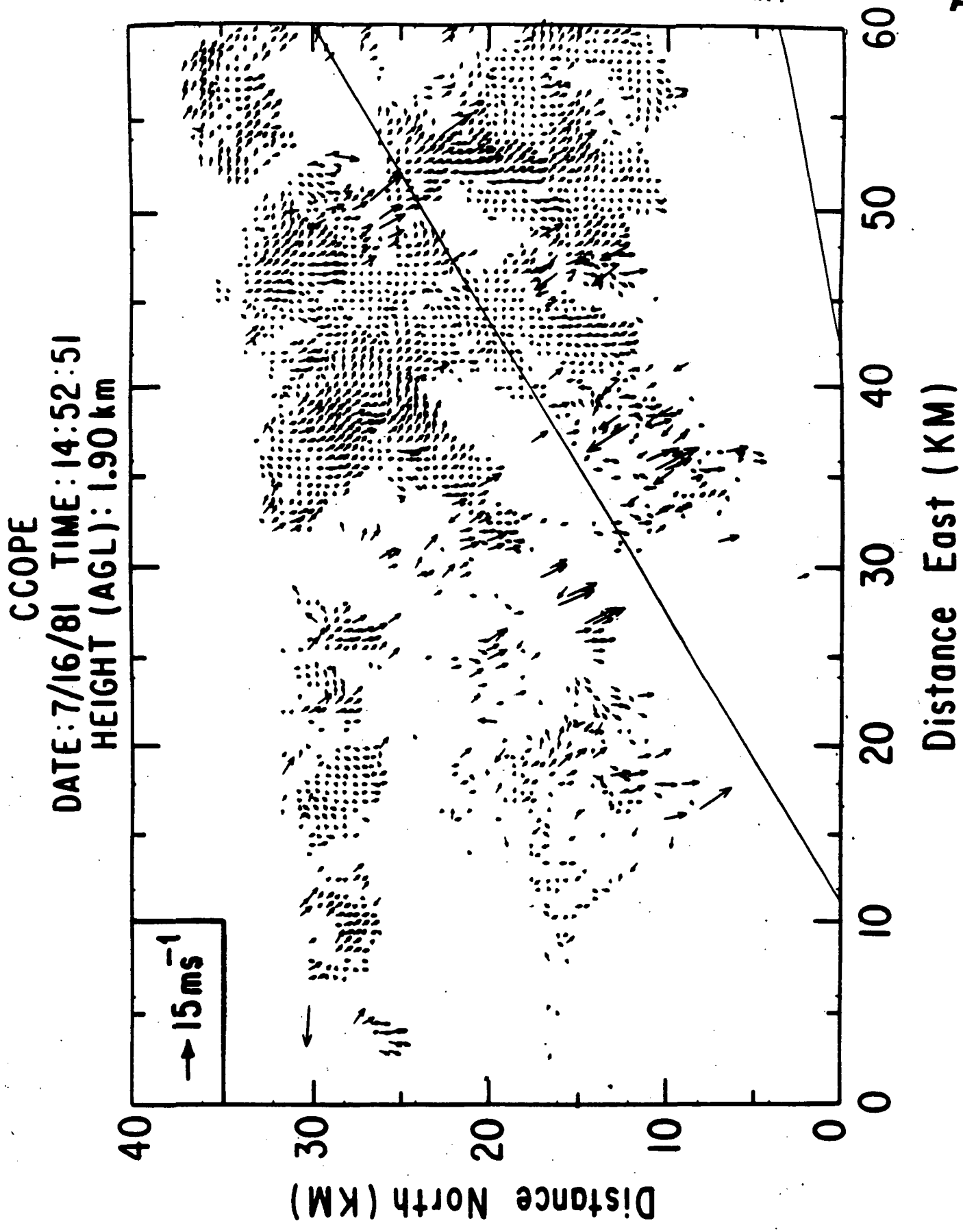

A40

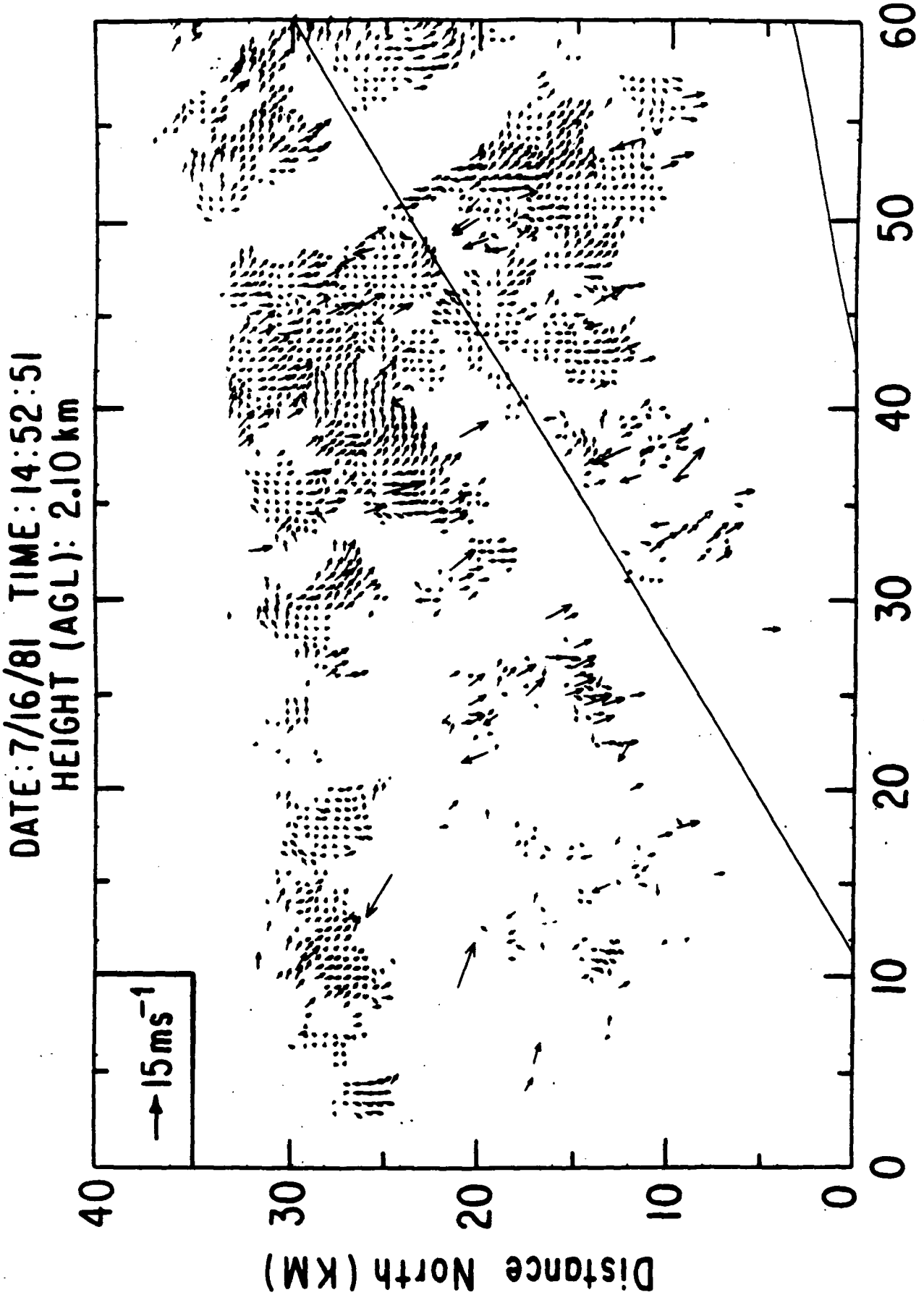
CCOPE
DATE: 7/16/81 TIME: 14:52:51
HEIGHT (AGL): 2.10 km
15 ms⁻¹
Distance East (KM)
Distance North (KM)
0
10
20
30
40
50
60

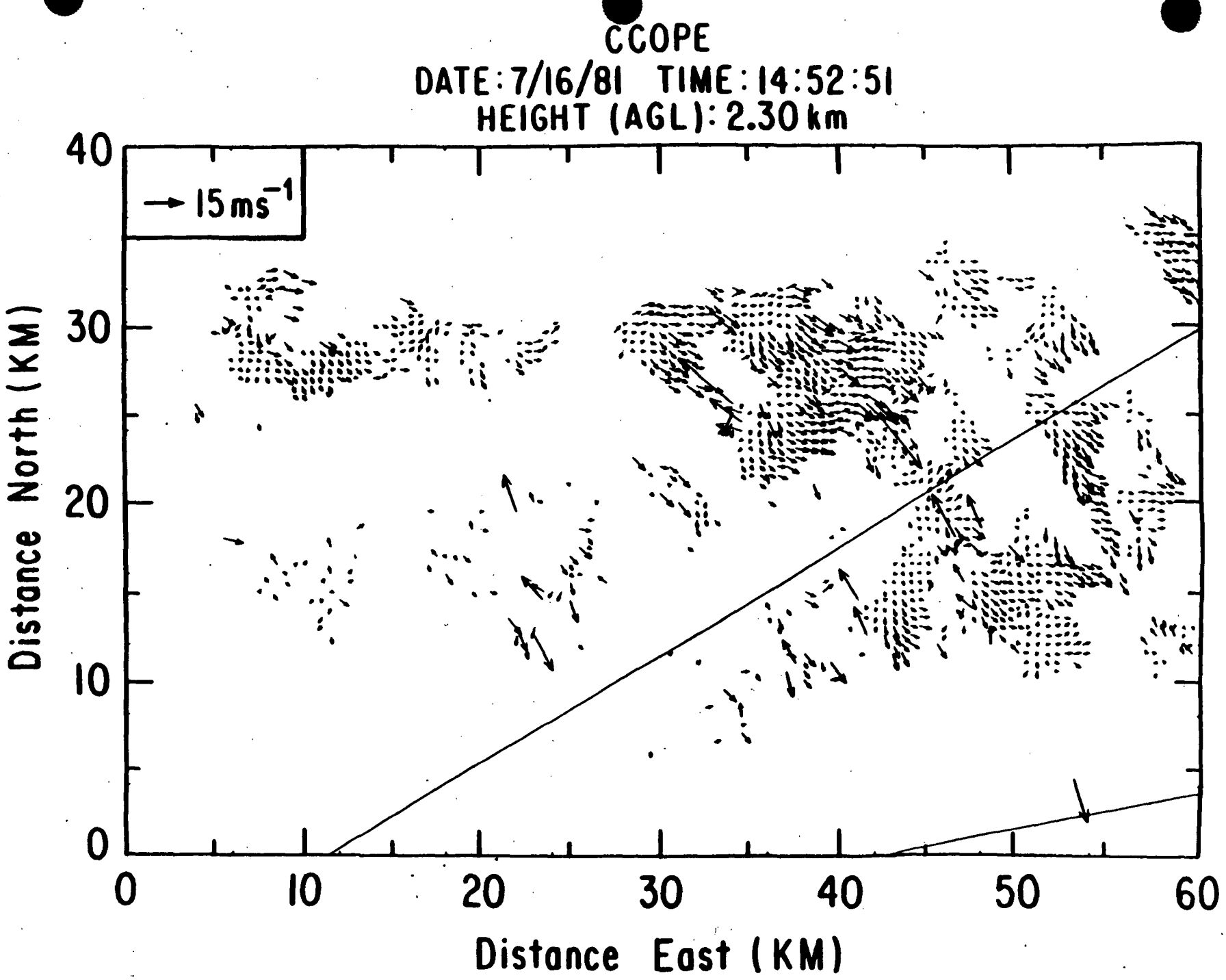
CCOPE
DATE: 7/16/81 TIME: 14:52:51
HEIGHT (AGL): 2.30 km
→ 15 ms⁻¹
Distance North (KM)
Distance East (KM)
0
10
20
30
40
50
60

A42

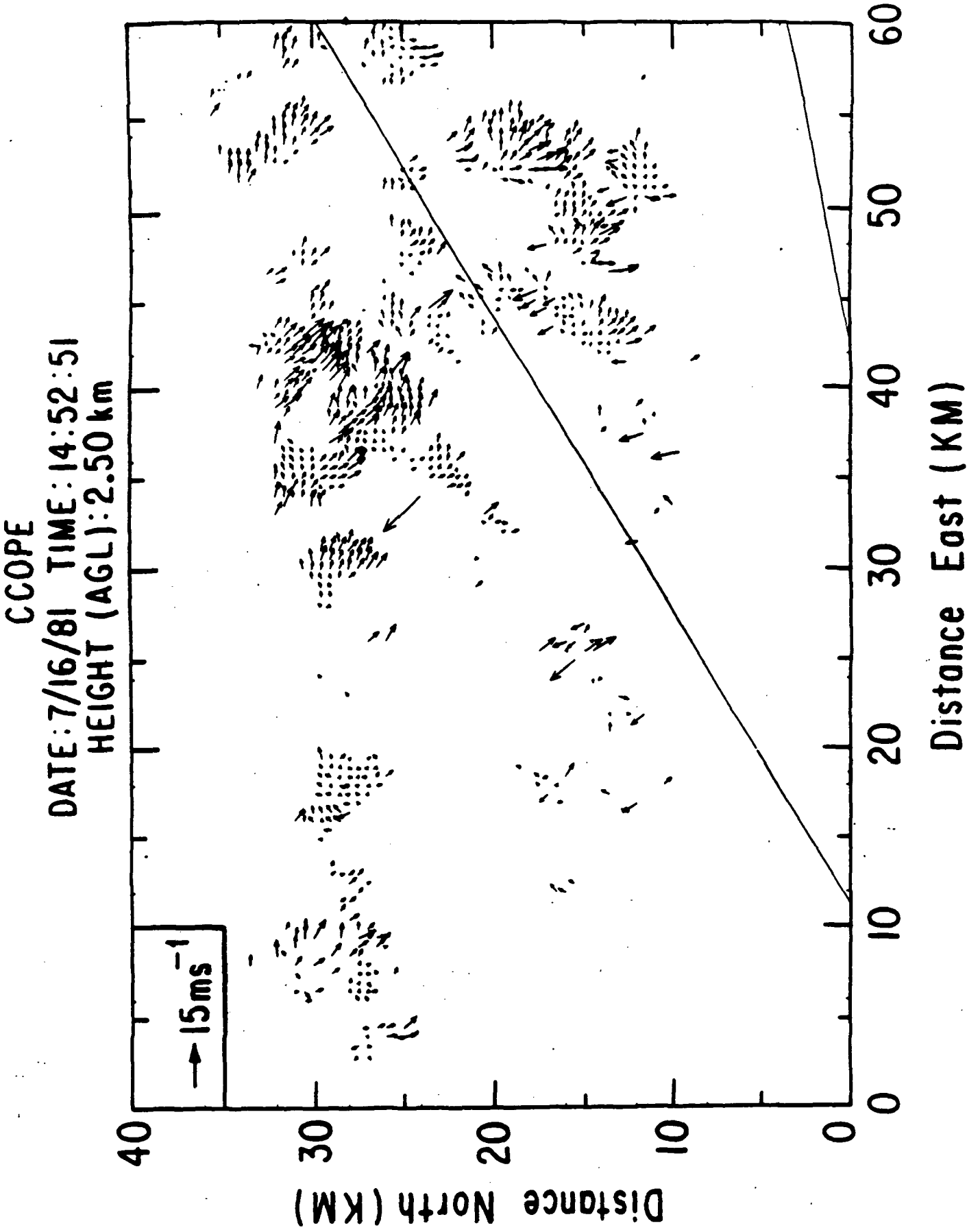
CCOPE
DATE: 7/16/81 TIME: 14:52:51
HEIGHT (AGL): 2.50 km
15ms⁻¹
Distance East (KM)
Distance North (KM)
0
10
20
30
40
50
60

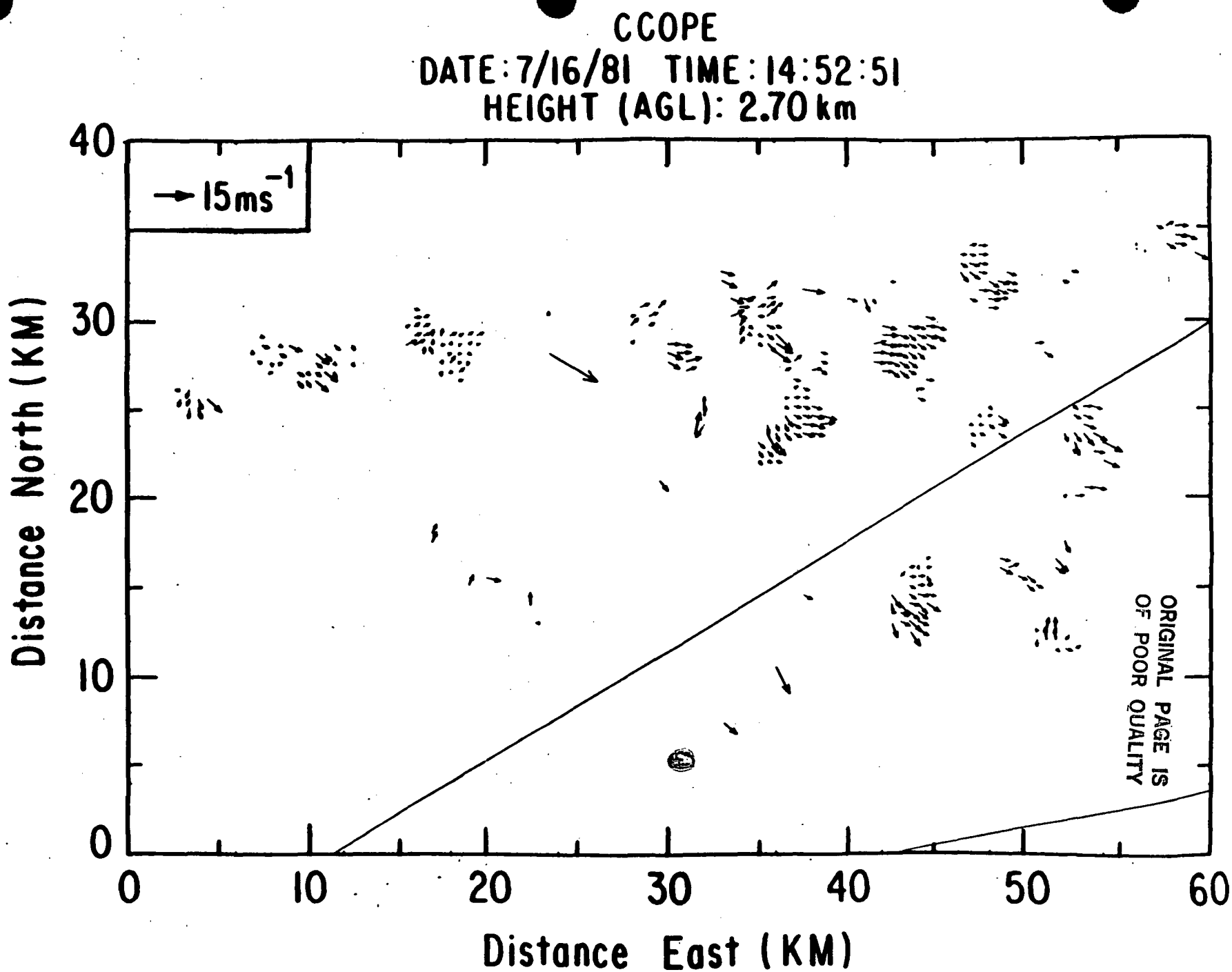
CCOPE
DATE: 7/16/81 TIME: 14:52:51
HEIGHT (AGL): 2.70 km
15 ms⁻¹
Distance North (KM)
Distance East (KM)
0
10
20
30
40
50
60
ORIGINAL PAGE IS
OF POOR QUALITY

CCOPE
DATE: 7/16/81 TIME: 14:52:51
HEIGHT (AGL): 2.90 km

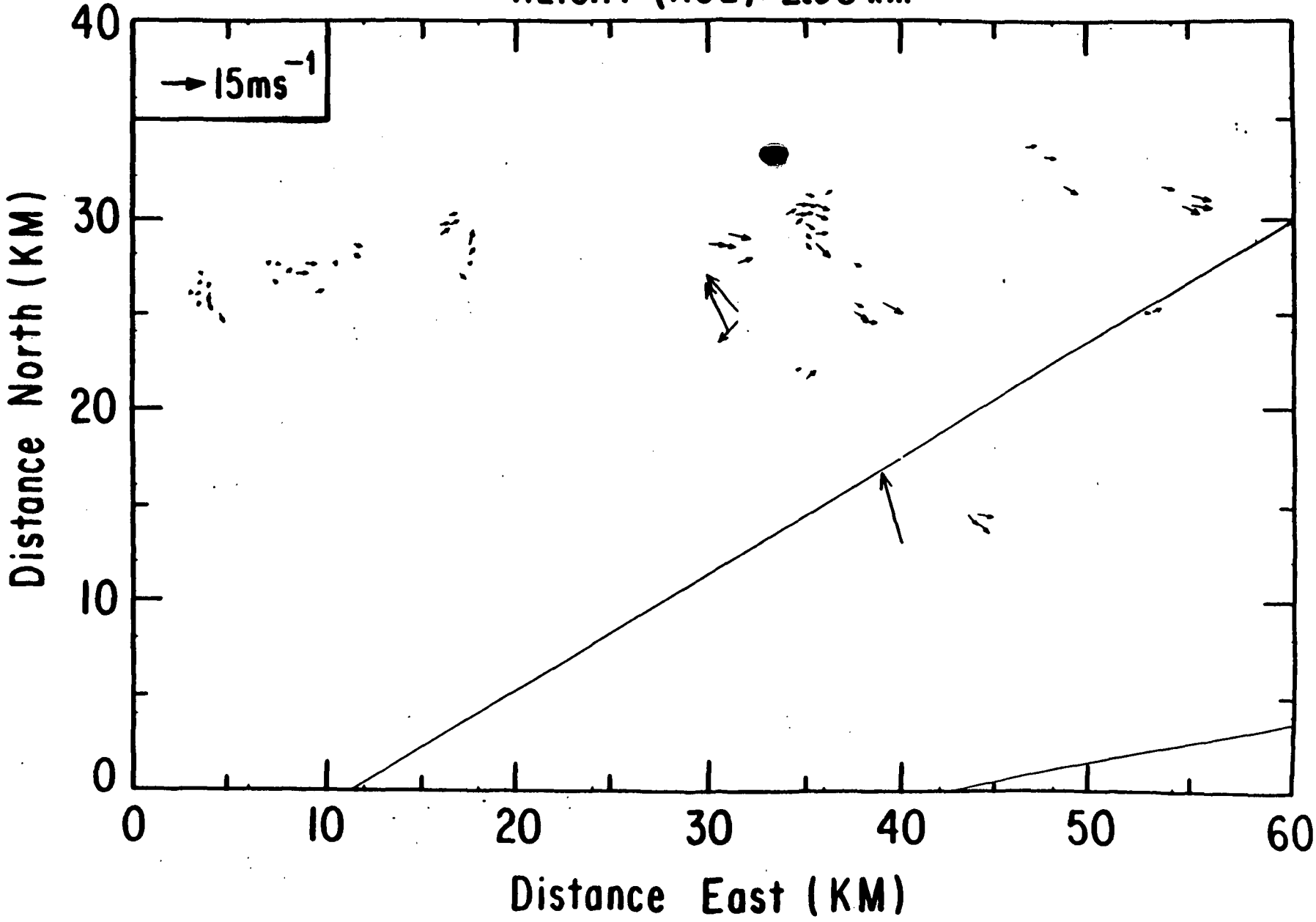

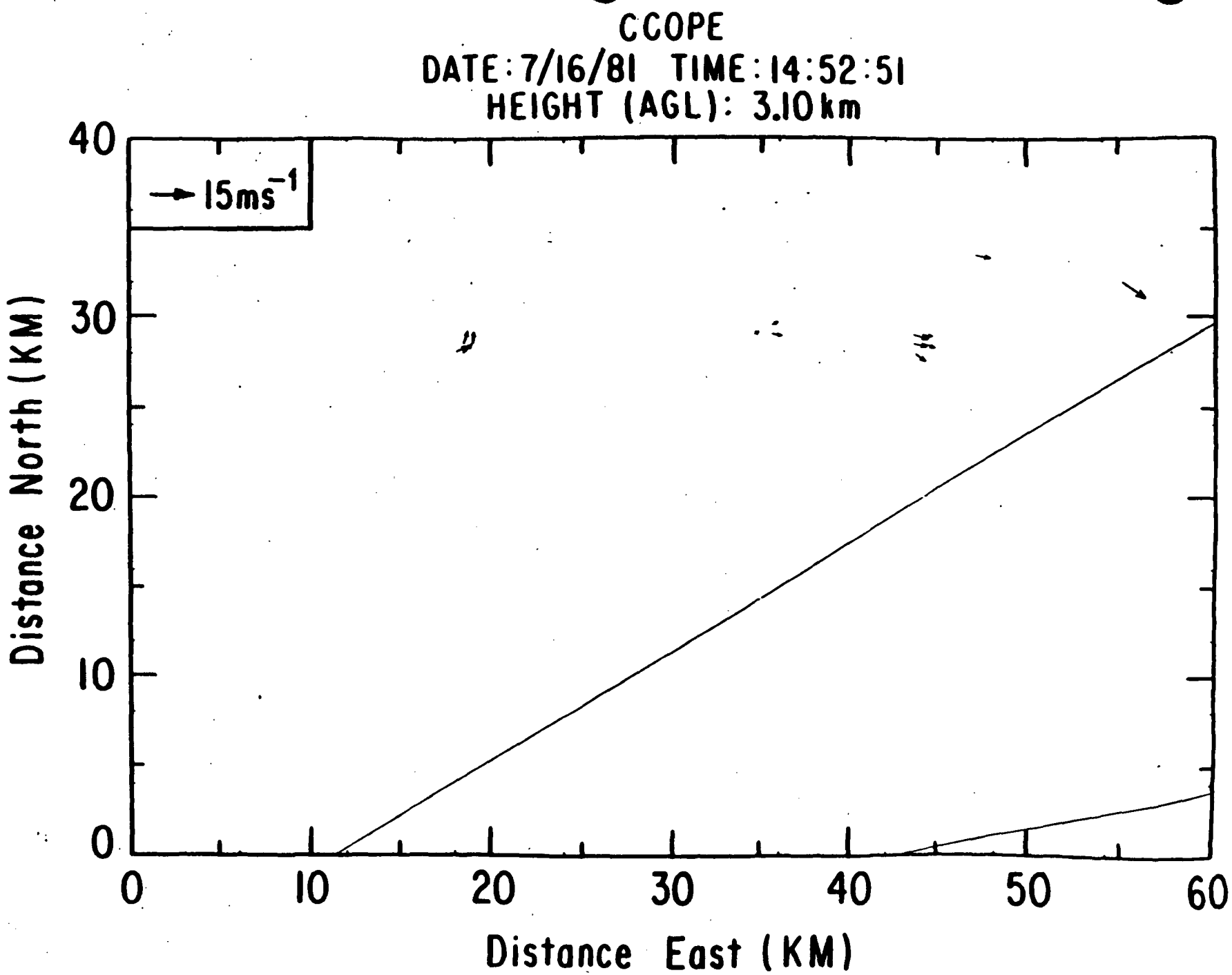
CCOPE
DATE: 7/16/81 TIME: 14:52:51
HEIGHT (AGL): 3.10 km
15ms⁻¹
Distance North (KM)
Distance East (KM)
0
10
20
30
40
50
60